FINAL REPORT

PHASE I

CONCEPTUAL APPROACH STUDY

200 W/Kg SOLAR ARRAY

CONTRACT NO. 954393

space division SD
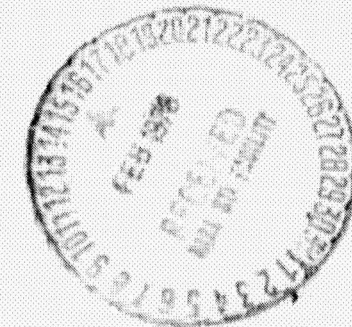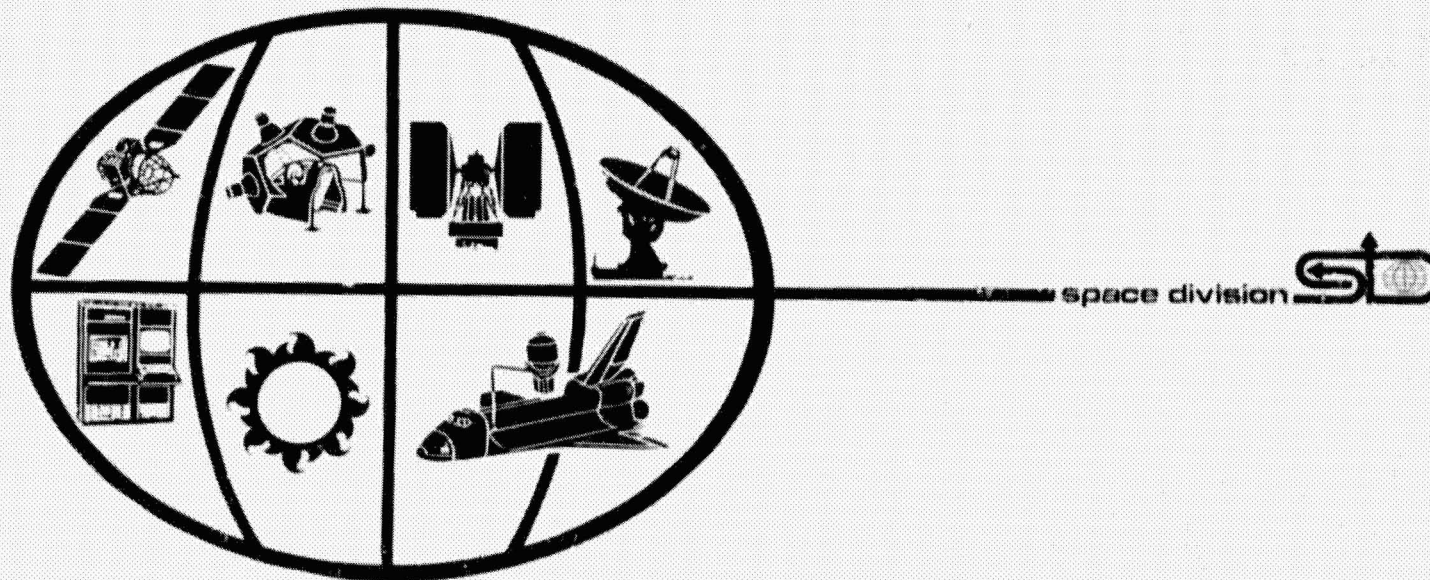
GENERAL ⬡ ELECTRIC

FINAL REPORT

CONCEPTUAL APPROACH STUDY

OF A

200 WATT PER KILOGRAM SOLAR ARRAY

PREPARED FOR

THE JET PROPULSION LABORATORY

CALIFORNIA INSTITUTE OF TECHNOLOGY

PREPARED BY: G. J. RAYL
K. M. SPEIGHT
R. W. STANHOUSE

APPROVED BY:

G. J. RAYL
PROJECT MANAGER

GENERAL ELECTRIC

SPACE DIVISION
Valley Forge Space Center
P. O. Box 8555 • Philadelphia, Penna. 19101

1

TABLE OF CONTENTS

iii

TABLE OF CONTENTS (Cont'd)

LIST OF ILLUSTRATIONS

LIST OF ILLUSTRATIONS (Cont'd)

LIST OF TABLES

REFERENCES

1.1   E. L. Ralph,
      "Performance of Very Thin Silicon Solar Cells,"
      6th Photovoltaic Specialists Conference - March 1967

1.2   P. A. Iles and D. K. Zemmrich,
      "Improved Performance from Thin Silicon Solar Cells,"
      10th Photovoltaic Specialists Conference - 1973

1.3   Joseph Lindmayer,
      12 Photovoltaic Specialists Conference - 1976

4.1   A. F. Forestieri and J. C. Broder,
      "Improvements in Silicon Solar Cell Cover Glass Assembly and Packaging Using FEP-Teflon,"
      NASA TMX-52875 - July 1970

4.2   J. D. Broder and G. A. Mazaris,
      "The Use of FEP-Teflon in Solar Cell Cover Technology,"
      10th Photovoltaic Specialists Conference - 1973

4.3   H. S. Rauschenbach,
      "FEP-Teflon Covered Solar Cell Array Advancements,"
      10th PVSC - 1973

4.4   A. F. Ratajczak and A. F. Forestieri,
      "Status of FEP Encapsulated Solar Cell Modules,"
      9th Intersociety Energy Conversion
      Engineering Conference - August 1974

4.5   H. S. Rauschenbach and M. D. Cannady together with A. F. Ratajczak,
      "FEP-Teflon Encapsulated Solar Cell Modules - Further Progress,"
      11th PVSC - 1974

4.6   H. S. Rauschenbach and M. D. Cannady,
       "Flexible, FEP-Teflon Covered Solar Cell Module Development,"
       Final Report, Contract No. NAS3-16742 - 13 October 1976

4.7   R. E. Schramm, A. F. Clark and R. P. Reed,
       "A Compilation and Evaluation of Mechanical, Thermal and Electrical Properties
       of Selected Polymers,"
       NBS Monograph 132 - September 1973

4.8   N. M. Bikales, Executive Editor,
       "Encyclopedia of Polymer Science and Technology,"
       Vol. 11 and Vol. 14

4.9   J. W. Hawkins, Silicone Products Dept., GE Co.,
       Private Communication

4.10   J. I. Vette, A. B. Lucero and J. A. Wright
       "Models of The Trapped Radiation Environment," Vol. II
       NASA SP-3024

4.11   J. H. King
       "Low Energy Protons," Vol IV
       NASA SP-3024

4.12   J. P. Lavine and J. I. Vette,
       "Inner Belt Protons," Vol V
       NASA SP-3024

4.13   J. R. Carter, Jr. and H. Y. Tada,
       "Solar Cell Radiation Handbook,"
       Report #21945-6001-RV-00
       JPL Contract #953362 - 28 June 1973

ABSTRACT

A conceptual design study was undertaken with a specific power of 200 Watts/kilogram, BOL (beginning of life) as the principal performance objective for a solar array at the heliocentric distance of one astronomical unit. Two alternative designs meet or exceed this specific power objective, one a retractable rollout design and the other a non-retractable foldout configuration. An end of life (EOL) power for either design of 0.79 BOL is predicted based on one solar flare during a 3 year interplanetary mission. High efficiency (13.5% @ 28°C, AMO) ultra-thin (75 microns) silicon solar cells were assumed, based on data furnished by the Jet Propulsion Laboratory. Both array configurations incorporate the features of flexible substrates and cover sheets. A power capacity of 10 kilowatt is achieved in a blanket area of 76 m^{2} with an area utilization factor of 0.8. A single array (or wing) consists of two identical solar cell blankets deployed concurrently by a single, collable-longeron boom. An out-of-plane angle of 8-1/4° is maintained between the two blankets so that the inherent in-plane stiffness of the blankets may be used to obtain out-of-plane stiffness. This "V-stiffened"" design results in a 67% reduction in the stiffness requirement for the boom. Since boom mass scales with stiffness, a lower requirement on boom stiffness results in a lower mass for the boom. These solar arrays are designed to be compatible with the shuttle launch environment and shuttle cargo bay size limitations.

SECTION 1
INTRODUCTION

SECTION 1

INTRODUCTION

This report concludes a 12-month study of possible conceptual designs for a 200-Watt per kilogram solar array. This study is the third of a series of study/development programs performed by the Space Division, General Electric Co. for the Jet Propulsion Laboratory since 1970 (see Table 1-1). This prior work showed that a flexible substrate, or blanket, was essential to the attainment of a high power-to-weight ratio. Two different methods of array stowage (flat pack and drum) were developed for those programs. The 110-Watt per kilogram study had shown the superiority of the lattice boom as a deployer for a flexible array. It was with this background of study and engineering development that this study was initiated with a principal goal of 200-Watt/kilogram.

Table 1-1. GE Design Studies and Development Program for JPL

	YEAR COMPLETED	BOL POWER, Kw	RETRACTION	PARTIAL RETRACTION	HARDWARE	STATUS & RESULTS
66 W/Kg ROLL-UP SOLAR ARRAY DEVELOPMENT	1971	2.5	X	X	FULL-SCALE ENGR UNIT PARTIALLY CELLED	FULLY QUALIFIED
110 W/Kg CONCEPTUAL SOLAR ARRAY DESIGN STUDY	1975	10	X	X	NONE	FEASIBLE DESIGN
200 W/Kg CONCEPTUAL SOLAR ARRAY DESIGN STUDY	1977	10	X (OPTIONAL)	X (OPTIONAL)	NONE	TECHNOLOGY READY BY 1980

1.1 A COMPARISON OF GE ARRAY CHARACTERISTICS

The advent of the ultra-thin solar cell concept made this study feasible. Although 75 microns thick solar cells were not readily available in early 1976, enough preliminary work has been done [1.1, 1.2] to lend credibility to the idea of ultra-thin cells. At the time of this report 50 microns thick solar cells are commercially available [1.3]. The significance of high-efficiency, ultra-thin cells in attaining very high specific powers may be seen by a comparison of pertinent characteristics of the 110 Watt per kilogram study, and this study is shown in Table 1-2. It will be noted that approximately 50% of the cell mass has been eliminated by a reduction in cell thickness and a 69% improvement in cell efficiency.

Table 1-2. A Comparison of GE Array Characteristics

Comparison	110 W/kg Study (Foldout Design)	200 W/kg Study (Rollout Design)
Cell Area (cm^2)	4	4
Cell Thickness (microns)	125	75
Mass per Cell (g)	0.13	0.093
Total Mass of Cells (kg)	29.3	15
Cell Mass/Blanket Mass (%)	60	48
Power per Cell (mW)	44 @ $57^{o}C$	86 @ $55^{o}C$
Cell Efficiency (%)	8	13.5
Specific Power (W/kg)	113	201
Total Array Power (KW)	9.86	10.5

1.2 MASS SUMMARY COMPARISON FOR GE ARRAYS

A mass summary comparison for the 110 W/kg and the 200 W/kg solar array designs in Table 1-3 illustrates the mass savings to be realized in the case of the 200 W/kg design in the blanket when 75 μm solar cells are used. The mass reserved for stowage and support is much less for the rollout or drum storage design. There is a weight penalty to be paid for retractability, as in the rollout design.

Table 1-3. Mass Summary Comparison for GE Arrays

Item	110 W/kg Study Foldout Design		200 W/kg Study			
	Mass (kg)	%	Foldout Design		Rollout Design	
			Mass (kg)	%	Mass (kg)	%
Blanket Assembly	48.5	55	28.36	60	31.22	63
Stowage & Support	30.6	35	11.10	19	9.17	14
Deploy & Retract	8.4	10	8.08	21	9.28	23
Total Mass (kg)	87.5	100	47.54	100	49.67	100
Power, Total (kW)	9.86		10.5		10.5	

1.3 A COMPARISON OF FLIGHT ARRAYS AND DEVELOPMENT ARRAYS

A comparison of characteristics for flight hardware and development hardware are listed in Table 1-4. From these comparisons it may be inferred that the two conceptual designs resulting from this study have extrapolated the state-of-the-art designs to a point where confirmation of the salient design features by engineering test and evaluation will be required if credibility is to be established.

Table 1-4. A Comparison of Flight Arrays and Development Arrays

	POWER DENSITY, W/Kg	BOL POWER, Kw	RETRACTION	PARTIAL DEPLOYMENT	HARDWARE	STATUS
COMMUNICATIONS TECHNOLOGY SATELLITE (CTS)	25	0.5			FLIGHT HARDWARE	FLOWN
FRUSA	45	0.75	X	X	FLIGHT HARDWARE	FLOWN
SPACE STATION	70	100	X	X	QUARTER-SCALE DEMONSTRATION UNIT	NOT TESTED
SEP TECHNOLOGY DEVELOPMENT PROGRAM	66	12.5	X	X	FULL-SCALE DEVELOPMENTAL WING	TO BE QUALIFICATION TESTED BY 1978

SECTION 2
PROGRAM SUMMARY

SECTION 2

PROGRAM SUMMARY

2.1 BASELINE SOLAR ARRAY

The baseline solar array is a fully retractable, rollout design consisting of two flexible solar blankets in a "V-stiffened" configuration. The solar array blanket consists of a sheet of 38 μm Kapton-F (laminate of Kapton and FEP-Teflon) as the substrate and 25 μm FEP-Teflon as the coversheet. FEP-Teflon is a thermoplastic that may be heat sealed to the cells and interconnects without the necessity of a cement.

A foldout solar array of the same 10.5 kW capacity was designed as an alternative to the rollout design. Unlike the rollout design, however, the foldout array is retractable.

One of the salient features of these two conceptual designs is the utilization of in-plane stiffness, inherent in the blanket construction, in an out-of-plane configuration as indicated in Figure 2-1. Approximately 1/3 of the required boom stiffness is obtained out of "V" stiffening with the blanket. With a lower requirement on boom stiffness, (approximately 2/3 that required with a planar configuration blanket) the boom mass may be reduced accordingly. The coilable lattice continuous longeron boom was selected for the best mass to stiffness ratio, relatively low sensitivity to thermal-induced bending, and low backlash characteristics.

Both of these array designs are compatible with the NASA Shuttle launch environment and payload bay stowage envelope.

CELL MODULE
2000 2 x 2 CM CELLS

80 MODULES
10.4 KW

4.74M (15.55 FT)

17.2M (56.45 FT)

12.7 CM DIAMETER LATTICE BOOM & DEPLOYER

DRUM 25.4 CM DIAMETER
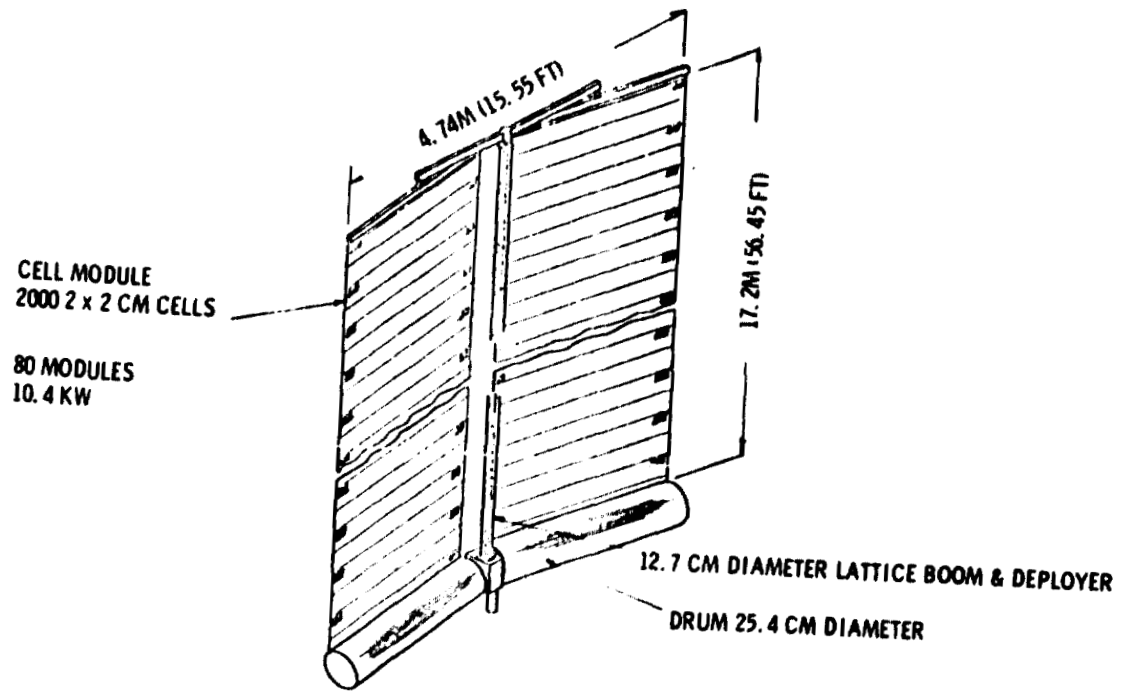
Figure 2-1. Baseline Solar Array

2.2 ALTERNATE DESIGN FOLDOUT ARRAY

The alternative to the baseline rollout design is a foldout design which uses a flat pack method of stowage. The blanket assembly is identical to that in the rollout design. A support truss, cantilevered from the boom storage and center support canister, provides a rigid base for the flat pack blanket stowage. This base, together with the rigid leading edge member, allows sufficient pressure to be applied to the folded array to prevent lateral or transverse motion of the blanket during launch. See Figure 2-2.
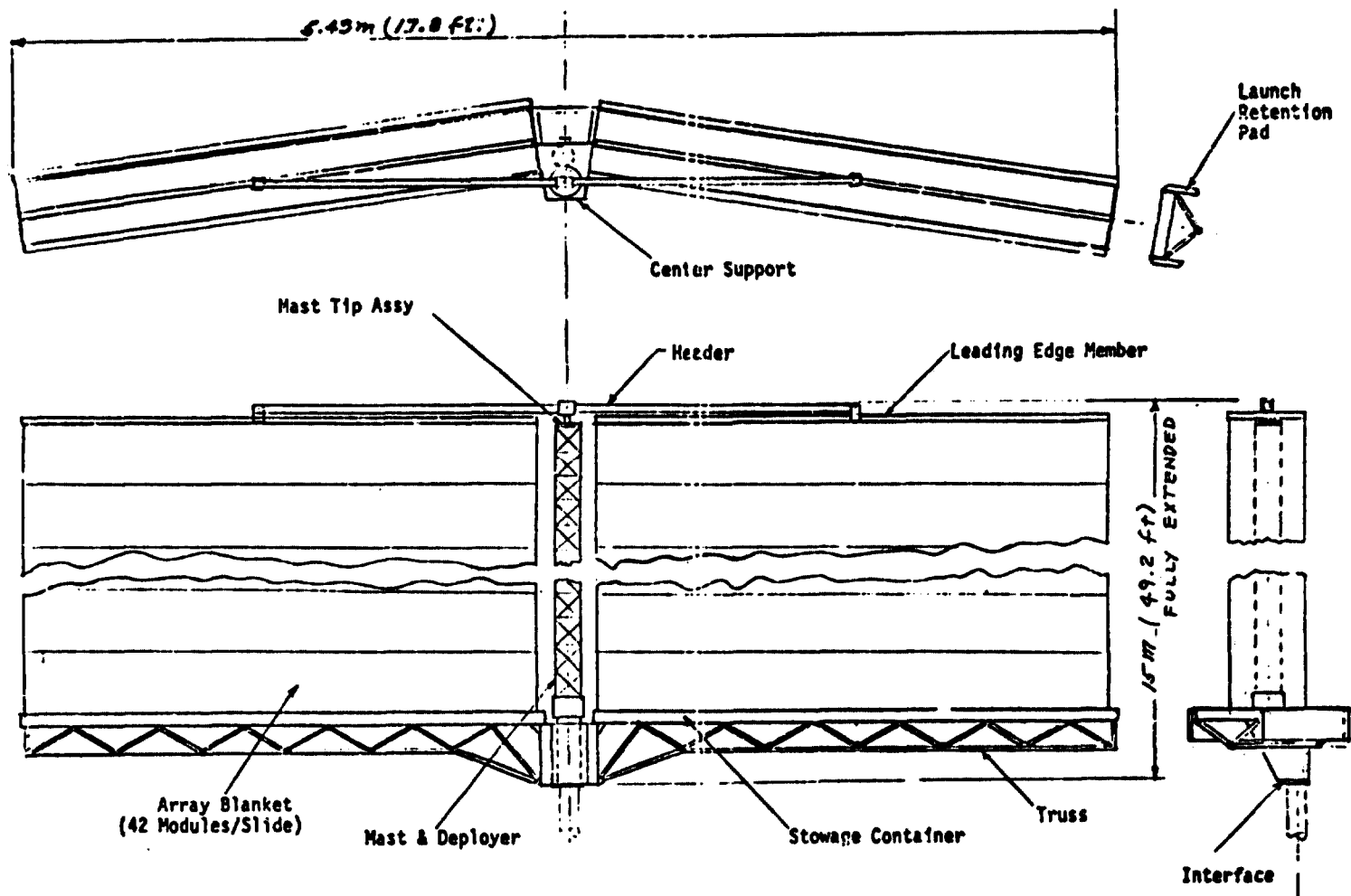
Figure 2-2.   Alternate Foldout Solar Array Design

2.3 RADIATION ANALYSIS - CONCLUSIONS

The calculated 1 Mev DENi electron fluence is used with an emperically derived function, supplied by the JPL, to estimate the power loss appropriate to this fluence. A summary of the calculated power losses for the interplanetary and earth orbital cases selected for this study is shown in Table 2-1. Figure 2-3 shows the normalized power versus particle fluence.

Table 2-1. Calculated Power Loss Summary

	DENI 1 MeV Electron Fluence		Total	$\dfrac{P_{Max_o}}{P_{Max_o}}$
	Front	Back		
Interplanetary-One Flare	1.12E15	1.08E15	2.20E15	0.79
Interplanetary-7 Flares	7.85E15	7.56E15	1.54E16	0.59
Geosynchronous 3 Year (trapped particles + 1 flare)	3.80E17	1.42E17	5.22E17	0.23
Low Earth Orbit 278 pm; 60 degree inclination Trapped Particles - 3 year Fluence	1.09E13	9.86E12	2.08E13	0.99
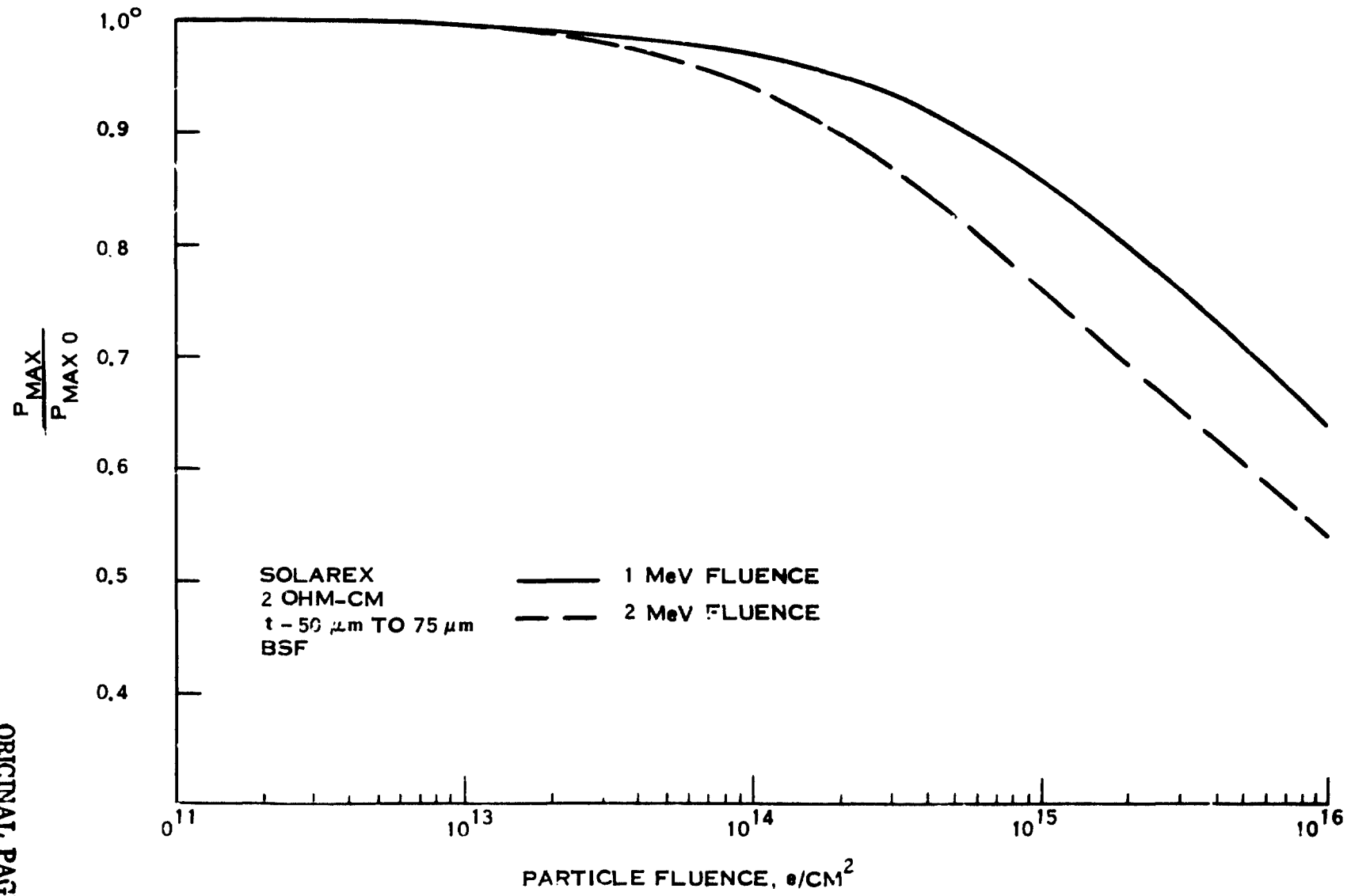
Figure 2-3. Normalized P_{Max} Vs Particle Fluence

SOLAREX
2 OHM-CM
t - 50 μm TO 75 μm
BSF

1 MeV FLUENCE
2 MeV FLUENCE

PARTICLE FLUENCE, e/CM^2

2.4 MASS SUMMARY

For purposes of mass estimation, the total solar array (1 wing) was broken down into four subsystems; electrical, mechanical, array structure and actuators. The associated mass estimates are based on measurements or published data in some cases; e.g., cells, substrate, adhesive and cover material. In other cases, related experience has been the guideline for items like interconnects, bus strips, slip ring assembly, cable, connector bearings, etc. Mass estimates for the longeron boom, boom deployer and center support were obtained from two sources, Astro Research and Able Engineering.

A total mass of 49.67 kg is predicted for the baseline 10.5 kW rollout array (wing). If a 5% contingency is applied, the resultant specific power is 201.3 Watts/kilogram. An alternate foldout design is listed for comparison purposes, showing the mass saving that may be expected where retractability of the array is not required. Both designs exceed the 200W/kg goal set for this conceptual design study. These mass estimates are based on

- 75 Microns thick silicon solar cells

- 38 Microns thick Kapton-F substrate

- 25 Microns thick FEP-Teflon coversheet

Table 2-2. Mass Summary - 10.5 kW Array (Aspect Ratio = 4:1)

Subsystem	Item No.	Item	Unit Mass (kg)	Quantity per 10kW	Total Mass (kg) Rollout	Total Mass (kg) Foldout
Electrical	1	Solar Cell	94×10^{-6}	160,000	15.04	15.04
	2	Substrate	1.4	2	2.80	2.80
	3	Adhesive	1.08	2	2.16	2.16
	4	Cover Material	2.97	2	5.94	5.94
	5	Interconnects	.87	2	1.72	1.72
	6	Bus Strips	.17	2	.34	.34
	7	Slip Ring Assembly	1.43	2	2.86	-
	8	Cable	.15	2	.06	.06
				Subtotal	31.22	28.36
Mechanical	10	Drum	2.95	2	5.9	-
	11	Shaft	.22	2	.44	-
	12	Bearings	.10	6	.60	-
	13	Container, Blanket	3.48	2	-	6.36
	14	Truss	.51	2	-	1.03
	15	Center Support	2.23	1	2.23	2.07
	16	Pad and Valve	.82	2	-	1.64
				Subtotal	9.17	11.10
Array Structure	17	Boom	.91	1	1.07	1.07
	18	Header	.90	1	.77	.77
	19	Leading Edge (LEM)	1.06	2	2.12	2.12
	20	End Strip	.05	4	.20	.20
	21	Misc. Hardware	-	-	.50	.50
				Subtotal	4.66	4.66
Actuators	22	Boom Deployer	3.18	1	3.18	3.18
	23	Tension Motor	.60	2	1.20	-
	24	Tension Spring	.24	1	.24	.24
		Net Mass			49.67	47.54
		5% Tolerance & Contingency			2.48	2.38
		Total Mass Estimate			52.15	49.92
		Specific Power (Watts/kg) (BOL)			201.3	210.3

SECTION 3
DESIGN REQUIREMENTS

SECTION 3

DESIGN REQUIREMENTS

3.1 PRINCIPAL STUDY REQUIREMENTS

The basic design requirements for the 200 Watt per Kilogram Solar Array Feasibility Study are given in GE document number 200W/kg - 2.76-004, Baseline Requirements, which is included in Appendix A of this report. These requirements were not intended to place undue restrictions on the solar array system design, but only to act as a guide in the formulation of a design approach. The intent was to develop high performance design concepts which are viable concepts for future interplanetary missions. These design requirements will be representative rather than specific, since a detailed optimization cycle would be a part of any flight hardware application. Table 3-1 summarizes the principal requirements.

Table 3-1. Principal Study Requirements

Power (BOL = 1 AU)	10 kW/Wing
Power Degradation	Less than 5% over 3 years including total fluence for 1 solar flare
Weight	50 kg (110 lbs)
Operating Temperature at 1 AU	$85^{\circ}C$ maximum
Flatness	± 10 degrees
Deployed Dynamics	Lowest $F_n \geqslant 0.04$ Hz
Quasi-Static Load	1×10^{-3} G_s maximum
Deployment/Retraction	Full deployment, 90% retraction an option
Steady State Operating Temperature	$-130^{\circ}C$ to $+140^{\circ}C$, 10^{-5} Torr
Thermal Shock	$-190^{\circ}C$ to $+140^{\circ}C$, 10^{-5} Torr 1000 cycles

3.2 OUTPUT POWER AND DEGRADATION

The output power of the fully deployed solar array is specified as 10kW in free space at 1AU and at the predicted solar array operating temperature at this intensity. ASTM Specification E490-73A defines the solar constant at air mass zero and 1 AU. A copy of this Specification is included in this report as Appendix B. The 10 kW power output is defined as the beginning of life (BOL) value measured at the spacecraft interface. Therefore, losses in solar cell interconnects and cabling (2-3 percent of total power output) must be added to define the array power required. Since the spacecraft power conditioning circuitry will include the necessary diode isolation, no diodes will be used on the array itself.

The solar array must be capable of operating over a three year period with a power degradation not to exceed 20%. The solar flare proton model on the preceeding page defines the proton fluence to be encountered in an interplanetary mission. The ultraviolet radiation intensity is specified as 1095 days at 2.002 calories/cm^2/minute. These environmental factors, along with thermal rejection considerations and overall weight, will be used to establish the type, thickness, and material employed for coverglasses, adhesives, coatings, etc.

Table 3-1. Principal Study Requirements (Continued)

Ionization Dose	10^7 rads
UV Exposure	2 cal/cm^2-min

Particle Fluence:	
Proton Energy, E(MeV)	Total Fluence ϕ E (P/cm^2)
1	2E12
10	4E10
30	9E9
100	1E9

3.3 POWER-TO-WEIGHT RATIO

The power-to-weight ratio is specified as 200 Watts of electrical power for each kilogram of total system weight. This ratio is based on the 10 kW, BOL, power output at 1 AU in free space. This requirement is the principal objective of the program. It represents approximately four times the capability of existing flight arrays. Several approaches were being considered to achieve this goal. Weight reductions were necessary in all elements of the array design. This includes lighter cells, coverglasses, substrates, deployment mechanisms, support structures, booms, and other materials and devices. A lower deployed mass means a lower requirement on boom stiffness and support mechanisms. This in turn means a lower boom and deployment mass. A low blanket mass, on the other hand, makes it more difficult to meet the 0.04 Hertz natural frequency requirement. When the principle of "V-stiffening" is applied to the blanket rigging, about 1/3 of the required boom stiffness can be met by the out-of-plane stiffness of the blankets themselves. The impact of cell thickness on the power-to-weight ratio is shown in Figure 3-1.
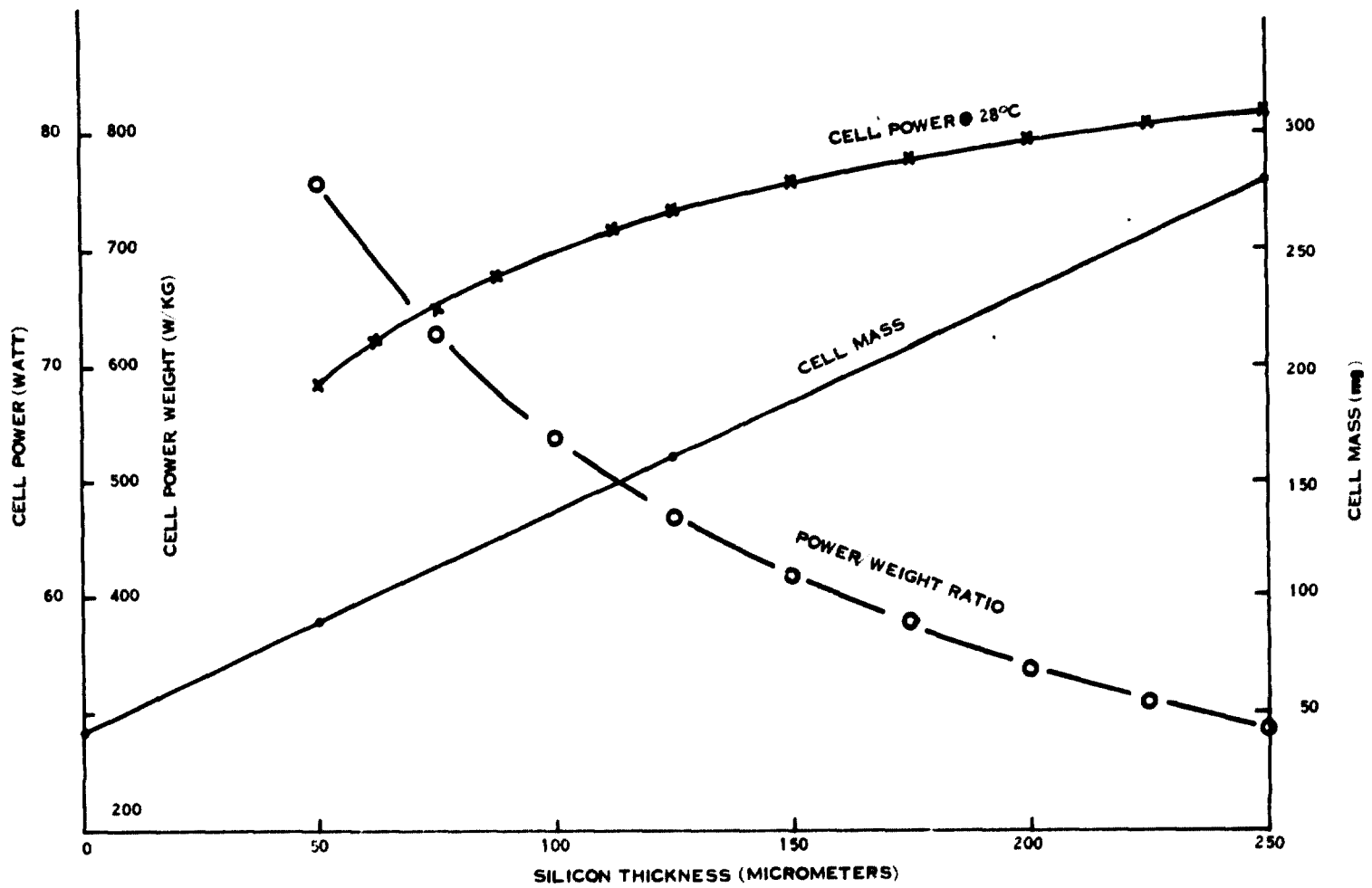
Figure 3-1. Cell Power and Mass vs Silicon Thickness

3.4 THERMAL ENVIRONMENT

3.4.1 TEMPERATURE, STEADY STATE

Paragraph 3.3.3.1 of the Baseline Requirements (Appendix A) specifies the steady state thermal vacuum environment of -130°C to $+140^\circ$C at 10^{-5} Torr. This requirement defines the range of steady state temperatures, at vacuum, over which the solar array shall be capable of operating. It is not required to produce 10 kW over this range, but it is required to be fully operational in both the electrical and mechanical modes. (The 10 kW of power output is defined as at BOL, 1 AU, and at the predicted array temperature for that intensity.) The solar cell sandwich, consisting of substrate, solar cell to coverglass adhesive, and coverglass, must be designed to withstand not only this temperature range, but also thermal shock. Solar cell interconnects must be capable of operating over these temperatures without applying undue stress on the cell contact areas. The induced thermal deformations caused by temperature cycling between -130°C and $+140^\circ$C must be kept to values low enough to meet the flatness requirement of 10 degrees specified in Paragraph 3.2.10 of the Baseline Requirements.

In the deployment mechanisms and boom area, the temperature range of -130°C and $+140^\circ$C implies the use of dry lubricants and materials with similar coefficients of thermal expansion, particularly in bearings, bushings, gears, and shafts.

3.4.2 THERMAL SHOCK

Paragraph 3.3.3.2 of the Baseline Requirements (Appendix A) defines the thermal shock environment. This requirement specifies a temperature range of $-190^{\circ}C$ to $+140^{\circ}C$ at 10^{-5} Torr. The time rate of change of temperature for cooling shall be the natural cooling rate of the solar panel in a simulated passage into a planetary shadow with an assumed planetary albedo of zero. The time rate of change temperature for heating shall be the natural heating rate of the solar panel in a simulated passage from a planetary shadow into a normal solar flux intensity corresponding to a steady state temperature of $+140^{\circ}C$ on the solar cells. The total thermal shock environment shall consist of 1000 complete heating and cooling cycles.

The thermal shock environment applies to a deployed array and is a survival environment rather than an operational one. This requirement has its greatest impact on the materials selected for the design. When any of these temperature requirements, as well as all other requirements, were found to restrict a potentially attractive design approach, a parametric review was performed to determine the impact on the ability to achieve the 200 Watt/kg goal.

3.5 DYNAMICS

The Shuttle launch environments specified in Paragraphs 3.3.2.1, 3.3.2.2, 3.3.2.3, and 3.3.2.4 of the Baseline Requirements Document define the vibration, acoustics, shock and acceleration values appropriate for the stowed array design. These environments are felt to be relatively "standard" for spacecraft design, and at this early stage of the program, did not unduly drive the array design to the detriment of overall weight penalties.

The lowest deployed natural frequency shall be equal to or greater than 0.04 Hertz, as specified in paragraph 3.2.8. Using this value of 0.04 Hertz and the quasi-static load of $1 \times 10g^{-3}$ studies have shown that the smallest practical size (4-inch diameter) of a deployment boom is sufficient to meet this frequency requirement.

3.6 SOLAR CELLS

Typical candidate solar cell data was provided by JPL for incorporation into this Study Program. Paragraph 3.4.5 of the Baseline Requirements (Appendix A) describes this data. Options regarding cell size, thickness, contact configuration and material, interconnecting materials, and grid line density were given. These options were evaluated to establish an optimum cell design for this program.

SECTION 4

TECHNICAL DISCUSSION

SECTION 4

TECHNICAL DISCUSSION

4.1 EXISTING SOLAR ARRAY CONCEPTS

4.1.1 GENERAL COMMENTS

A number of lightweight solar array system concepts have been developed, with experimental hardware and testing applied to many of the designs. The most recent example of large lightweight arrays is in the 25 kW system currently being developed by LMSC for the Solar Electric Propulsion Stage (SEPS).

These concepts can be categorized by three basic approaches, namely: rollout, foldout, and folding panels. Rollout designs require a complete flexible blanket type of array. Foldout configurations usually involve a series of either flexible or semirigid panels which fold accordian fashion into a lightweight container. Folding panels are rigid in construction utilizing a frame or structural material such as honeycomb for a substrate. The frames are large and hinged to form two or more layers when stowed. A comparison summary of efficiencies and power levels of many of these concepts is shown in Table 4-1.

Table 4-1. Summary of Existing Lightweight Solar Array Designs

Type	Efficiency		Power Level kW	Description Array/Support/Stowage	Source	Remarks
	Watts/kg	Watts/M²				
Rollout	77.6	118	2.75	Blanket/Pantograph/Graphite Epoxy Drum	Fairchild-Miller	
	71.7	118	2.75	Blanket/BI-STEM/Beryllium Drum	General Electric	Eng'g Model Tested
	68.1	118	2.75	Blanket/Ryan boom/Magnesium Drum	Ryan	
	48.5	107	1.5	Blanket/BI-STEM/Magnesium Drum	Hughes	1971 Flight Experiment
	38.5	118	0.08	Blanket/STEM/Drum	British Aircraft Corp.	
Foldout	110	95	10	Blanket/Astro Mast/Be Container	General Electric	Study
	83	118	2.75	Panels/BI-STEM/Container	TRW	
	79	118	14.2	Panels/Inflatable Framework/ Magnesium Frame	Messerschmitt	
	78	118	2.7	Panels/BI-STEM/Frame Attached to S/C	LMSC	
	75	118	0.75	Rigid Panel/Telescopic Mast/Container	RAE	
	66	99	25	Blanket/Astro Mast/Honeycomb Container	LMSC	SEPS Array
	105	148	(2 panels)	Blanket/BI-STEM/Container	AEG Telefunken	1976 CTS Flight
Folding Panel	80	90	10.4	Hollow Core Substrate Beryllium Box Frame	EOS	
	40	118	15.7	Fiberglass Be Frames	Boeing	

4.1.2 GE/JPL 110W/Kg ARRAY (BASELINE CONCEPT)

A study of the design of the 110 Watt/Kg systems was completed by General Electric, Space Division in May of 1973. The baseline configuration which meets those requirements is illustrated in the sketch on the opposite page and summarized in Table 4-2.

This concept consists of a single, central, deployable boom which supports two flexible solar cell blankets. The 10,000 Watt beginning-of-life output is generated by 226,800 solar cells which are interconnected to supply power at a 193 Vdc maximum power voltage. These solar cells are nominal 125 μm thick, 2 x 2 cm, N/P silicon with a nominal base resistivity of 10 Ohm-cm. A plated nickel-copper-nickel-gold bottom wraparound contact configuration is used in conjunction with an ultrasonically bonded aluminum wire interconnector system. The active solar cell surface is protected from low energy proton damage by a nominal 38 μm thick integrally deposited coverglass. A Kapton-H film substrate supports the solar cell modules without the aid of a bonding adhesive. Holes in the substrate allow for this direct radiation heat transfer from the rear of the solar cells. The exposed portion of the rear cell contacts are coated with adhesive to provide the necessary low energy proton protection.

Tension in the solar cell blanket substrates maintains the deployed natural frequency above the minimum specified value of 0.04 Hz. The flexible solar cell blankets are stowed for launch by folding into a flat-pack package which is retained in compression between a bottom honeycomb panel and spring driven hinged honeycomb panel doors on the top. These doors are held closed during launch by the tabular leading edge member (LEM) which is attached to the deployable boom at the center and retained at each end by a launch retention cable mechanism. Solar array deployment is accomplished by firing redundant cable cutters at each end of the array which releases the end of the LEM and the restraint at each end of the supporting truss work. Application of power to the deployable boom actuator will cause the LEM to move off the door panels allowing them to swing open. Continued deployment of the boom will cause the LEM to pull each fold of the blankets from the stowed package. Interlayer cushions of Kapton-H film are retained by the bottom panel. At the end of the deployment travel, the further deployment of the blanket applies the required tension load by extending a spring mechanism at the base of each blanket.

Table 4-2. Design Features 110 W/kg Baseline Solar Array Panel Configuration
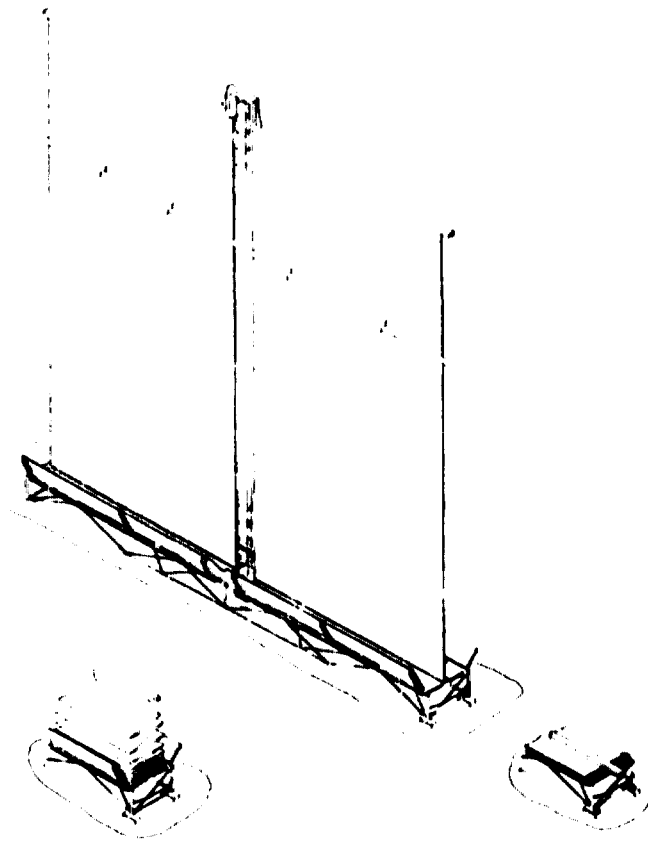
Parameter	Value
1. Deployed length (L)	18.565 m
2. Total width (W)	5.915 m
3. Blanket width (w)	2.830 m
4. System aspect ratio (L/W)	3.14
5. Total gross blanket area	105.08 m^2
6. Total number of solar cells (2 x 2 cm)	326,800
7. Lowest deployed natural frequency	0.04 HZ
8. Electrical power output at V_{mp} = 193 Vdc	9869 Watts
a. Beginning-of-life (BOL)	
b. 57°C	
c. 1 AU, AMO illumination	
d. Measured at panel interface connector	
9. Expected maximum power degradation after 3 year interplanetary mission	30%
10. Total system mass	87.5 kg
11. BOL power-to-mass ratio	112.7 Watt/kg
12. EOM power-to-mass ratio	78.9 Watt/kg

4.1.2.1 1110W/Kg Array Blanket

Each solar cell blanket consists of an interconnection of 30 identical strips as shown in Figure 4-1. Each strip consists of two series connected solar cell modules, with each module being composed of 1890, 2 x 2 cm solar cells which are interconnected 135 in series by 14 in parallel. The two modules on one strip are connected electrically in series with the two modules on an adjacent strip to form a complete electrical circuit. Thus, each electrical circuit is composed of 7560 cells connected 540 in series by 14 in parallel.

Each circuit has a calculated 335-Watt maximum power output at 196 Vdc measured at the circuit terminals. If a 2-percent bus strip distribution loss is accounted for, the total calculated panel output is 9860 Watts measured at the panel interface connector.

MODULE (135 s X 14 p)

FOLD

JUMPER LOOP

FOLD

BUS STRIP

FOLD
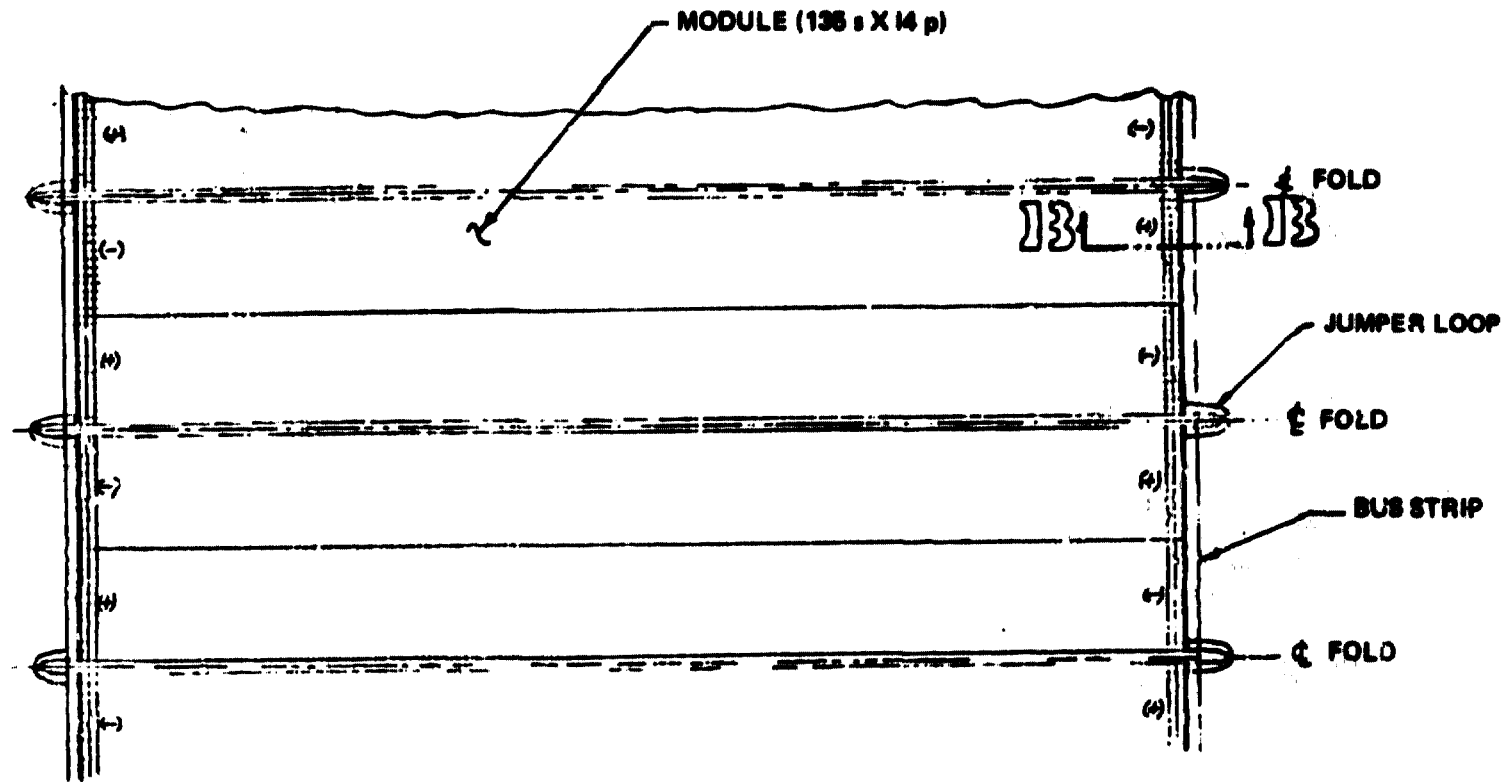
Figure 4-1. Detail of Module Arrangement on
110 Watt/kg Solar Cell Blanket

4.1.2.2 110W/kg Solar Cells

The solar cells are nominal 125 μm thick, 2 x 2 cm, N/P silicon with a nominal base resistivity of 10 Ohm-cm. Table 4-3 summarizes the significant characteristics of this cell. The solar cells are shielded from the damaging effects of low energy protons by the deposition of an integral cover of Corning 7070 glass. A nominal integral coverglass thickness of 37 μm should provide the necessary protection within the weight constraints of this program.

Table 4-3. Design Characteristics of Ferranti 125 μm Thick Solar Cells
(Ferranti Cell Type MS36)

Thickness	125 ± 25 μm
Size	20 ± 0.15 x 20 ± 0.15 mm
Resistivity	7 to 12 Ohm-cm Float zone silicon
Contact Configuration	Bottom wraparound 24 finger drid geometry
Contact Material	Plated - nickel, copper, nickel, gold
Anti-reflective Coating	TiO_x
Minimum Lot Average Electrical Performance (covered)	123 mA at 0.445 Volts (AMO, 1 AU, $25^oC \pm 2^oC$)
Maximum Lot Average Cell Mass	0.129 gm/cell

4.1.2.3 110W/kg Solar Array Mass Breakdown

A detailed mass breakdown for the solar cell blanket is given in Table 4-4. Note that about 75 percent of the total mass is assigned to the 125 micron cell and the 37 micron coverglass. This mass breakdown clearly identifies the cell and its cover as the place where weight reduction may materially affect the array specific power. A reduction in blanket weight is reflected in a lower stiffness requirement on the boom. This in turn permits a lighter boom, deployment mechanism and stowage canister.

Table 4-4. Mass Breakdown for Solar Cell Blanket - 110W/kg
Array (Total for Both Blankets)

Items	Mass (kg)
Solar Cells (.129 gm each)	29.26
Integral Coverglass	7.26
Interconnectors	1.81
Substrate	4.04
Adhesive (rear contact low energy proton protection)	3.50
Bus Strips and Insulators	1.50
Inboard and Outboard Leaders	0.27
Circuit Terminations	0.15
Strip Hinge Joints and Bus Strip Jumpers	0.71
	48.50

4.1.3 LMSC/MSFC SEPS ARRAY

The SEPS array currently under development by LMSC is a large array consisting of two wings with a total output of 25 kW. The baseline configuration is shown in Figure 4-2.

This array is a blanket foldout type using a continuous longeron lattice lightweight extendible boom. The array is stored in a supporting container when retracted. The total density of the blanket is 0.86 kg/m^2 (.176 lbs/ft^2). Specific power for the total array is approximately 66 Watts/kg.
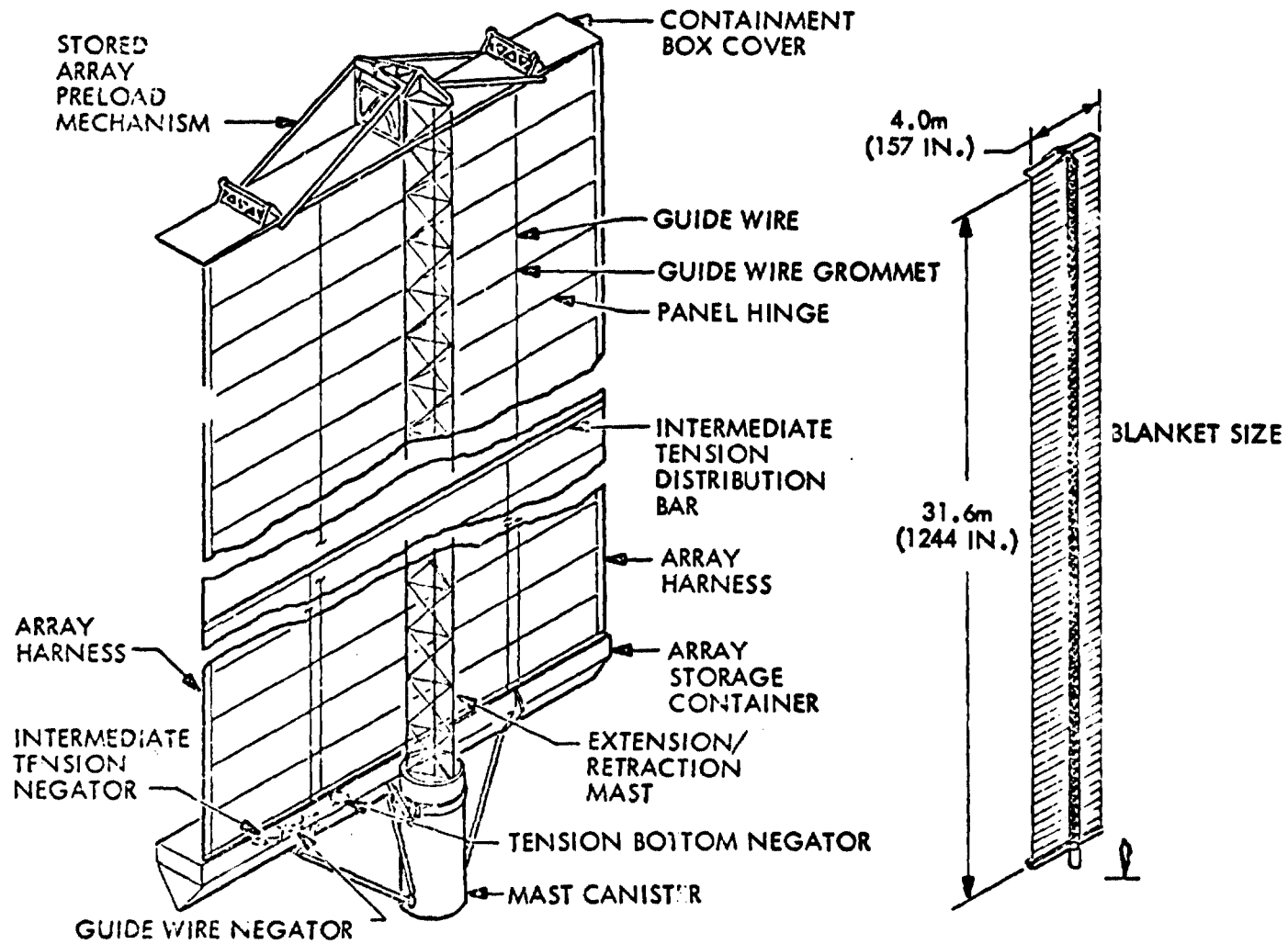
Figure 4-2. LMSC/MSFC SEPS Array

4.1.3.1 SEPS Solar Array Requirements

The solar cell blanket is 30.99 m (101.6 ft) x 3.99 m (13.09 ft) in size and is made up of individual panels which are attached to each other by means of a fiberglass and graphite/epoxy piano hinge. When retracting the blanket, the panels are guided by means of wires which are maintained in tension by negator spring motors. The stowage container cover also serves as an outboard header for the blanket array.

The SEPS baseline calls out 200 micron cells and 150 micron coverglass cemented to the cells. A copper-Kapton laminate is selectively etched to produce the required cell interconnect pattern. The Baseline Requirements are shown in Table 4-5.

Table 4-5. SEPS Basic Array Requirements

Parameter	Requirement
Deployment	Full development and retractions from intermediate positions
Stowage Volume	0.46 m x 0.46 m x 4.06 m
Weight	380 kg maximum
Deployed Natural Frequency (1st mode)	0.04 Hz
Docking Loads	0.5 G
Solar Operating Range	Between 0.3 and 6.0 AU from Sun
Array Power (2 wings)	25 kW BOL 21 kW BOL
Voltage	V_{oc} 420 Vdc V_{mp} 200 Vdc
Boom Length (extendible)	32.0 m (105 ft)
Boom Bending Stiffness	5.45×10^4 N-M^2 (19.1×10^6 lb-in^2)
Boom Life	50 cycles full as partial extensions over 5 year period in space. 200 cycles ground test.

4.1.4 GE/JPL 66 WATT/KILOGRAM SOLAR ARRAY

In February 1971 General Electric completed a program to develop the technology of the rollup solar array concept under contract to The Jet Propulsion Laboratory. This array, shown in Figure 4-3 provides 2.75 kW at an efficiency of 71 Watts/kg. A flexible Kapton substrate blanket 1.17 m (46 inches) wide by 10.2m (402 inches) long is stowed by rolling it up on an 8" diameter drum of beryllium. A negator spring motor on the drum provides the blanket tension. The array is deployed and retracted by means of an Astro Research "BI-STEM" deployable boom 3 4 cm (1.3⁴ inches) in diameter.

GE/JPL 66 WATT/KILOGRAM ARRAY

RA250 SOLAR ARRAY

STATUS: DESIGN, DEVELOPMENT, & ENVIRONMENTAL TESTS COMPLETED FEB. 1970

CHARACTERISTICS

- POWER   2.75 KW
- SPECIFIC POWER   71 WATTS/KG
- STOWAGE   BE DRUM
- MAST   BI-STEM
- ARRAY SIZE   2.5M x 10.3M
- MASS   34.6 KG
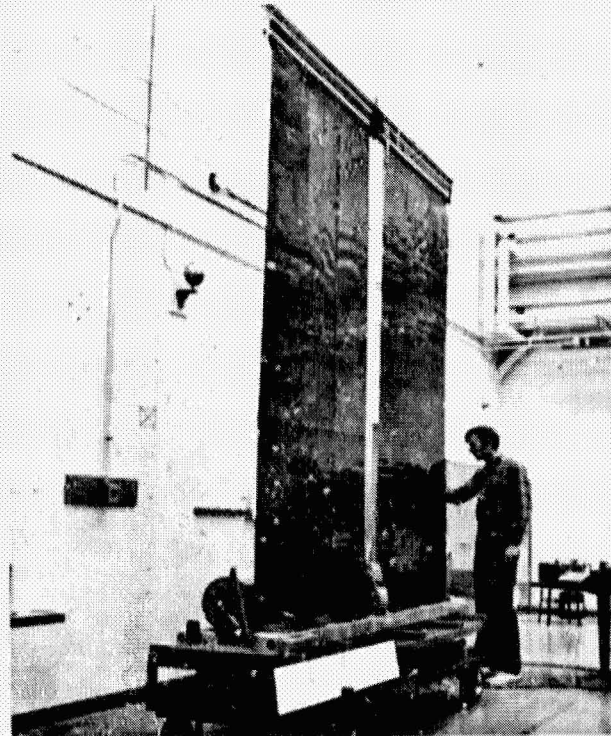
Figure 4-3. RA250 Solar Array
(Partially Deployed)

4.1.4 GE/JPL 66 WATTS/KILOGRAM SOLAR ARRAY (CONTINUED)

The array was fabricated with partial solar cell coverage and the remaining area with dummy glass modules. Cell modules were procured from several suppliers to provide a representative sampling of interconnection approaches used by the industry. Suppliers included Heliotek (Spectrolab), Boeing, EOS, and Centralab (OCLI). Slip rings conducted power from the array to electrical interface connectors. The total weight of the array was 37.4 kg (82.5 lbs). A prototype model was fabricated and tested for performance and response to the environments of vibration, pyrotechnic shock and thermal vacuum. The prototype array demonstrated that a 23.2-square meter array could be made to exceed the baseline target of 66 Watts/kilogram. It provided valuable information on such items as cell module variations in weight and construction, rollup extension and retraction, dynamic response, damping characteristics, and thermal radiation effects. The RA250 Prototype Test Model is pictured in Figure 4-4.
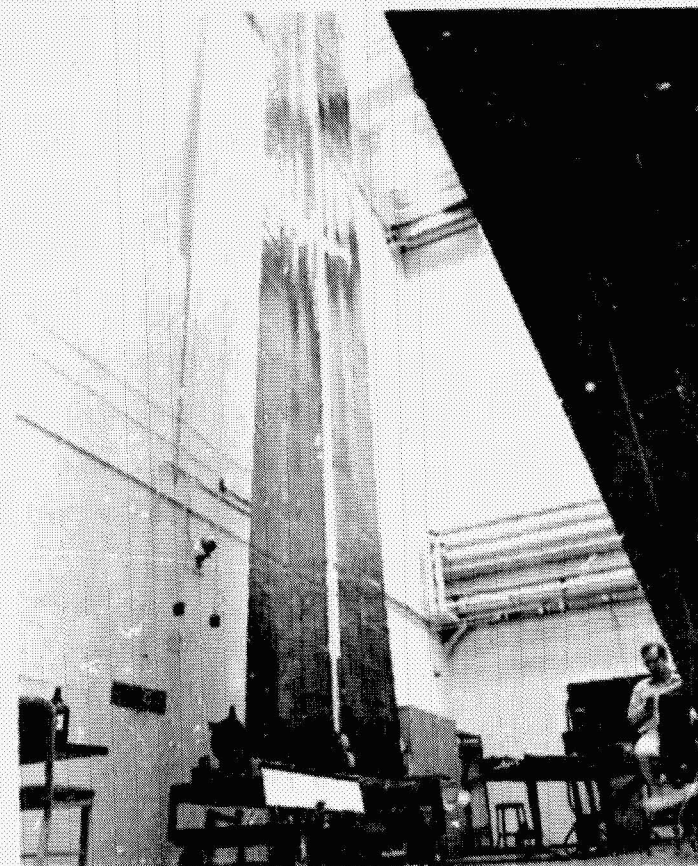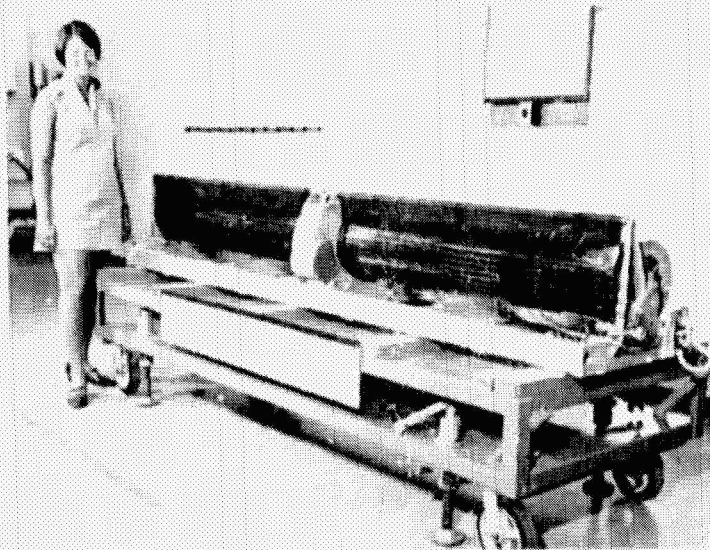
Figure 4-4. RA250 Prototype Test Model –
66 W/kg Solar Array

4.1.4 GE/JPL 66 WATTS/KILOGRAM SOLAR ARRAY (CONTINUED)

The mass summary (Table 4-6) for the RA250 Prototype represents the actual components and subassemblies used in the fabrication of this module. It may be noted that the mass of the two blankets that make up an array is not the same. This resulted because modules from the different sources noted above had slightly different masses.

Table 4-6. 66-Watt/kg Solar Array Actual Mass Summary (Prototype Model RA 250)

Nomenclature	Drawing No.	Unit Weight (kg)	Qty/ Next Assy	Total Weight (kg)
RA250 Prototype Assembly	47E214519G2	-	-	37.50
Center Support	47E218547	0.60	-	0.60
Leading Edge Member	-	0.38	1	0.38
Boom Actuator	-	5.33	1	5.33
LEM Support Brackets	-	0.05	2	0.10
Outboard End Support	-	0.93	2	1.86
Movable Portion	-	0.60	1	-
Fixed Portion	-	0.31	1	-
Bolt	-	0.02	1	-
Drum Assembly	47E218804-G3 & G4	4.00	2	8.00
Guide Flange	47D218535-G3 & G4	0.17	2	-
Drum Shell	47E218144G4	1.27	1	-
Outboard End Cap Assembly	47E218194G3	0.20	1	-
Inboard End Cap Assembly	47E218544-G1 & G2	2.18	1	-
Mounting Hardware (Drum-to-Center Support)	-	-	-	0.06
Prototype Array Blanket Assembly	47E218819G1	10.55	1	10.55
Prototype Array Blanket Assembly	47J218819G2	10.62	1	10.62

4.2 EXISTING COMPONENT TECHNOLOGY

4.2.1 SOLAR CELLS

The attainment of the specific power goal of 200W/kg is dependent in large part on the reduction of the total weight of the solar cells required to output 10.2 kW, BOL (assumes 2 percent electrical loss). Cell efficiency, cell thickness, and configuration will all impact the requirement for light weight. Solar cell efficiency for any given cell configuration is a function of cell temperature and solar flux (insolation) incident on the cell. The Solar flux spectral distribution is defined by ASTM Standard Specification E490-73a.

4.2.1.1 Cell Efficiency Vs. Cell Thickness

The impact of cell thickness on cell efficiency is indicated in Figure 4-5. The falloff in power output as the cell thickness decreases is associated with the low absorptivity of red and infrared photons in silicon. At the baseline thickness of 75 microns the cell power output has dropped to 89.5 percent, that of a 250 microns thick cell. Conversely, 11.7 percent more cell area is required with the 75 micron cell to provide the same power as the conventional 250 micron cell.
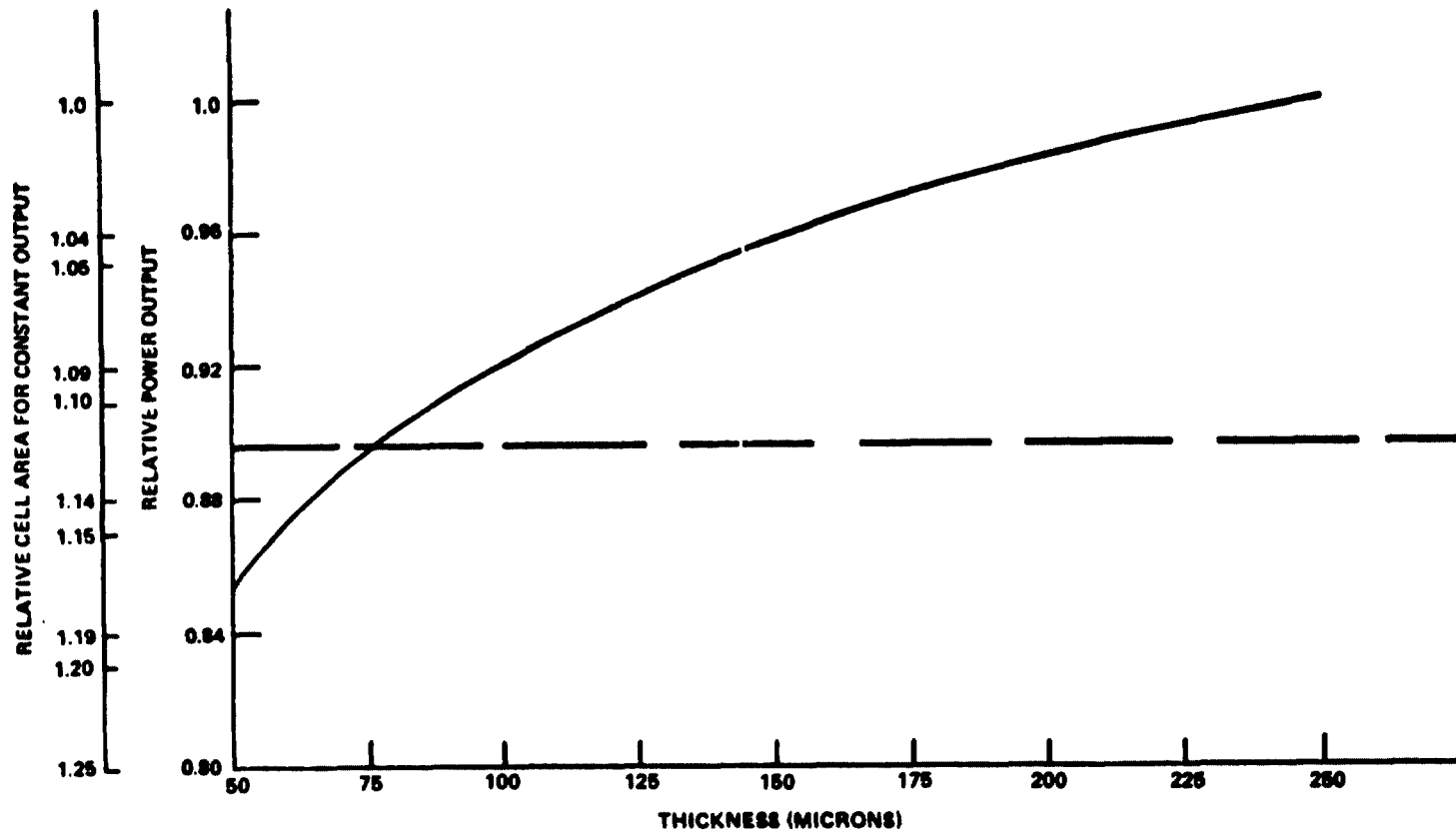
Figure 4-5. Cell Power vs Cell Thickness

4.2.1.2 Solar Cell Temperature Coefficients

Temperature coefficients for voltage and current of $-2mV/^{\circ}C$ and $30\ uA/cm^2 - ^{\circ}C$ respectively were provided by JPL for the 75 micron cell. A power coefficient was calculated to be $-264uW/^{\circ}C$ for a $2 \times 2\ cm^2$ cell. The normalized voltage and power coefficients became:

Voltage: $\quad \Delta V/V_{o} \quad = -0.4\%\Delta T$

Power: $\quad \Delta P/P \quad = -0.33\%\Delta T$

Temperature dependence of solar cell power is presented in Figure 4-6.
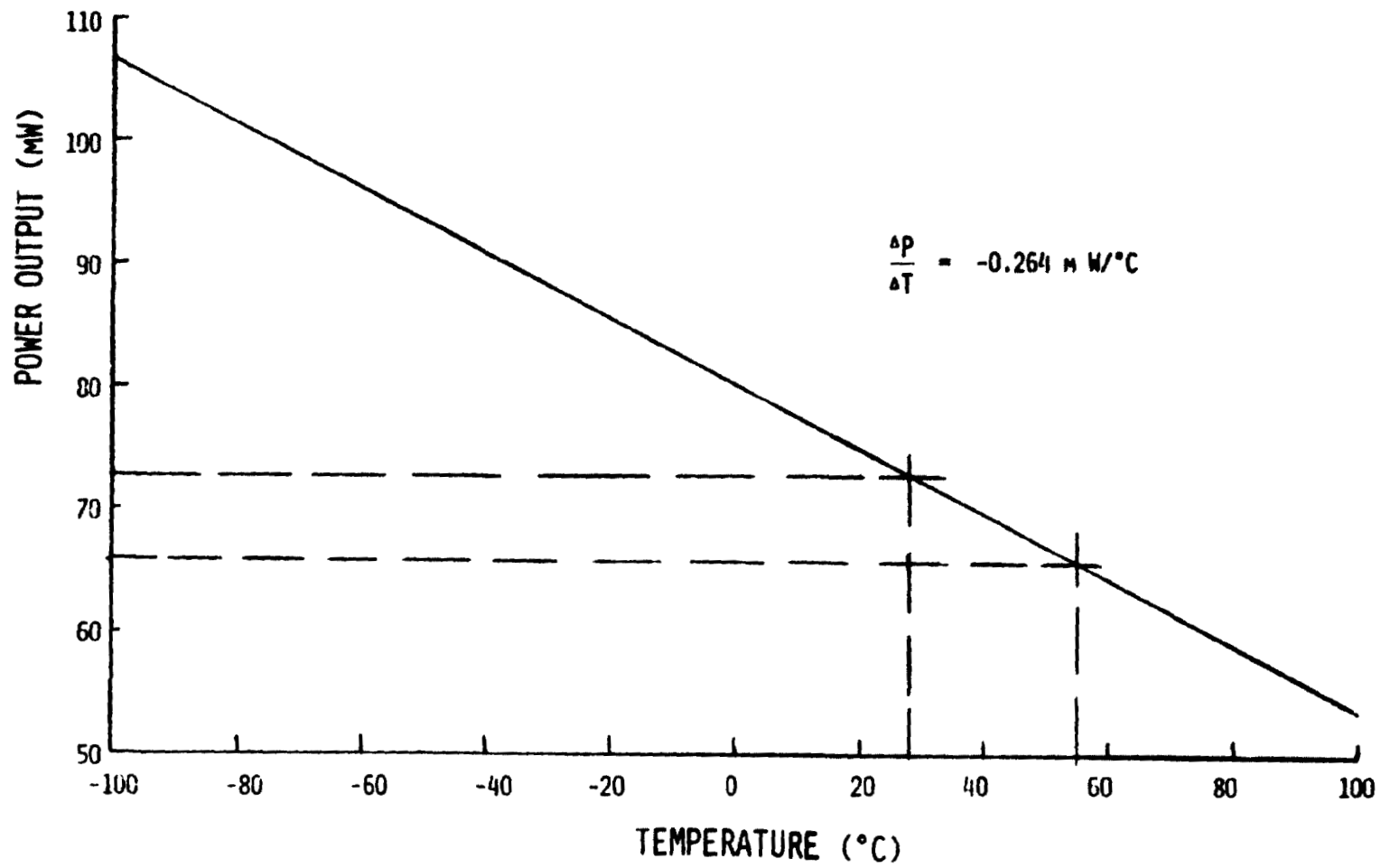
Figure 4-6. Temperature Dependence of Cell Power for
2 x 2 Cm^2 Cell, 3 Mil Thick

4.2.1.3 Solar Cell Maximum Power and Current

JPL furnished data on the electrical performance of an advanced state-of-the-art solar cell that was to be used in the present conceptual design study. This data is for a non-glassed cell, 250 microns thick, at 28°C. Additional data on cell power versus thickness and temperature coefficients for current and voltage made it possible to convert the 250 micron cell performance data to that assumed for the 75 micron baseline cell. The metallization is $A_g - T_i - P_d$ on both terminals. Wraparound contacts are not assumed.

E/I and power for the baseline cell is shown in Figure 4-7.
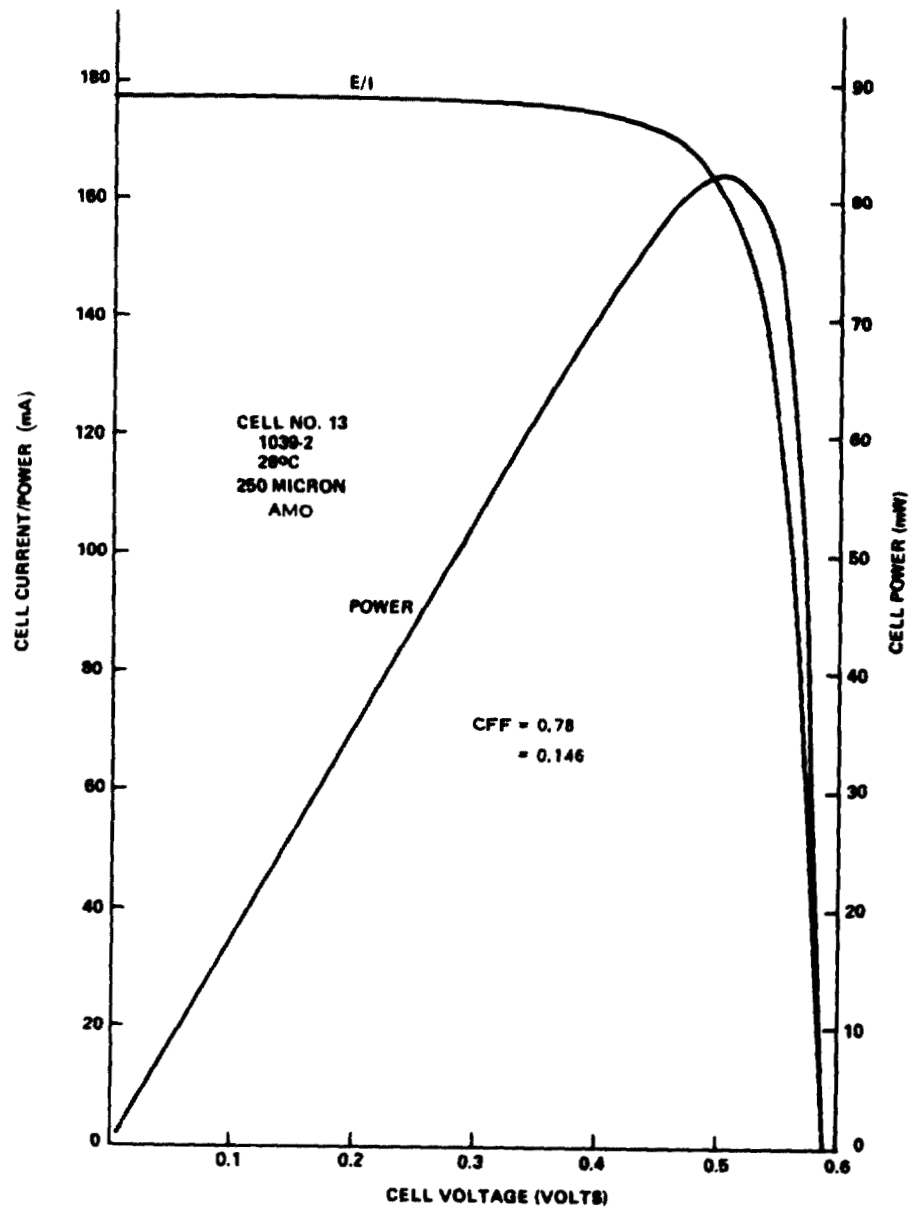
Figure 4-7. Baseline Cell E/I and Power

4.2.2 DEPLOYABLE BOOMS

Extensive surveys of deployable booms have been made in the past, particularly in connection with the Space Station Array Program. This study has utilized these findings. The deployable booms, which appear to be good candidates at present, are (1) the Astromast Coilable Lattice Boom, Figure 4-8, made by Astro Research Corporation, and (2) the BI-STEM (Storable Tubular Extendible Member) boom, Figure 4-9, also manufactured by Astro Research. The Coilable Lattice Boom has continuous longeron members running the entire length of the boom. When retracted, these longerons coil on top of each other as shown in Figure 4-8. When longeron stresses generated by the coiling of the boom are excessive, as in case of high temperature, segmented steel longeron members are utilized. These fold on retraction. In general, lattice structures have the advantage of a high strength to weight ratio in applications where a relatively high EI (modulus of elasticity) and low mass are needed. Their disadvantage is the large stowage volume and actuator weight required.
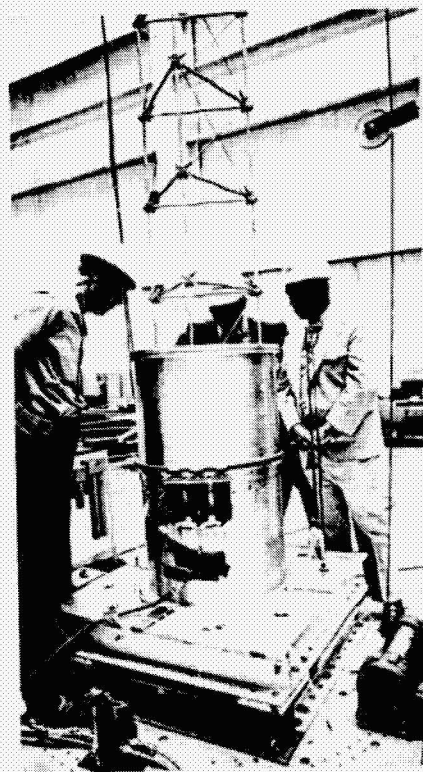
Astromast Deploying
Automatically
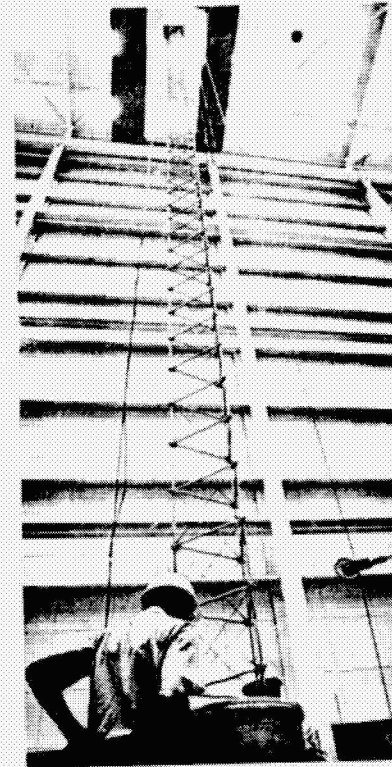
Fully Extended Mast
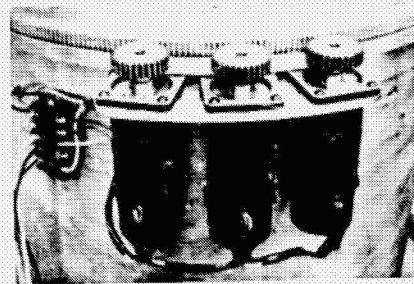
Deployment Motors
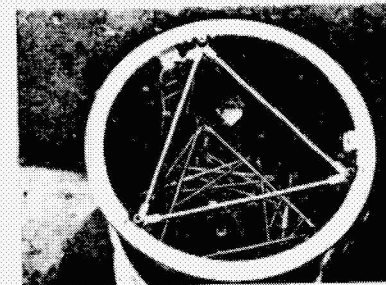
Retracted Configuration

Figure 4-8.   ASTROMAST Articulated Lattice Boom

4.2.2 DEPLOYABLE BOOMS (CONTINUED)

The widely used BI-STEM boom is essentially a ribbon of thin metallic material which assumes a tubular shape of high strength when unwound from a spool. Additional strength is obtained by using two tapes which wrap around each other as shown in Figure 4-9. The actuator has a motor driven spool and tubular guide mechanism. The unit shown in Figure 4-10 is the A-631 model containing a 3.4 cm diameter boom that was used in the GE/JPL 66W/Kg solar array. This device is compact and weighs less than 2.73 kg, less BI-STEM element.
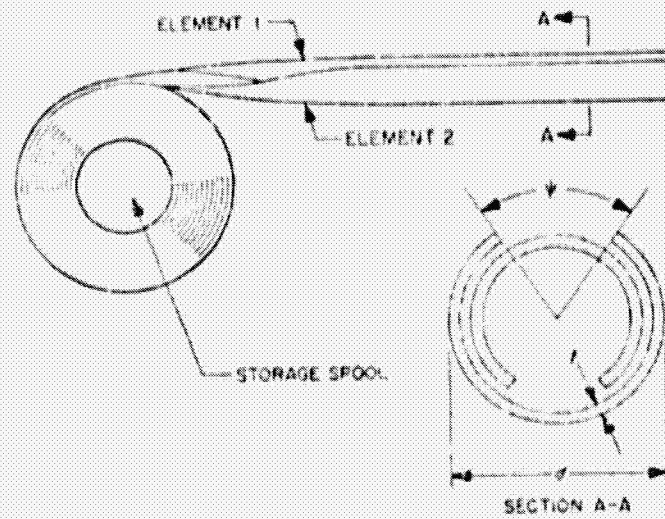
Figure 4-9.   The BI-STEM Principle
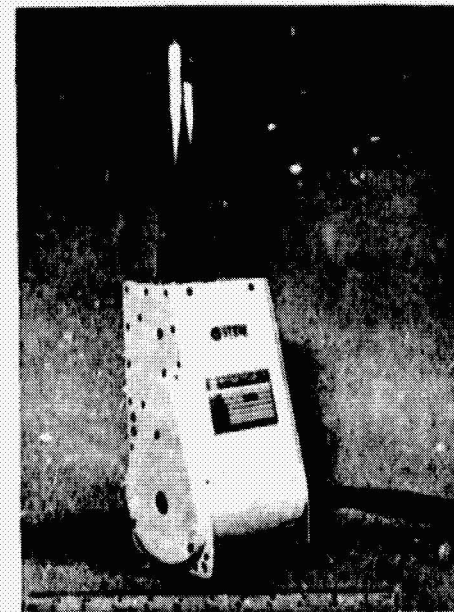
Figure 4-10.   BI-STEM Deployable
Boom and Actuator

4.3 ELECTRICAL DESIGN

4.3.1 ELEMENTS OF DESIGN OPTIMIZATION

The design philosophy adopted in this conceptual study to meet the design goal of 200W/kg, was to take the extreme position regarding weight in all elements of the design. This led, in some cases, to design margins that are subject to question and readjustment in a subsequent design iteration. The principal value of this approach is that each element of design may be minutely examined for characteristics that may lead to the desired ultra-lightweight design. The principal elements of design are shown in Figure 4-11, together with the options that exist with each element. It will be noticed that several elements normally associated with solar arrays are missing from this figure. Coverglass adhesives have been eliminated on the basis that either integral coverglass, heat-sealed sheet materials, or sprayable coatings will be used. Substrate adhesive is missing on the basis that a heat-sealed substrate will be used. Isolation diodes are not shown as an element in the array design since they are accounted for in the power conditioning circuitry, which by direction, is not part of the array mass summary. Also shown in this figure are the major design requirements and the characteristics of the baseline design that results when unique design elements are chosen. This selection process will be discussed in the succeeding paragraphs of this section.
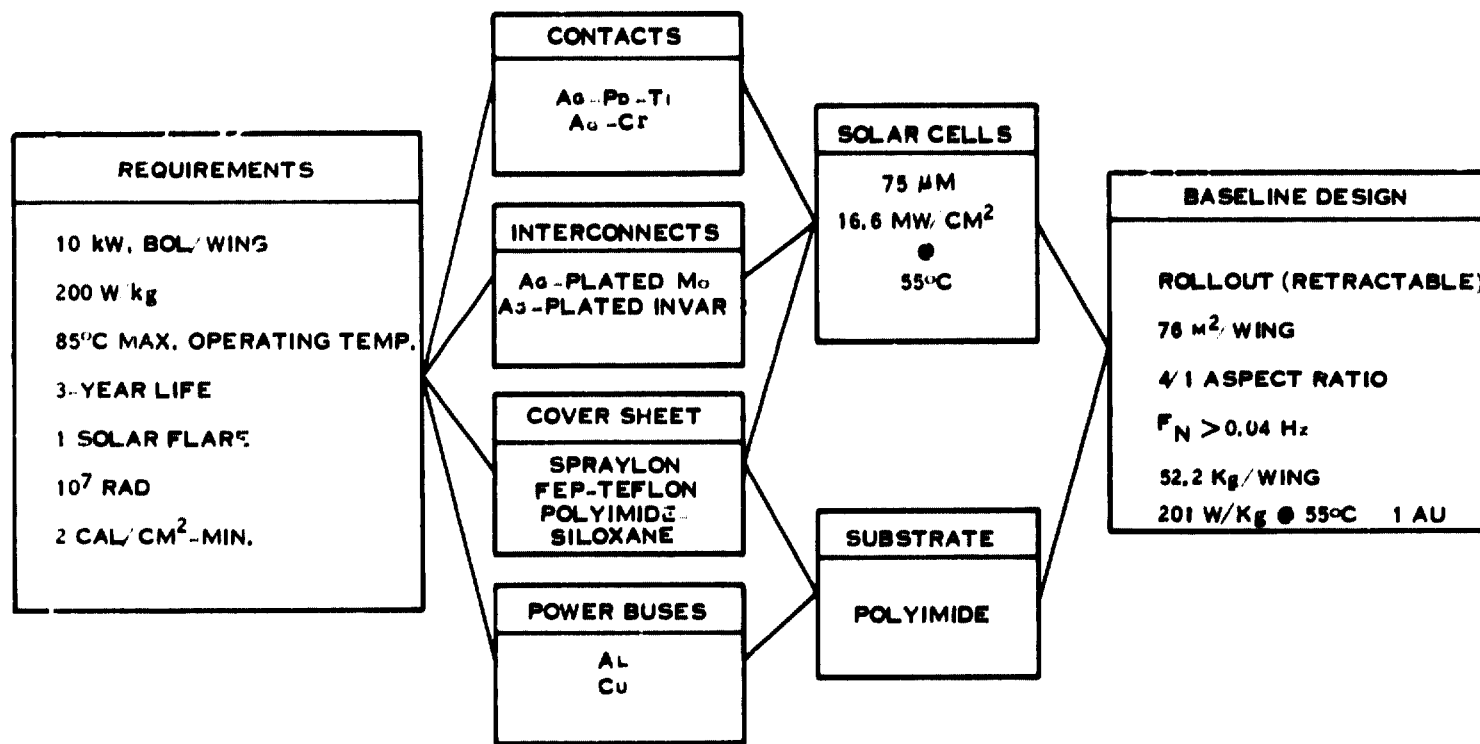
Figure 4-11. Elements of Design Optimization

4.3.1.1 Baseline Solar Cell Option

Of the many options that exist (Table 4-7) for the baseline cell and cover material, the thinnest cell (75 microns) and cover material (12.7 microns) were selected on the basis of minimum impact on the mass budget. The electrical performance cited for solar array designs resulting from this study is based on solar cell performance data enumerated in the Baseline Requirements document. The baseline cell thickness assumed for this study was 75 microns. Based on an earlier study, the baseline operating temperature was assumed to be 55°C. Using the given current/voltage characteristic for a 250 microns, 2×2 cm^2 cell (Figure 4-2), the change of output power with thickness (Figure 4-3), and the temperature coefficients for this cell (Table 4-1), the expected maximum power output for the baseline cell is calculated to be 66.3 mW at 1 AU and 55°C. The space radiation analyses reported upon later in this report shows that sufficient density thickness product is obtained for the interplanetary mission when 12.7 microns of FEP-Teflon is used. No additional cement is required, since FEP-Teflon may be heat sealed to the cell/interconnect/substrate materials. It is a moot question as to whether wrap-around contacts are feasible with a 75 microns thick cell.

Table 4-7. Solar Cell Options

Type	Pro	Con
• Conventional, 10 ohms-Cm (250 μm + 150 μm Fused Silica)	• Flight Qualified	• To Heavy (61 kg)
• Wraparound, rear contacts (125 μm + 30 μm 7070)	• Avoids Heat Damage to Junction • Flat Connectors Top Surface Clean	• 50% of Weight Budget • No Flight Experience
• Conventional or Wraparound, rear Contacts (75 μm + 13 μm FEP)	• FEP Cover Doubles as 1/2 Blanket • Cells Only 29% of Weight Budget	• No Experience With Cells of this Thickness

4.3.1.1 Solar Cell Options (Continued)

The tradeoff areas for solar cells are limited to cell thickness and configuration, cell cover material thickness and density and the optional use of coverglass cements as may be necessary if integral coverglass is not used. The lower bound for cell thickness was set at 75 microns in the Baseline Requirements document of this contract (see Appendix A). While no lower bound per se was set for the cell cover material, the radiation environment defined in this same document for the interplanetary mission does imply a minimum thickness sufficient to protect the cell from radiation damage. The impact of the solar cell/cover material mass contribution to the total mass budget of 50 kg may be judged by two examples. The 200 microns silicon solar cell and the 150 microns cemented coverglass chosen for SEPS (Paragraph 4.1.3) requires 1/2 the total mass budget in the SEPS 66W/kg design. In accompanying Figure 4-12, the affect of cover material thickness on specific power is illustrated. This plot is normalized to the "standard" 254 microns thick cell with a 152 microns thick fused silica coverglass. The 75 microns thick cell with a cover of 12.7 microns thick FEP-Teflon is 2.9 times as effective as the standard.
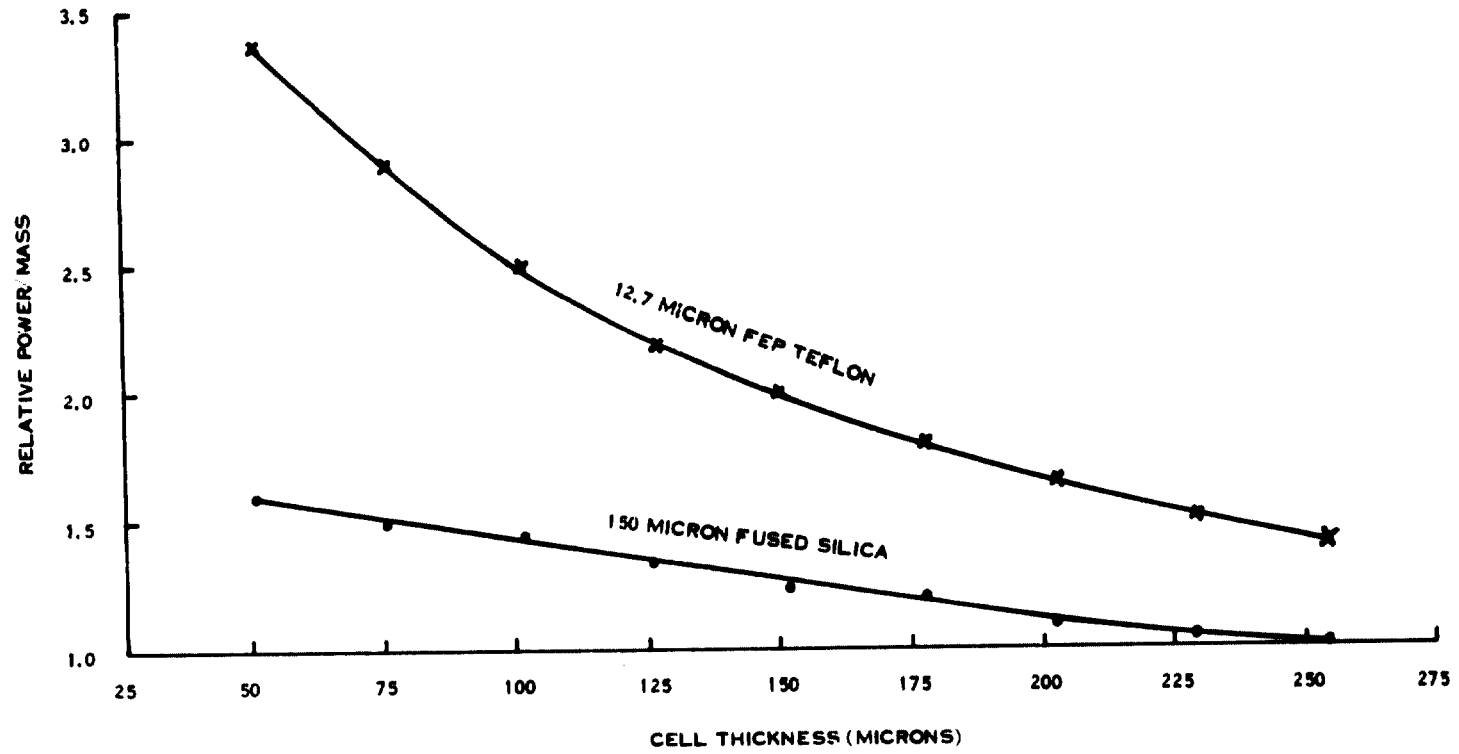
Figure 4-12. Relative Specific Power at the Cell Level vs Solar Cell Thickness

4.3.1.2 Cell Interconnects

The Baseline Requirements Document stipulates that the cell interconnect material option be limited to Beryllium-copper (Be-Cu), Kovar, molybdenum (Mo) and silver (Ag). A selection of characteristic properties for these materials, and several others, appear in Table 4-8. A limited amount of parametric analysis has been done regarding the design of the interconnect. One design criterion followed early in the program is that the relative power loss in the interconnect shall be in the same ratio as the mass of the connector to the total mass of the blanket assembly; i.e.,

$$\frac{\Delta P}{P} = \frac{W_{cn}}{W_{tot}}$$

This proved to be an impractical arrangement. For any nominal value of power loss; i.e., 2%, the corresponding interconnect mass was judged to be too high. The interconnect was designed on the basis of its physical relationship to the cell and the encapsulants, rather than a power loss criterion. There are no out-of-plane service loops, for instance, that might lead to stress risers in the encapsulant.

Table 4-8. Candidate Materials - Interconnects and Buses

Material	Density x Resistivity $\frac{G - Ohm}{cm^2}$ (10^{-6})	Thermal Coeff. $10^{-6}/{}^{\circ}C$	Thermal Cond. $W/cm-{}^{\circ}K$	Specific Stiffness E/D 10^6 in.
Aluminum	7.1	23	2.2	102
Copper	15	16	3.9	49
Molybdenum	49	5	1.5	128
Silver	17	19	4.1	29
Silicon	NA	2.8 to 7.3	0.84	115

Conclusions: Aluminum for power buses
Molybdenum for cell interconnects

4.3.1.2 Cell Interconnects (Continued)

Three principal concerns impact the selection of an interconnect material and design layout; viz, thermally induced stress, strength to weight ratio, electrical and thermal conductivity. A comparison of these properties relative to silver will point up some significant differences (Table 4-9). Molybdenum is judged to be the best among these materials, especially when the thermal coefficient of expansion of molybdenum is compared to silicon (see Table 4-8). The large specific stiffness of this material suggests that a molybdenum interconnect could be thought of as a structural element of the array design, as well as an electrical conductor. A thin (2.5 microns) plating of silver on the molybdenum is desired to minimize the voltage drop across the connector.

Table 4-9. A Comparison of Materials for Cell Interconnections

Material Comparison	Material Properties						E/D	Comments
	Density (D) Ratio	Resistivity (ρ) Ratio	D-ρ	Thermal Coefficient of Expansion (α) Ratio	Thermal Conductivity (K) Ratio	Youngs Mod (E) Ratio		
$\dfrac{Be-Cu}{Ag}$	0.79	4.17	3.3	0.89	0.27	1.54	1.96	Density favorable 3rd choice
$\dfrac{Kovar}{Ag}$	0.80	30.3	24.0	0.31	0.03	1.73	2.17	Density favorable α is favorable - 2nd choice
$\dfrac{Mo}{Ag}$	0.97	2.94	2.8	0.26	0.36	4.27	4.4	Best choice on 6/7 counts - 1st choice

4.3.1.2 Cell Interconnects (Continued)

A sketch of the baseline interconnect is shown in Figure 4-13. This layout has been drawn for the case of a conventional contact. Multiple weld tabs are shown. The conductor width (W) was examined on the basis of a 2% power loss criterian, on the one hand, and practical minimum width on the other. Because of the redundancy in electrical paths, it turns out that the latter criterian dominates; i.e., for any practical minimum width, the power loss is much less than 2%. A conductor width of 0.3 mm was chosen. The surface area of 0.033 cm^2 and thickness of 25 microns for Mo and 2.5 microns of Ag (each side) together with associated densities gives a connector unit mass of 10.8 mg/cell.

For an array of 160,000 cells, a total interconnector mass of 1730 grams results.

W
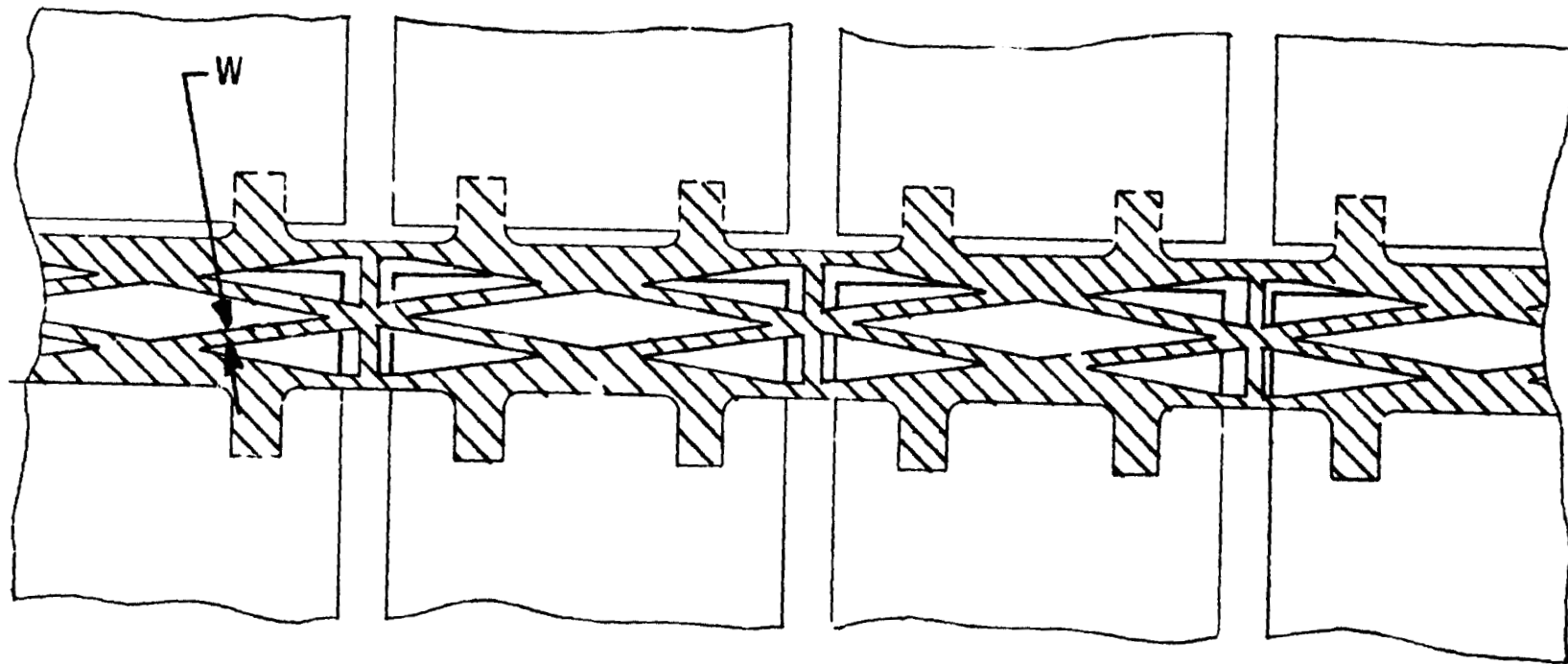
1 MIL INVAR
0.5 MIL AG
BOTH SIDES

Figure 4-13. Baseline Cell Interconnections

4.3.1.2 Cell Interconnect - Alternate Design (Continued)

A flexible interconnect design, with in plane service loops, is offered as an alternative design. Thermal stress relief is provided by the serpentine design of the conductor. Because of the additional conductor length the conductor width has been increased to 0.6 mm. The mass for this design is estimated to be 32 mg/cell.
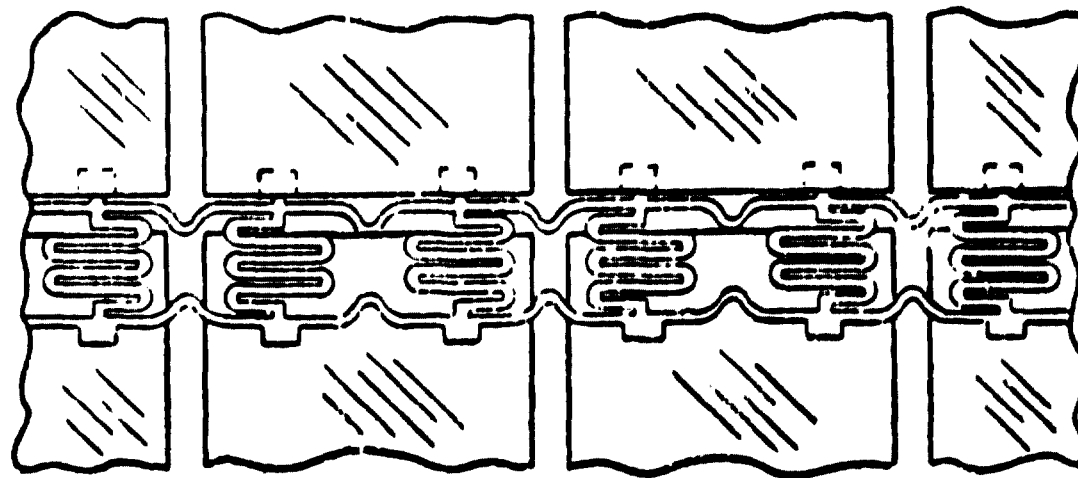
1 MIL INVAR
0.5 MIL Ag
BOTH SIDES

Figure 4-14.   Flexible Interconnect Design

4.3.1.3 Power Buses

The Baseline Requirement stipulates that diode isolation for the array shall be provided off the blanket in the power conditioning circuitry. For this reason, both electrical terminals from each module will be brought out to the spacecraft interface. The Baseline Requirement also requires that module layout and interconnection result in a minimum magnetic field. This condition is obtained when successive modules alternate in polarity position, as indicated in Figure 4-15. This conceptual layout results in both polarities at both sides of the blanket. While one of the polarities could be served by a common line and thus eliminating 41 individual lines on each side of the blanket, the total mass of conductive runs would not change. The most flexibility is obtained by bringing all module terminals out to the inboard end of the blanket. At this point the 80 individual lines may be switched into any desired series - parallel hookup, as desired.

Using the same criterian that was applied to the interconnects; viz, the relative power loss in the buses should be comparable to the relative mass of the buses, the point of equality for aluminum buses results in a larger cross-sectional area than is desirable from a minimum weight point of view. A more appropriate design guide, it would appear, is to design for an equal and maximum power loss in each of the module buses. Accordingly, a design goal of 1 percent was established for all the power loss in the buses. If the bus thickness is kept constant, the width of the buses serving modules successively more remote from the terminus at the spacecraft must increase so that the bus length-to-width is in the same ratio.

PACKING FACTOR = 0.8   2 X 2 CM^2 CELLS
MODULE OUTPUT @ 55°C, 1 AU & 8-1.4° SUN ANGLE: 133 W @ 223 V
TOTAL POWER FOR 80 MODULE: 10.5 KW

25 CIRCUITS/MODULE
500 CELLS IN SERIES X 4 IN PARALLEL, 2000 TOTAL

1 CIRCUIT, 20S X 4P
(2.03 CM X 2.03 CM CELL)

2.21 M

2.03 M

40.6 CM

17.2 M

17.6 M

(40 CONDUCTORS, EACH SIDE)
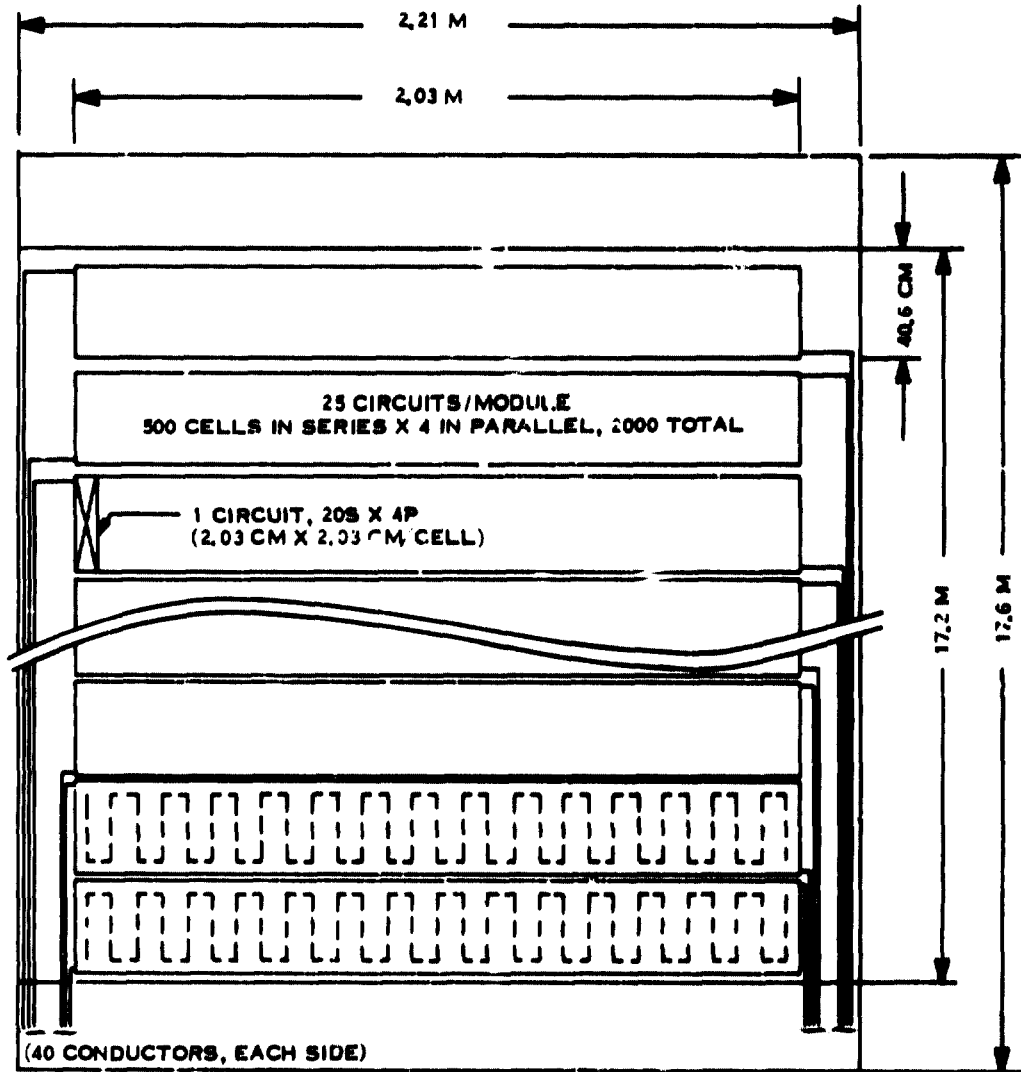
Figure 4-15. Conceptual Design - 40 Module Half Blanket

4.3.1.4 Substrate and Coversheet Materials

The basis for the rollout and foldout arrays described in this report lies with the concept of a flexible blanket whereby the solar cells, interconnects and power buses are encapsulated in contiguous films of polymer plastics. Kapton has no competition as the selected material for the substrate, or bottomsheet, of this blanket. Kapton has excellent strength-to-weight (specific stiffness), low density, good creep resistance and a wide usable temperature range. Kapton-F, being a laminate of Kapton-H and FEP-Teflon, is specified in the baseline design because it is heat-sealable to the p-contact of the cells and interconnects.

The choice of a coversheet material is more difficult. In addition to those properties demanded of the bottomsheet, the topsheet must have excellent optical transmittance. This stipulation eliminates Kapton, where the transmittance is 66%.

Polymer coversheet properties are given in Table 4-10.

Table 4-10. Required Properties for Polymer Coversheet Materials

- HIGH OPTICAL TRANSMITTANCE
- LOW THERMAL EXPANSION
- LOW CURE (OR PROCESSING) TEMPERATURE
- HIGH TENSILE STRENGTH AT ALL TEMPERATURES
- GOOD CREEP RESISTANCE
- HIGH RESISTANCE TO RADIATION EMBRITTLEMENT AT 10^7 RADS DOSAGE
- EASE OF APPLICATION; I. E., BY HEAT SEALING OR SPRAYING
- APPLICABLE IN THIN FILMS 1-2 MIL THICK

4.3.1.4 <u>Substrate and Coversheet Materials</u> (Continued)

One of the guidelines adopted early in the study was that separate cements were to be avoided, if at all possible. The concept of heat-sealable thermoplastics was adopted as the preferred means of sealing cover materials and substrate materials to the cell/interconnect assembly. A limited materials search identified several coversheet candidates (Table 4-11). Each had some shortcomings; such as transmittance in the case of polyimide, radiation resistance with FEP-Teflon, and limited temperature range for Tedlar and Kynar.

Table 4-11. Material Properties Coversheet Candidates

Characteristics	Kapton-H [1] Polyimide	Teflon FEP	Tedlar [2] PVF	Kynar [2,3] PVF_2
Optical Transmittance, BOL (25 Microns)	0.66	0.96	0.90	0.9
Heat Sealable	No	Yes	Yes	Yes
Coefficient of Thermal Expansion (^{o}C)	$2 (10^{-5})$	8.3 to $32 \cdot 10^{-5}$	$1.6 (10^{-5})$	$1.5 (10^{-5})$
Specific Gravity	1.42	2.15	1.48	1.78
Creep Resistance	Good	Poor	Good	Good
Usable Temperature Limit (^{o}C)	-269 to 400	-240 to 200	<-70 to 110	<-62 to 315
Processing Temperature (^{o}C)	NA	280	204	150
Radiation Tolerance (mrad)	1000	2	32	100

1) Final report, Solar Array Technology Evaluation, LMSC No. D384250, 1 September 1974

2) Encyclopedia of Polymer Science and Technology, Volume 14

3) R. Timmerman, Journal of Applied Polymer Science, Volume VI, No. 22, Page 456

4.3.1.4 Substrate and Coversheet Materials (Continued)

Based on its excellent optical properties, heat-sealability, wide temperature range and a large body (4.1, 4.2, 4.3, 4.4 and 4.5) of prior experience, FEP-Teflon was selected in the Mid-Term Report (17 June 1976) as the baseline coversheet.

Subsequent to the selection of FEB-Teflon as the coversheet and bottomsheet adhesive, a report was issued (4.6) that negated the earlier evidence that this material could perform adequately in a space thermal and ionizing particle environment. A limited search was made to uncover data that would point to a radiation resistant material. From the evidence uncovered (4.7, 4.8, 4.9) it would appear that the most radiation resistant polymers are those which incorporate the benzine aromatic ring in their structure. Highly oxidized or halogenated polymers are to be avoided. Based on this, several potential alternatives to FEP-Teflon have been identified. Tedlar (PVF) and Kynar (PVF$_2$) shown in Table 4-11 are both commercially available. Their lower coefficient of thermal expansion and high radiation tolerance are major points of interest.

A developmental material, polyimide-siloxane, now being used on an experimental basis at GE to encapsulate solid state devices, is compared to polyimide and silicone in Table 4-12. This new material, a copolymer of polyimide and silicone, is not fully characterized at this juncture. Its range of properties may be inferred from those of polyimide and silicone, however. Particularly noteworthy is the tolerance to ionizing radiation to be expected from this copolymer. An experimental program for material screening and characterizing is needed to allow a selection of a suitable coversheet material.

Table 4-12. Polyimide-Siloxane Copolymer Comparison

Properties	Polyimide (Kapton-H)	Polyimide Siloxane	Methyl-Phenyl RTV-655 Silicone
Optical Transmittance (25 microns)	0.66	0.95	0.90
Coefficient of Thermal Expansion ($10^{-5}/^{\circ}$C)	2	4 to 10 [1]	12
Cure Temperature ($^{\circ}$C)	NA	125	20
Tensile Strength at -190°C	35,000	NA	850-1000
-200°C	17,000	NA	NA
Creep Resistance	Good	NA	NA
Radiation Tolerance (1 Mrad)	1000	NA	100
Method of Application	Sheet	Solution	Solution
Usable Temperature Range ($^{\circ}$C)	-269 to 400	NA	<-73 to 140

1) Depends on percent of each component used.

4.3.2 THERMAL ANALYSIS

The equilibrium temperature of the blanket is of concern, because of the adverse power coefficient with temperature (-0.33%/degree Celsius). The radiosity of the two sides of the blanket and the electrical power outputted from the blanket promote cooling of the blanket, while the heat absorbed from solar insolation causes the temperature to rise. At equilibrium:

$$SA \cos \theta = \rho \, SA \cos \theta + (\epsilon_F + \epsilon_R) \, \sigma \, AT^4 + NPc$$

where the in ant solar power is on the left side of the equation. The first term on the right is the reflected component, the second term is the quantity radiated and the last term is the electrical power generated. Here A is the total blanket area, S is the solar constant, θ is the solar angle (angle of incidence), ρ is the reflectivity and the complement of absorbtivity (α), $(\epsilon_F + \epsilon_R)$ the emissivities of the front and rear surfaces respectively, σ is the Stefan-Boltzmann constant, N is the number of solar cells and P_c is the maximum power per cell. Let $f = NA_c/A$, where A_c is the area per cell. By definition, the electrical efficiency is

$$\chi = \frac{P_c}{A_c S \cos \theta}$$

Substituting and solving for the equilibrium temperature

$$T = \left[\frac{(\alpha - \chi f) \, S \cos \theta}{(\epsilon_F - \epsilon_R) \, \sigma} \right]^{1/4}$$

This function is plotted in Figure 4-16 in parametric form for the case where f = 0.95, χ = 0.12 @ 55°C, α = 0.84 and θ = zero degrees.
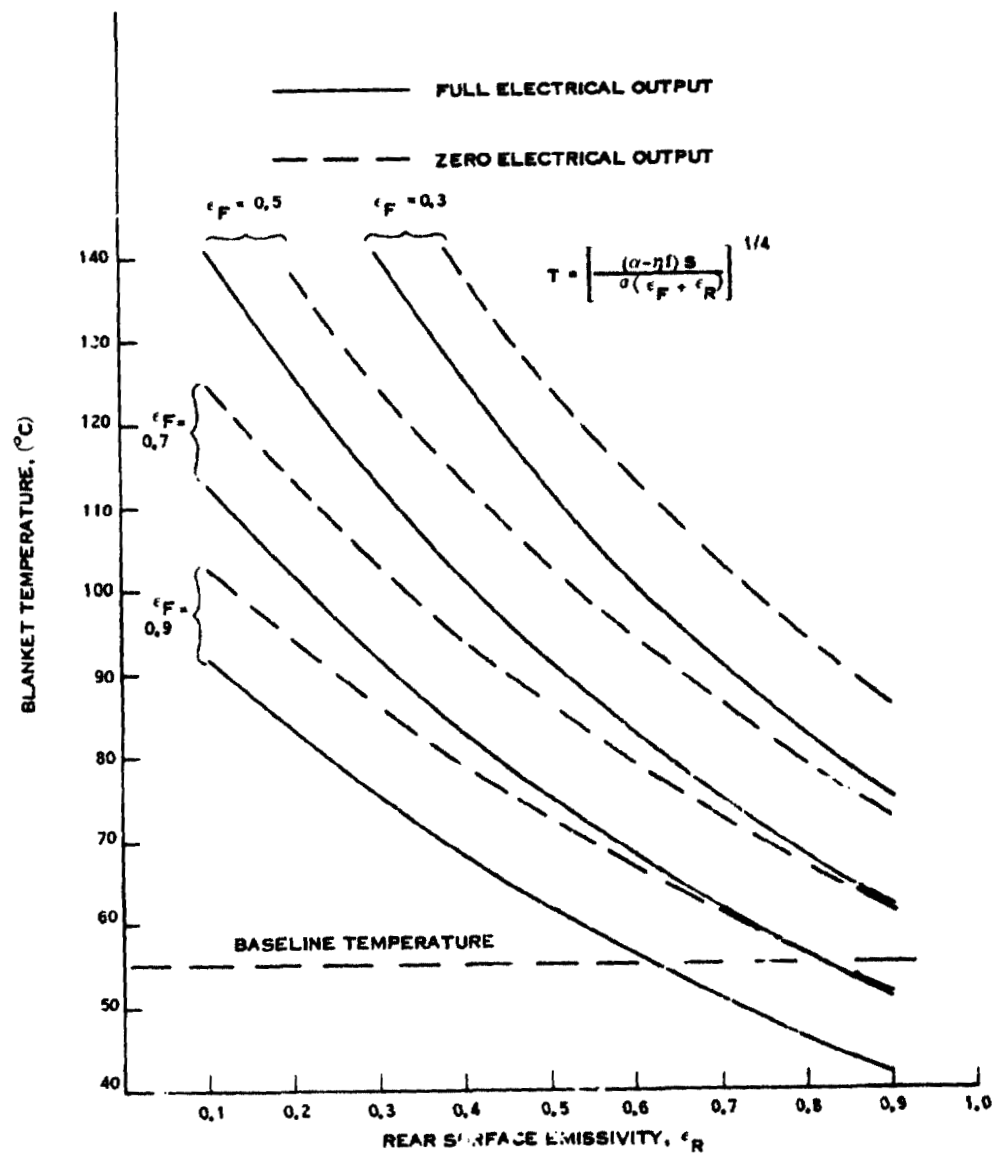
Figure 4-16. Blanket Temperature at 1 AU Insolation Normal Incidence

The chart includes the following labels:

- FULL ELECTRICAL OUTPUT
- ZERO ELECTRICAL OUTPUT
- $\epsilon_F = 0.5$
- $\epsilon_F = 0.3$
- $\epsilon_F = 0.7$
- $\epsilon_F = 0.9$
- BASELINE TEMPERATURE

$$T = \left[\frac{(\alpha - \eta f)\, S}{\sigma(\epsilon_F + \epsilon_R)} \right]^{1/4}$$

Y-axis: BLANKET TEMPERATURE, (°C)

X-axis: REAR SURFACE EMISSIVITY, ϵ_R

4.3.2 THERMAL ANALYSIS (Continued)

A summary of measurements of front and rear surface emissivity and the calculated cell equilibrium temperature for several different rear surface materials combinations is shown in Table 4-13. Materials were heat and pressure bonded to silver-backed solar cells.

The front surface emissivity of 0.730 shown for 12.7 microns FEP-Teflon will satisfy requirements for the front surface.

A 25 microns FEP/50 microns Kapton composite film heat-sealed to the rear cell surface will adequately satisfy the thermal rejection criteria mentioned above.

Table 4-13. Summary of Emissivities for Various Samples of FEP-Teflon and
Kapton Bonded to Silver-Backed Solar Cells

Sample	Solar Cell Surface	E 37.78°C	100°C	Cell Temperature with 12.7 Microns Front Cover of FEP and Back as Indicated by Sample Line (°C)
12.7 microns FEP	Front	0.730	0.721	
12.7 microns FEP	Back	0.491	0.467	72.5
25 microns FEP/ 50 microns Kapton	Back	0.843	N/A*	51.3
25 microns FEP/ 50 microns Kapton	Back	0.851	N/A*	50.9
25 microns FEP/ 50 microns Kapton	Back	0.851	N/A*	50.9
·) microns FEP	Back	0.645	N/A*	62.4

*Not Applicable

e-2

4.3.3 IONIZING RADIATION ANALYSIS

4.3.3.1 Radiation Models

Solar wind, solar flare protons, trapped electrons and protons, and alpha particles are components of the space radiation environment that are capable of introducing lattice damage in the solar cell material and resultant degradation of solar cell output parameters. The low energy component (0-10 keV) of the proton spectrum is probably the least well characterized region and represents the energetic proton contribution of the Solar Wind. This region of the solar proton spectrum may be an important contributor to total solar array degradation in array designs which utilize thin (0 to 75 microns) shielding material. Its impact on solar array end-of-life output power is not weighed in this analysis due to the lack of relative damage coefficient data in this low energy region. Immediate en᷈ g᷈ ᷈ ᷈᷈ons with energies between   100 keV and 1. 0 MeV and solar flare protons with energies between 1. 0 and 200 Mt᷈᷈ ᷈᷈᷈ ᷈ considered the primary causitive factors of proton induced array power loss.

Alpha particle contributions to array degradation are not included in any of the calculations.

The following models, based on NASA reports (4. 10, 4. 11, 4. 12) are presented here for three mission types:

1.   Interplanetary - One and seven flare ambient

2.   Geosyndronous Earth Orbit Three Year Mission - Trapped particle and one solar flare ambient

3.   Low Earth Orbit (278 km, 60 degrees) - Three year trapped particle ambient

The flare model shown in Figure 4-17* represents the solar flare contenet of the worst known period (cycle 19) and as such is a conservative model.

*Energy Spectra given in JPL Spec ES506080B

4-58
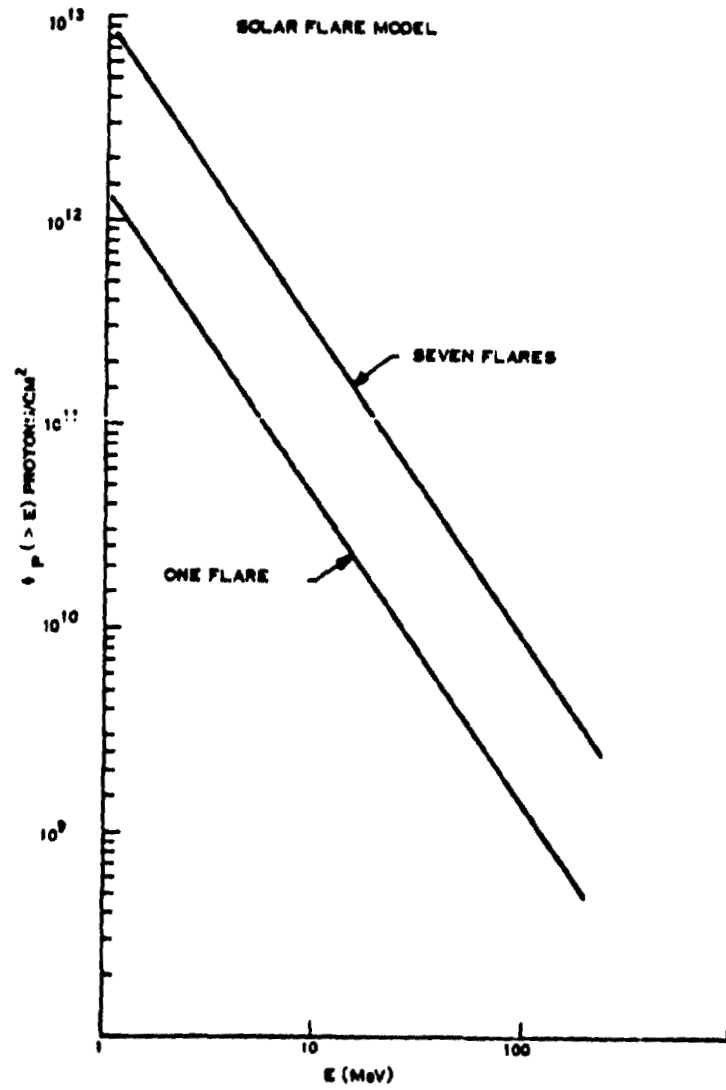
Figure 4-17. Interplanetary Solar Flare Model

4.3.3.1 <u>Radiation Models</u> (Continued)

A 3-year fluence for trapped electrons and protons at synchronous orbit is based on Vette's AE4 model.

See Figure 4-18.

PROTONS
0.01 ≤ E ≤ 1.0 MeV
$\phi(>E) = 2.9 \times 10^7$ EXP $(-9.0E)$ $\dfrac{P}{CM^2 \cdot SEC}$

ELECTRONS
E ≤ 0.3 MeV
$\phi_e(>E) = 5.0 \times 10^7$ EXP $(-6.91\ E)$
e/CM^2-SEC
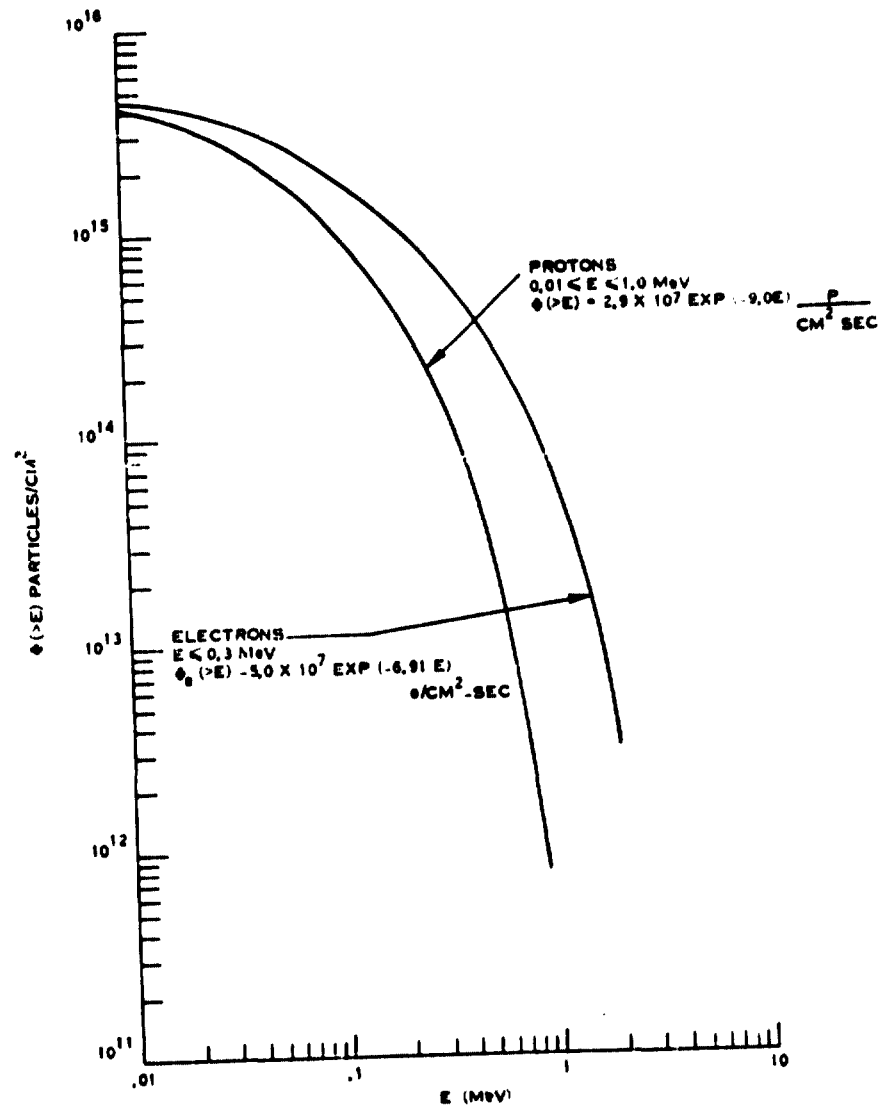
Figure 4-18. 3-Year Fluence Trapped Protons and Electrons for Synchronous
Orbit Based on Vette's AE4 Model

4.3.3.1 <u>Radiation Models</u> (Continued)

The trapped electron and proton environment at 258 km attitude is based on Vette's AE2 and AP6 models. While the AE2 model has been superceded by Vette's AE6 model, this model is not available in the format necessary for our analysis. See Figure 4-19.
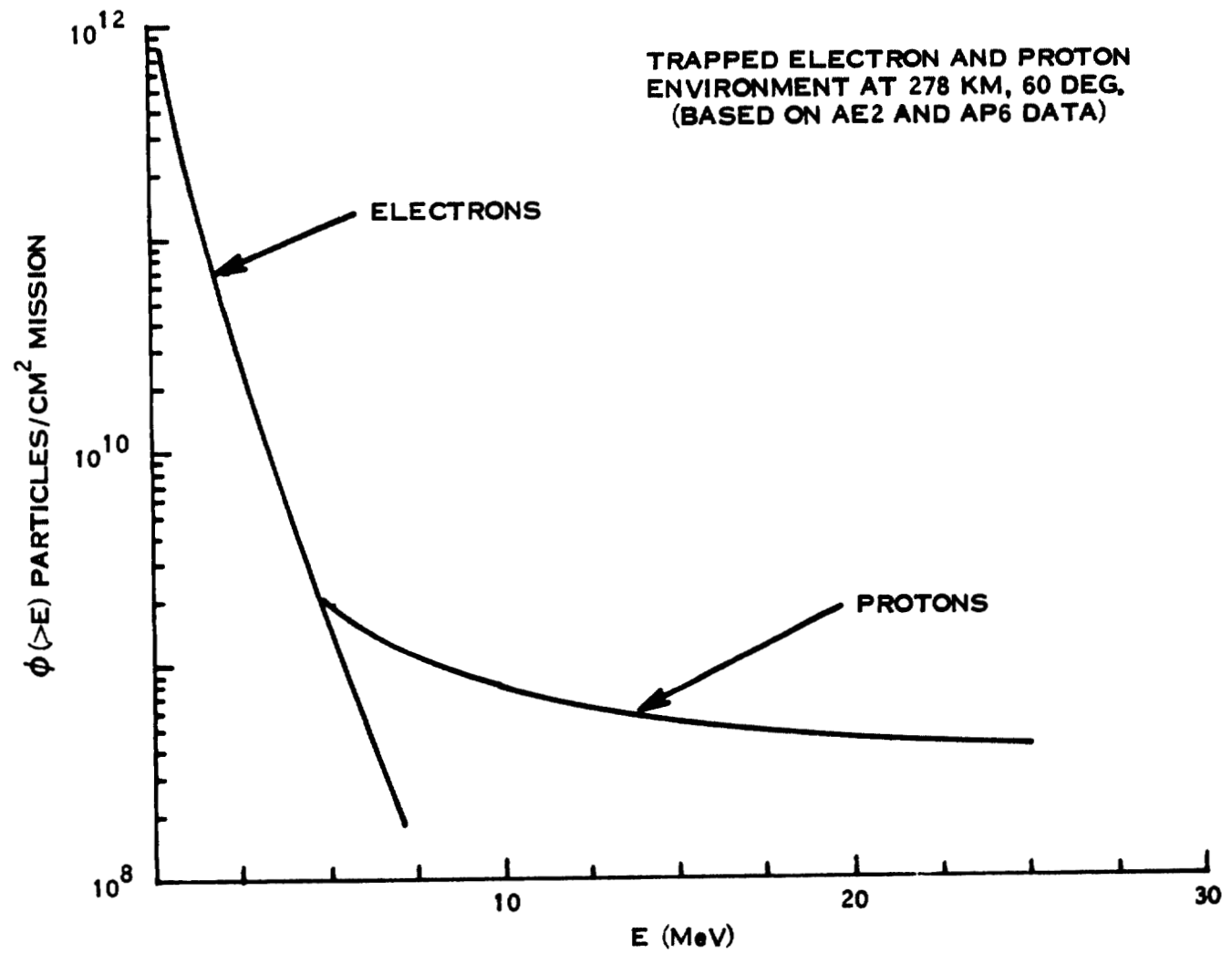
Figure 4-19. Low Earth Orbit Fluence

4.3.3.2 Particle Radiation Analysis

End of life (EOL) power was calculated for the 3-year interplanetary mission, a 3-year geosynchronous earth orbit (GEO) and a low earth orbit case, also 3 years in length. In both cases the array was assumed to be exposed to one solar flare as defined in Table 4-14,

Table 4-14. Single Solar Flare Fluency

Proton Energy, E (MeV)	Total Fluence, ϕ Where $\phi > E$ (p/cm^2)
1	$2 (10^2)$
10	$4 (10^{10})$
30	$9 (10^9)$
100	$1 (10^9)$

The physical model of the solar array blanket used in this analysis shows a 75 μm cell with silver contacts heat sealed to a Kapton-F substrate and overcoated with heat sealed FEP-Teflon. The quantities referenced to the left of Figure 4-20 are the density thickness products for those materials.

0.00273 G/CM^2 → FEP TEFLON OR EQUIVALENT

SOLAR CELL

0.00525 G/CM^2 → SILVER
0.00273 G/CM^2 → FEP TEFLON
0.0036 G/CM^2 → KAPTON

FRONT
$0.0027 \dfrac{GM}{CM^2}$

BACK
0.0053 GM/CM^2
0.0027
0.0036
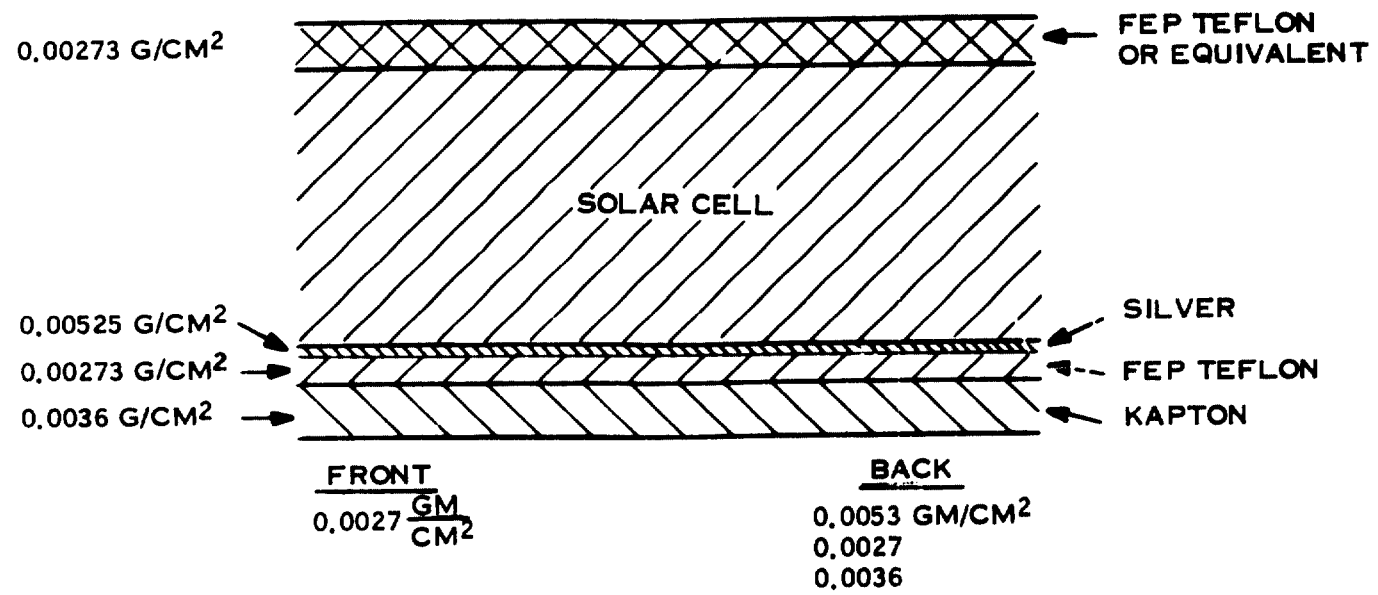
Figure 4-39. Solar Array Blanket Radiation Model

4.3.3.2 Particle Radiation Analyses (Continued)

The analytical procedure for the earth orbit case is shown in Figure 4-21. Each contributor to particle fluence is converted to the Damage Equivalent Normally Incident (DENI) 1 Mev electron fluence using the above physical model and relative damage coefficients derived from data published in the TRW Solar Cell Radiation Handbook (4.13). The DENI from all three classes of radiation particles are summed together for the earth orbital case. Only solar flare protons are of consequence in the case of interplanetary missions.

TRAPPED

VIA TRW → DENI · 1 MeV ELECTRON FLUENCE

TRAPPED

VIA TRW → DENI · 1 MeV ELECTRON FLUENCE

SOLAR FLARE

VIA TRW → DENI · 1 MeV ELECTRON FLUENCE

SUM OF DENI 1 MeV ELECTRON CONTRIBUTIONS FROM THREE SOURCES

• ALL PARTICLE FLUXES ARE ISOTROPIC
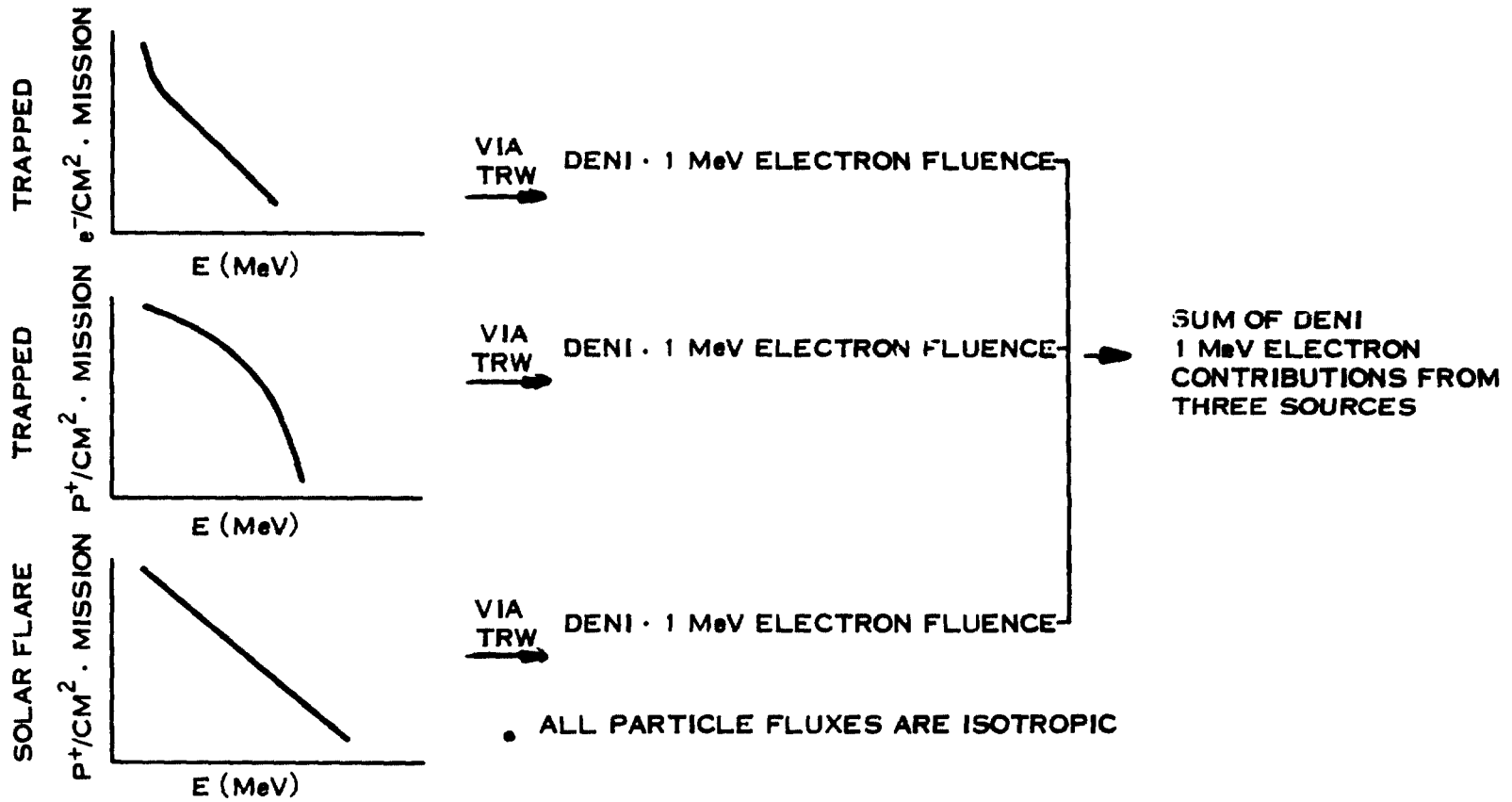
Figure 4-21. DENI 1 · MeV Electron Calculation Procedure

4.3.3.2 Particle Radiation Analysis (Continued)

Environmental radiation models that contribute to array degradation are converted to their total fluence in damage equivalent 1 MeV electrons. The conversion, performed by computer calculation, is based on the TRW algorithm (4.13) and yields the damage equivalent normally incident (DENI) 1 MeV electron fluence as a function of shield density-thickness product. Such relationships are graphically illustrated in Figures 4-22 thru 4-24.

DENI 1 MeV electron fluence contributions from the various radiation sources are summed. Linear interpolation is now employed to find the DENI 1 MeV electron fluence for front end and rear surface radiation shielding structures shown in Figure 4-20.
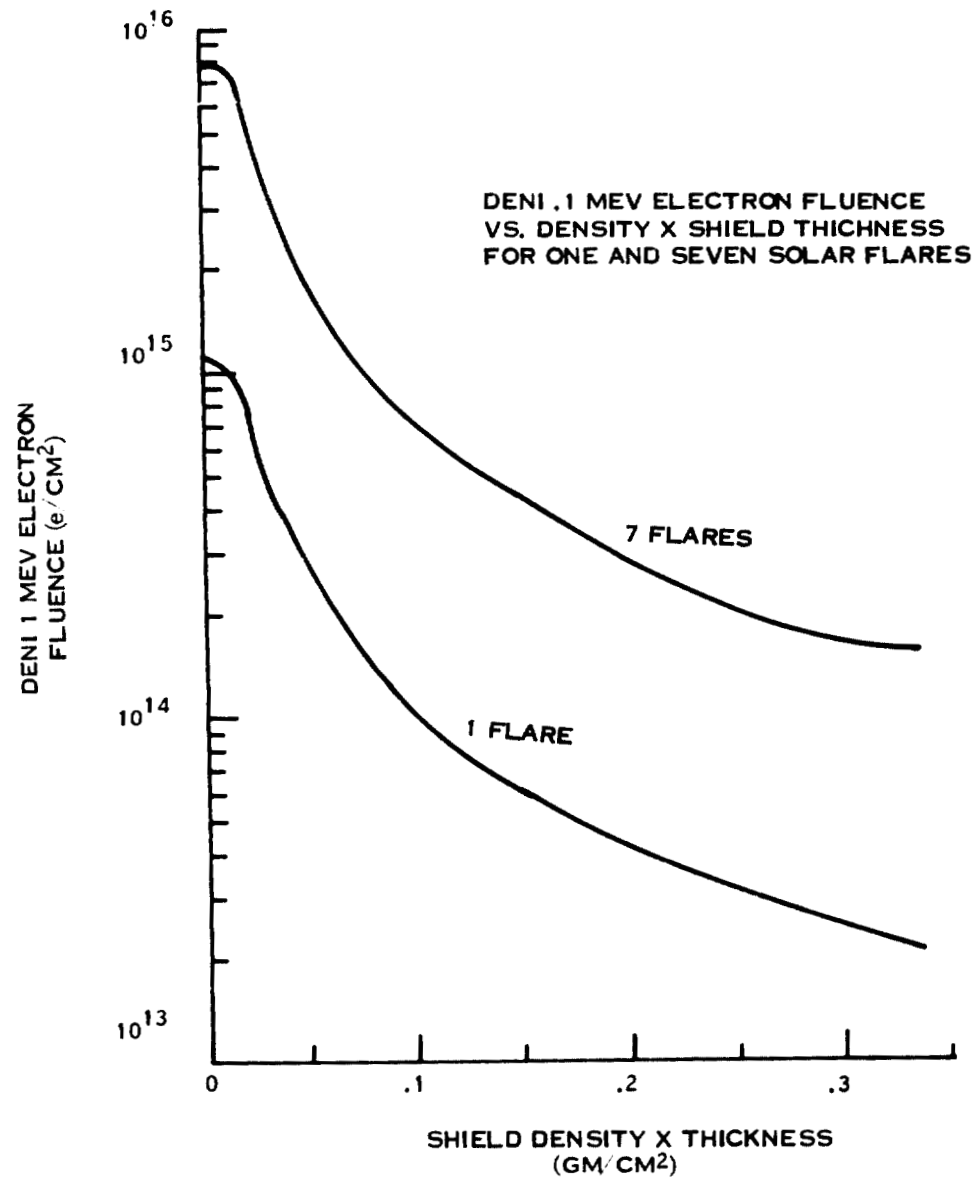
Figure 4-22. DENI 1 MeV Electron Fluence - Interplanetary Case
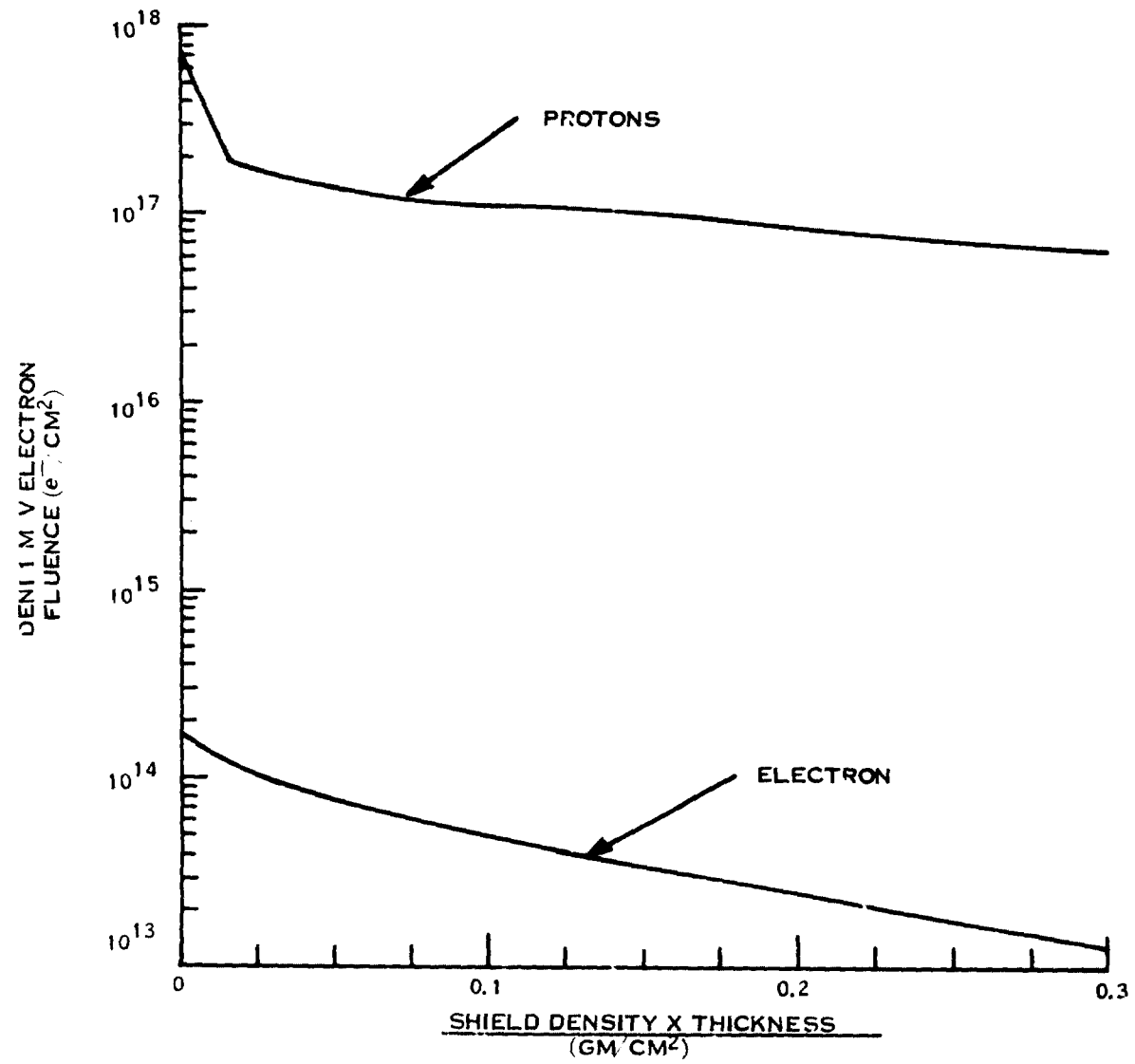
Figure 4-23. DENI 1 MeV Electron Fluence - Geosynchronous Case
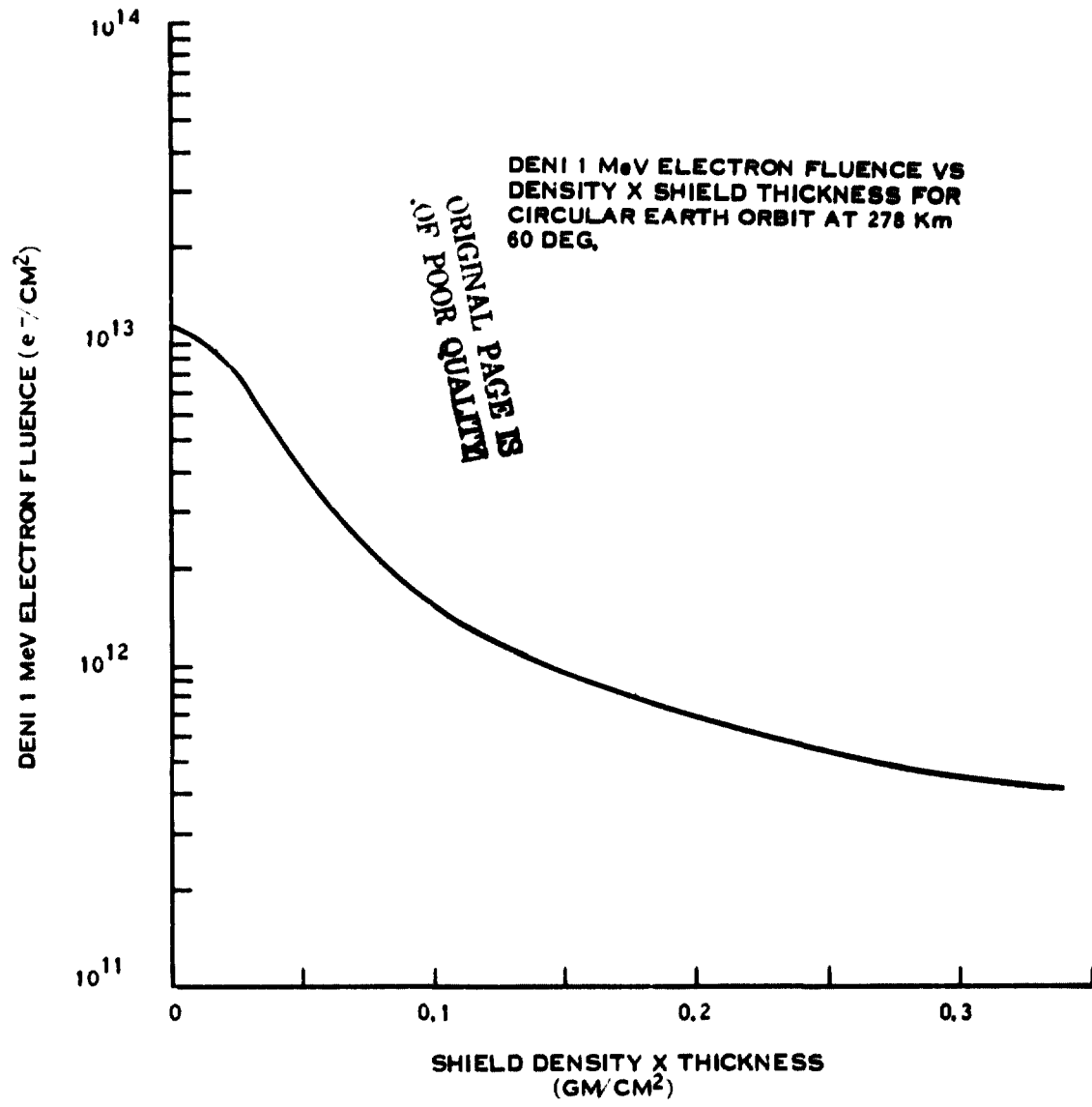
Figure 4-24. DENI 1 Electron Fluence - Low Earth Orbit Case

4.3.3.2 Particle Radiation Analysis (Continued)

The end-of-life (EOL) power maximum is predicted based on data presented in Figure 4-25 (same as Figure 2-3 in the Summary Section). This curve represents empirical data gathered by JPL on a developmental cell that has been thinned to the range of 50 to 75 microns.

The EOL power for the interplanetary (1 flare), geosynchronous and low earth orbits is calculated to be 0.79, 0.23 and 0.99 respectively. The EOL power output of 0.99 x BOL, predicted for a low earth orbital mission of three years duration is representative of this mission only. Solar flare degradation is not included in this estimate. It is expected that the occurrence of a large flare (i.e., magnitude at or close to that specified for the one flare model in Figure 4-17 will reduce EOL power to a value closer to the 0.79 x BOL value noted for the interplanetary, one flare case.
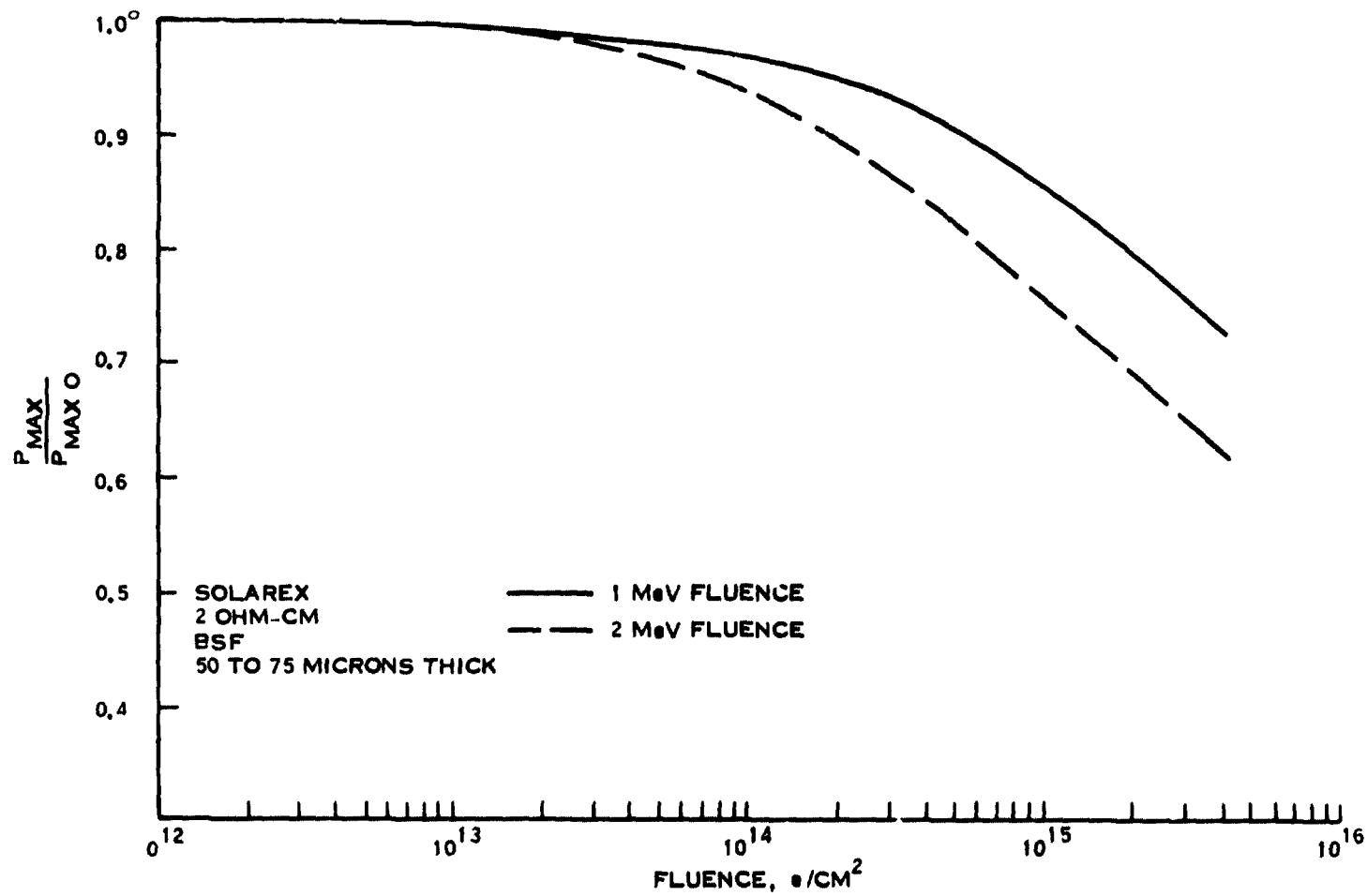
Figure 4-25. Normalized P_{max} vs 1 and 2 MeV Fluence

4.3.4 BLANKET LAYOUT

The layout for the baseline half-blanket is shown in Figure 4-15. Approximately 80% of the blanket is occupied by 2 x 2 cm^2 cells. Each half-blanket consists of 40 electrically independent modules. Each module in turn is made up of 2000 cells grouped into 25 circuits of 20 series by 4 parallel connected cells, see Figure 4-15. The encapsulated cells occupy an area 40.6 cm high by 2.03 m wide, allowing for 0.3 mm all around between cells. Each circuit of 80 cells terminates in an end connector which is used to join adjacent circuits to form a series string of 25 circuits. Each cell interconnector bridges 4 cells in parallel. A cross-section through the balnket is shown in Figure 4-26.

CELL THK
75 MICRON

SPOT WELD

COVER THK
12.7 TO 50 MICRON

SUBSTRATE
25 MICRON THK
KAPTON

INTERCONNECT
25 MICRON THK MOLYDBENUM
SILVER PLATED

F.E.P. ADHESIVE
12.7 MICRON THK
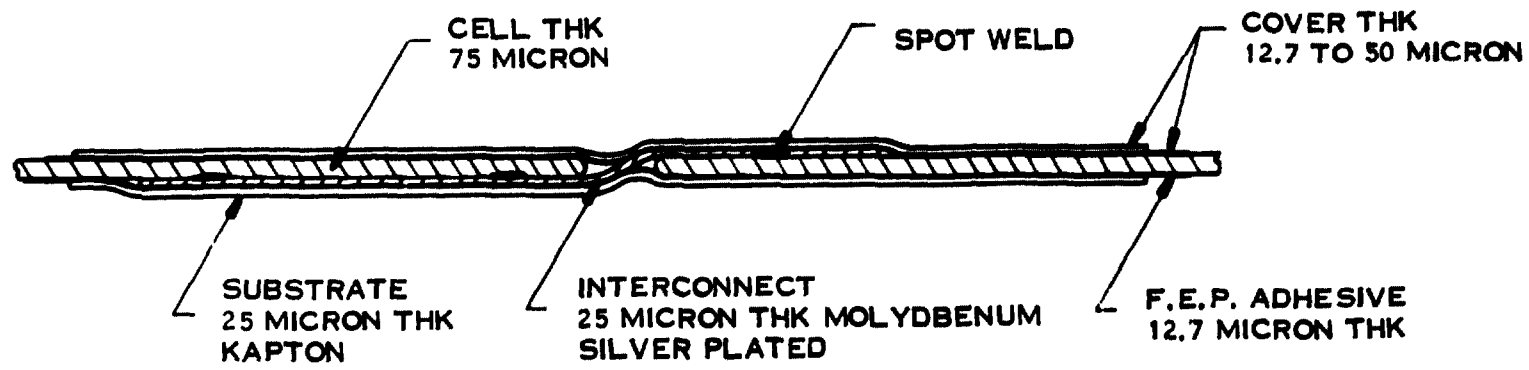
Figure 4-26. Blanket Cross-Section

4.3.5 BLANKET FABRICATION

The assembly of the blanket is seen to occur in the following way. Cells with matched current output will be welded together in parallel at the N-contact as a unit of four. Twenty of these units will be welded together in series at the P-contact to form a circuit 20 cells long. One end connector is welded to the P-contact of the appropriate end unit. These circuits are then assembled ready for final end connector welding on top of the substrate material. Heat sealing of the unconnected circuits to the substrate appears to be advisable at this point in order to maintain positional tolerances between circuits. The final welding of the end connector follows. At this juncture the individual modules may be heat sealed together with junction strips. End strips incorporating the flat conductor cables (FCC) are to be heat sealed to both sides of the assembled modules. The FCC lines are then welded to the appropriate module end terminals. The blanket is then ready for the top sheet material, which may be in the form of a sheet or liquid polymer. The latter form would appear to be preferred, especially since cast film may be cured at low temperature ($\sim 135^{\circ}$C).

4.3.6 BLANKET REPAIR

A conceptualization of how the array might be repaired, as necessitated by a broken or inoperative cell, is schematically shown in Figure 4-27. This concept trades heavily on the thermoplastic properties of materials use in the blanket and the relative ease with which it may be softened and repaired. In the case of open electrical connections or high resistance joints, the repair procedure may only involve use of the parallel bar welding tool.

① CUT AROUND CELL FRONT & REAR

② REMELT TEFLON BOND FRONT & BACK REMOVE CUT PIECES

ELECTRICALLY HEATED TOOL

③ BREAK WELDS

THIN BLADE

④ FUSE FEP TEFLON ON TOP SIDE OF NEW CELL

OVERLAP

⑤ REWELD - HAND HELD TOOL

⑥ BOND TOP PATCH TO ARRAY COVER

⑦ BOND SUBSTRATE PATCH (SEE ②)
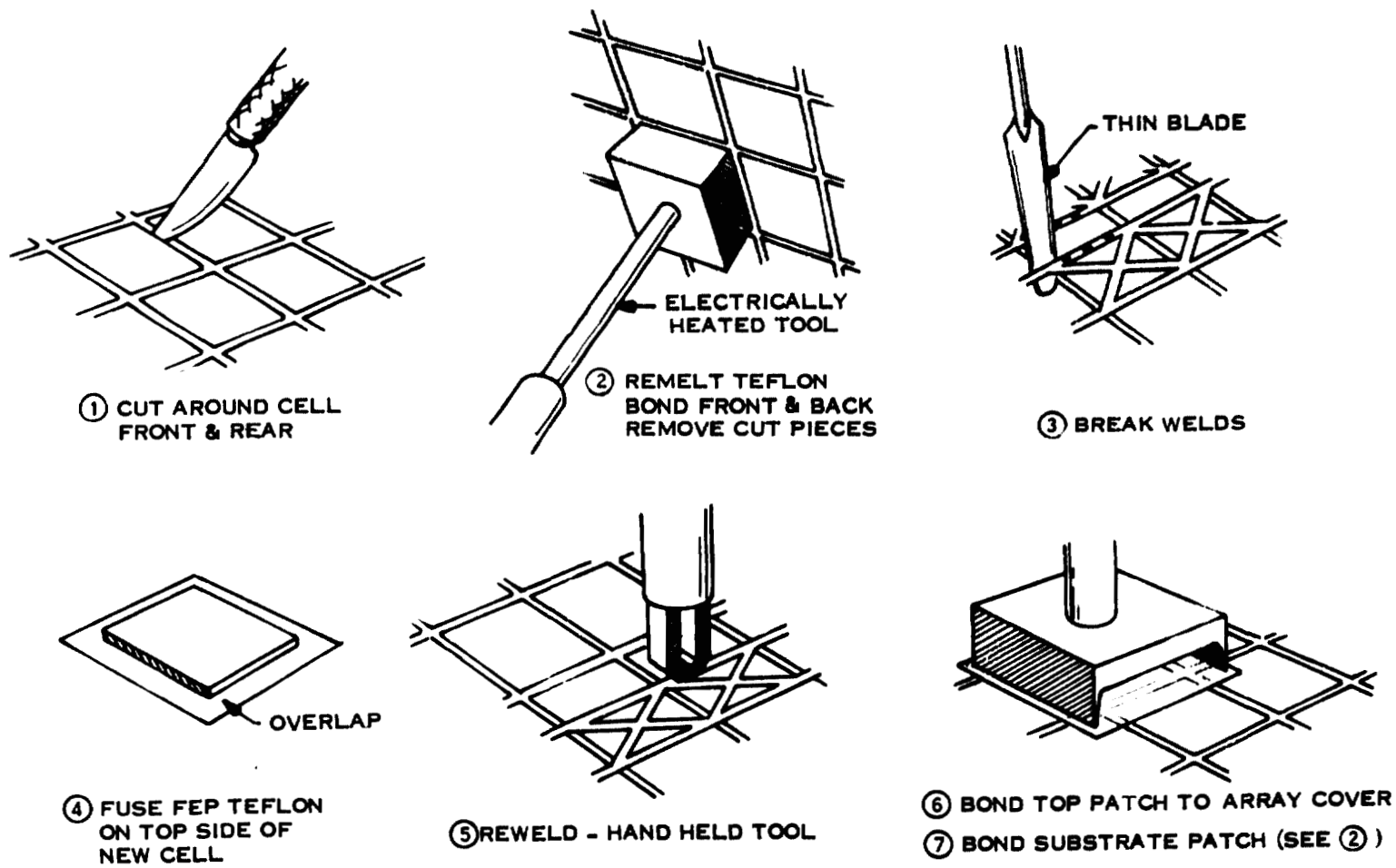
Figure 4-27.   Conceptualization of Blanket Repair

4.4 MECHANICAL DESIGN

4.4.1 BASELINE DESIGN CONCEPT

The baseline selected for the 200W/kg solar array is a rollout lightweight blanket type. (See Figure 4-28). The array is divided into two sections which are canted at a small angle to form a "V-stiffening" effect permitting the use of a smaller extendible boom with associated savings in mass. This "V-stiffening" concept was a new technology development that came out of the GE/JPL 110W/kg Solar Array study.

The blanket sections are 2.21 m wide by 17.2 m long including cells and electrical busses for a total array area of 76 m^2 per wing. The boom is a standard type Astromast 12.7 cm in diameter with a stiffness (EI) of 532 $N-m^2$. The boom supports the outer end of the blankets through a "header" which is free to rotate on the boom axis. Leading edge members rigidly attached to the header secure the blanket at the outer end.

The array is held flat by boom tension on the blanket. The substrate (or bottom sheet) of the blanket is composed of a 12.7 microns thick layer of heat-sealable FEP Teflon backed up by a 25.4 microns thick layer of Kapton for strength. In the baseline design a second sheet of FEP will serve as the cell cover-sheet.

8.25°

4.74M (15.55 FT)

LEADING
EDGE
MEMBER

HEADER

17.2M (56.45

CELL MODULE
2000 2 X 2 CM CELLS
80 MODULES
10.4 KW

12.7 CM DIAMETER LATTICE
BOOM & DEPLOYER

DRUM 30.48 CM DIAMETER
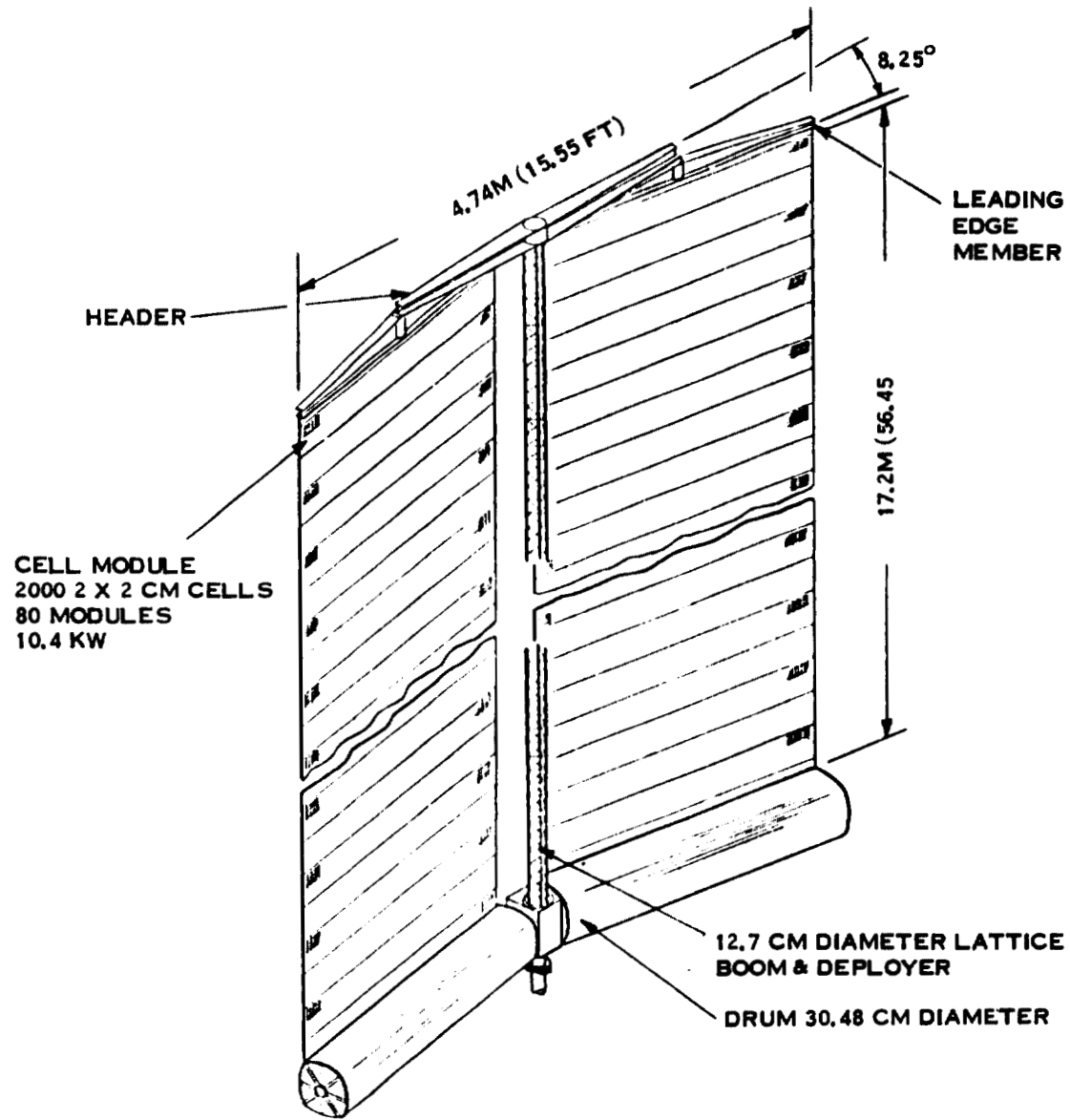
Figure 4-28. Baseline Solar Array

4.4.1 BASELINE DESIGN CONCEPT (CONTINUED)

4.4.1.1 Boom and Stowage Drum

The Astromast assembly is mounted in a center support. The stowage drum is flange mounted to each side of this support by means of a preloaded bearing assembly.

A negator spring motor attached to the bearing assembly housing imparts a nearly constant torque of 1.02 Nm (9 in. lbs.) to the drum resulting in a blanket tension of 7.12 N (1.6 lbs.).

A slip ring assembly is also mounted on the inner stationary shaft of the bearing assembly. This device is a standard type design for space use with capacity for 40 power leads and a number of signal leads.

The stowage drum is 25.4 cm in diameter by 2.31 m long. It is constructed of a graphite composite for low weight and high stiffness. See Figure 4-29.

DEPLOYER MOTOR

STOWAGE DRUM

NEGATOR SPRING
MOTOR

SLIP RING ASSEMBLY

DEPLOYER
NUT

CANISTER

CENTER SUPPORT
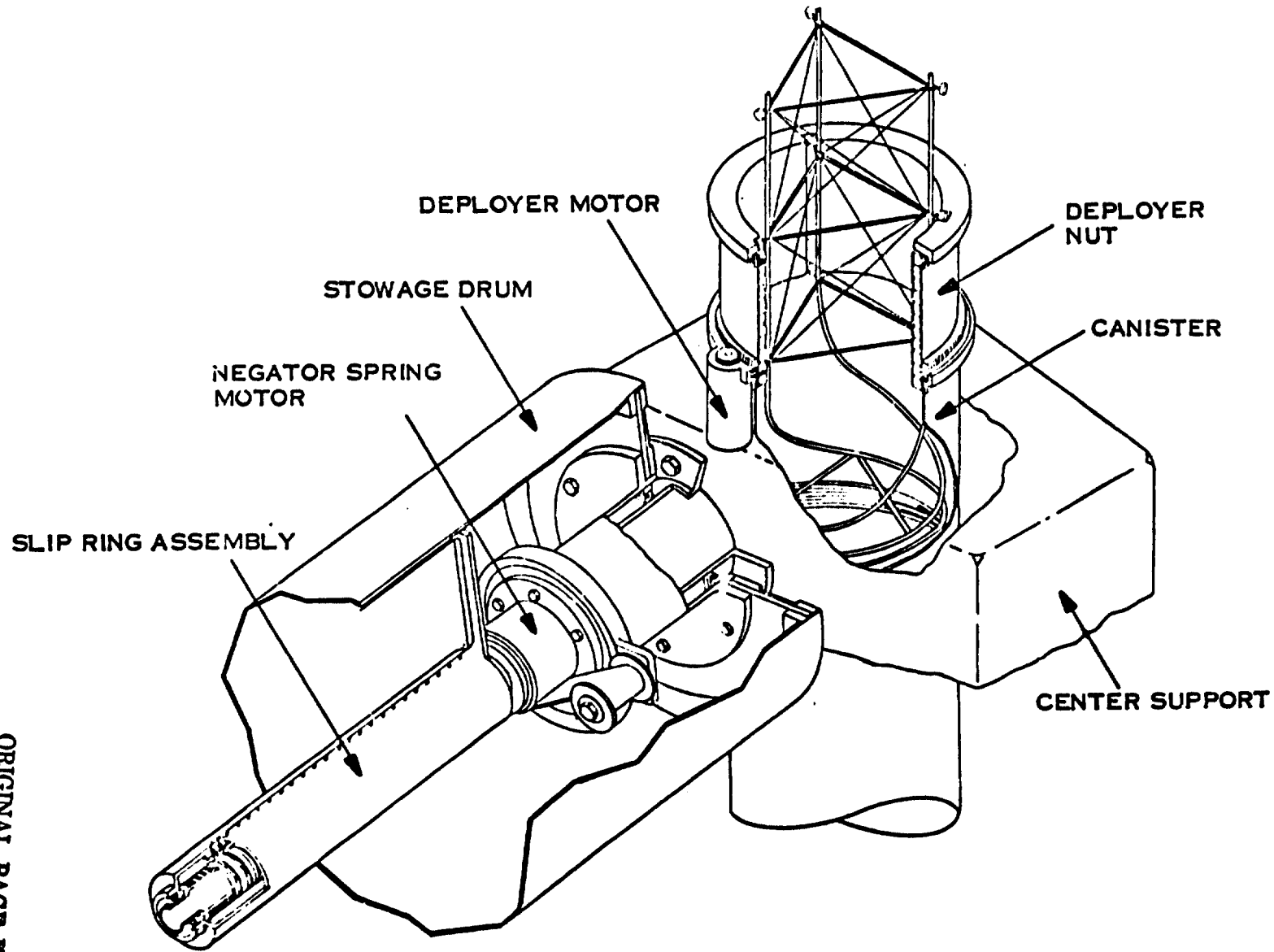
Figure 4-29.   Cut-Away View of Boom and Storage Drum

4.4.2 BASIC ARRAY STRUCTURES

Three basic array candidates were considered in this study. The <u>rigid array</u> has a stiff substrate such as aluminum honeycomb on which the cells are bonded. This method of construction is often adequate for small arrays. Although some good advances have been made, such as the EOS hollow core panel, rigid panels can be expected to be a limiting item in optimizing weight for large arrays.

An example of a <u>semi-rigid</u> array is the concept proposed by Convair for the SEPS application. This is an array bonded to very lightweight isogrid stricture (machined from plate). The material is curved to create stiffness but will fold into a flat pack configuration for stowage much the same as a carpenter's rule.

The third basic type is the <u>flexible blanket</u> which depends upon tension in the blanket to maintain itself in a flat plane in zero G environment. Stowage of the flexible blanket is accomplished by either rolling or folding. See Figure 4-30.
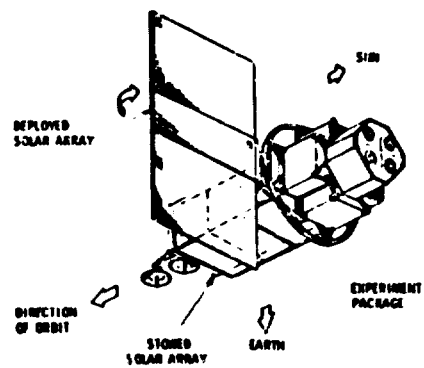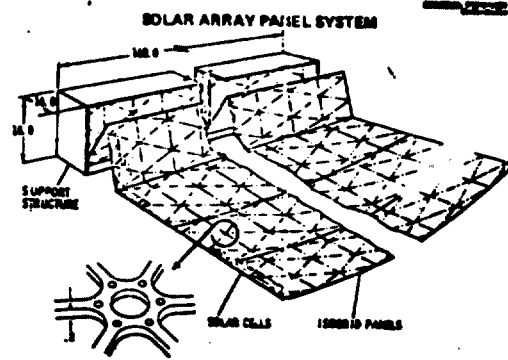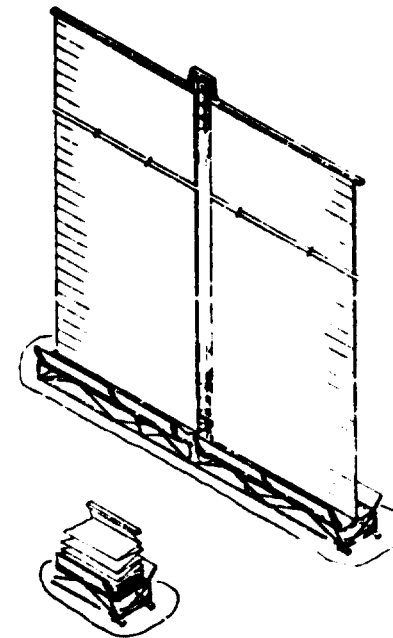
RIGID   SEMI RIGID   FLEXIBLE

Figure 4-30. Basic Array Candidates

4.4.3 DESIGN TRADEOFFS

By comparison ·exible blanket is superior in respect to high specific power (Power/Unit Mass). It has low mass bec...ᵤᵤᵉ the supporting structure can be supplied by a single lightweight element. Stowage is compact because the thickness of the substrate is reduced to a sheet as thin as 1 mil of Kapton-H film. As an added feature, retraction and re-deployment of the array on command can be readily accomplished if the blanket is rolled-up on a drum.

Table 4-15 lists a mass density comparison for the three basic types. Table 4-16 shows a comparison of array types.

Table 4-15. Array Structure Mass (Typical)

Type	Array Examples	Mass per* Unit Array Area Kg/M^2
Rigid	GE Broadcast Satellite Experiment	1.67
Semi-Rigid	Convair Proposal (Iscgrid Structure)	0.09
	GE 30 Watt/Lb Rollup	0.246
Flexible	LMSC SEPS Array	0.272
	GE 110 Watt/kg (Study)	0.059

*Support Structure Only (Deployer Not Included)

Table 4-16. Array Type Comparison

TYPE	RIGID	SEMI-RIGID	FLEXIBLE
ADVANTAGES	• STRUCTURALLY STIFF • GOOD CELL SUPPORT • FLIGHT PROVEN	• INHERENT STIFFNESS AT HINGE LINES • RELATIVELY LOW MASS	• LOW MASS • COMPACT STOWAGE • COMPATIBLE WITH LIGHTWEIGHT EXTENDIBLE BOOMS • EASILY RETRACTED BY ROLL-UP
DISADVANTAGES	• HIGH STOWAGE VOLUME FOR LARGE ARRAYS • BULKY FOR LAUNCH VEHICLES • LOW POWER WEIGHT RATIO	• NEW CONCEPT, UNPROVEN • REQUIRES COMPLEX DEPLOYER & RETRACT MECHANISMS	• REQUIRES SEPARATE SUPPORT STRUCTURE • DIFFICULT TO CONTROL FOLD-UP

4.4.4 EXTENDIBLE BOOM CANDIDATES

The boom for the array assembly was selected from known extendible booms. Among the devices considered are (1) the "BI-STEM" pioneered by SPAR and used on many space applications, (2) the Bi-Convex Tubular boom manufactured by Celesco and used on the soil sampler for Viking, and (3) the coilable lattice boom developed by Astro Research Corp. See Figure 4-31.

A semi-rigid structural boom proposed by Convair was also given consideration in this study.
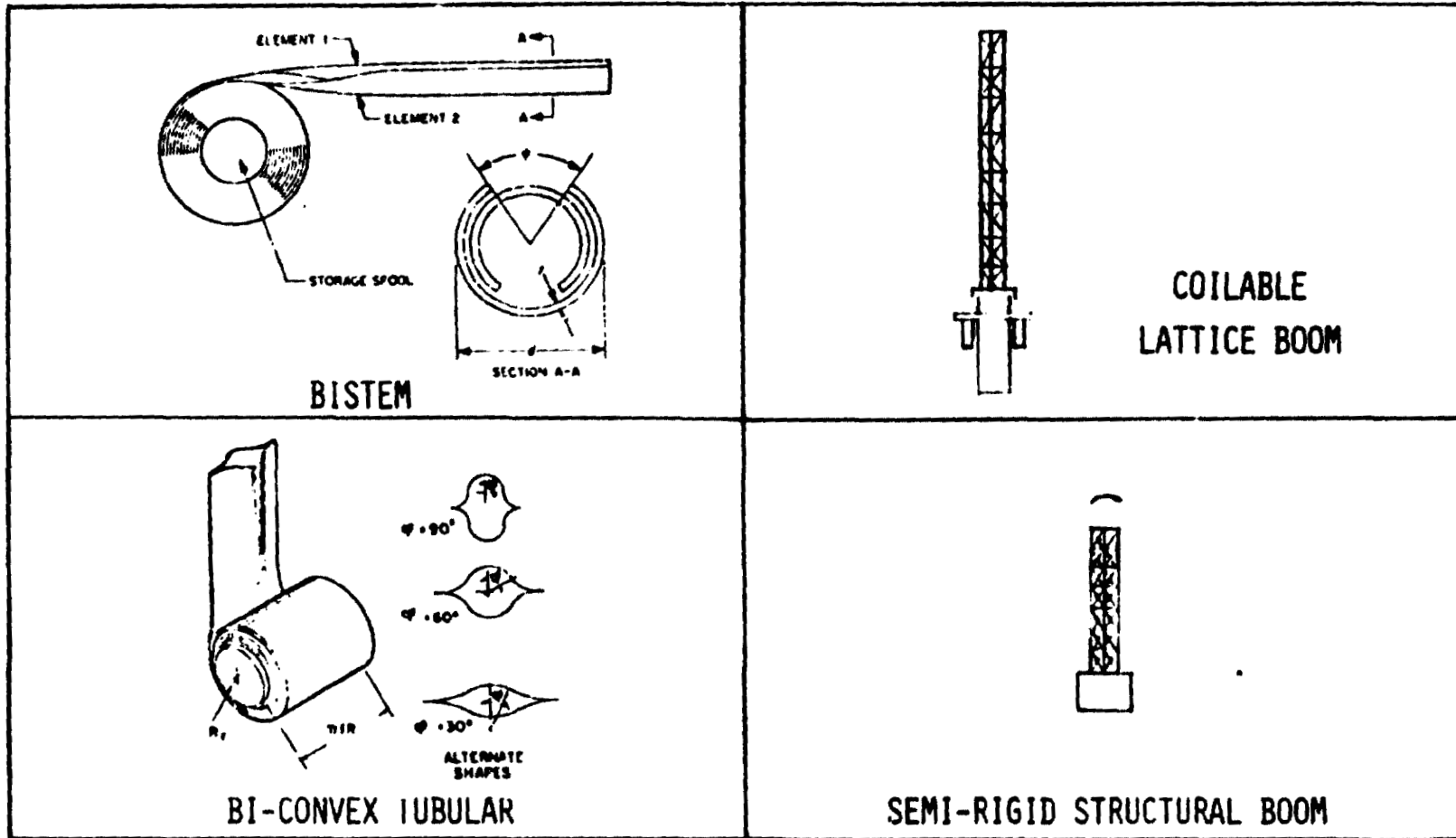
Figure 4-31. Extendable Boom Candidates

4.4.4 EXTENDIBLE BOOM CANDIDATES (CONTINUED)

Boom Mass Comparison

The continuous longeron astromast can provide best low-mass benefits as shown by the curves in Figure 4-32. To meet the design requirement of a stiffness of 1×10^5 lb-in^2 (287 N-M^2), an element mass of approximately 0.04 lb/ft (0.06 kg/m) is attainable.

The coilable lattice (continuous longeron) boom has been selected for the following reasons:

1. Best mass-to-stiffness ratio

2. Lowest boom plus deployer mass

3. Relatively low sensitivity to thermal bending

4. Low backlash characteristics

5. Related application (LMSC SEPS array)
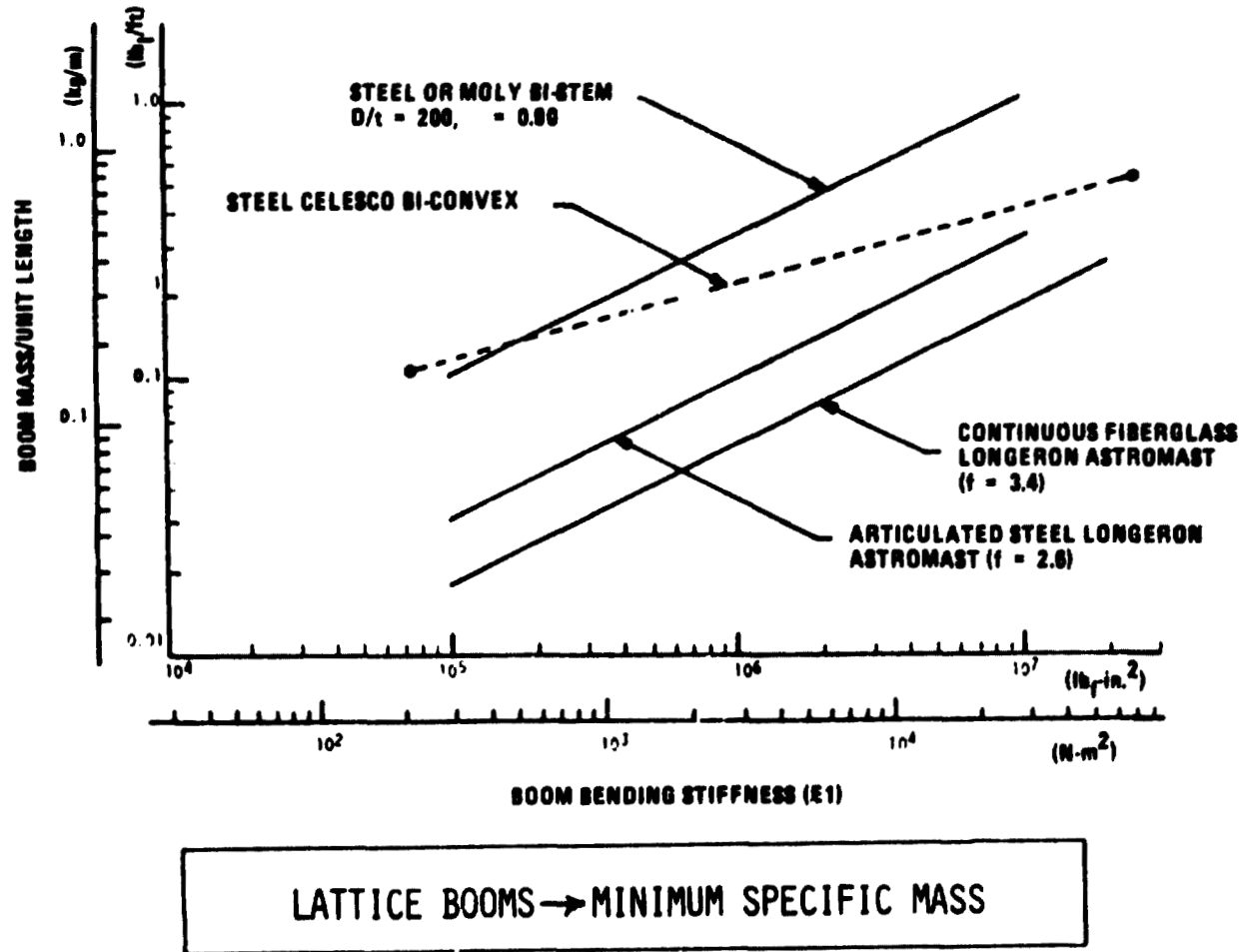
Figure 4-32. Boom Mass Comparison

4.4.5 ARRAY STOWAGE CONFIGURATION OPTIONS

Three options considered for the stowage of the flexible array are shown in Figure 4-33. The flat pack (foldout) method and the drum (or rollout) approach are the most conventional.

Option 3 is a combination of Options 1 and 2. Since the amount of bending which a thin cell blanket could withstand without degradations was unknown, the curved sided drum was conceived as a way to keep the curvature independent of the nominal drum radius. Stowage surface curvature may be specified in accordance with blanket flexing limitations. The presence of some curvature on the surface results in a radical force which helps to secure the blanket to the drum during launch.
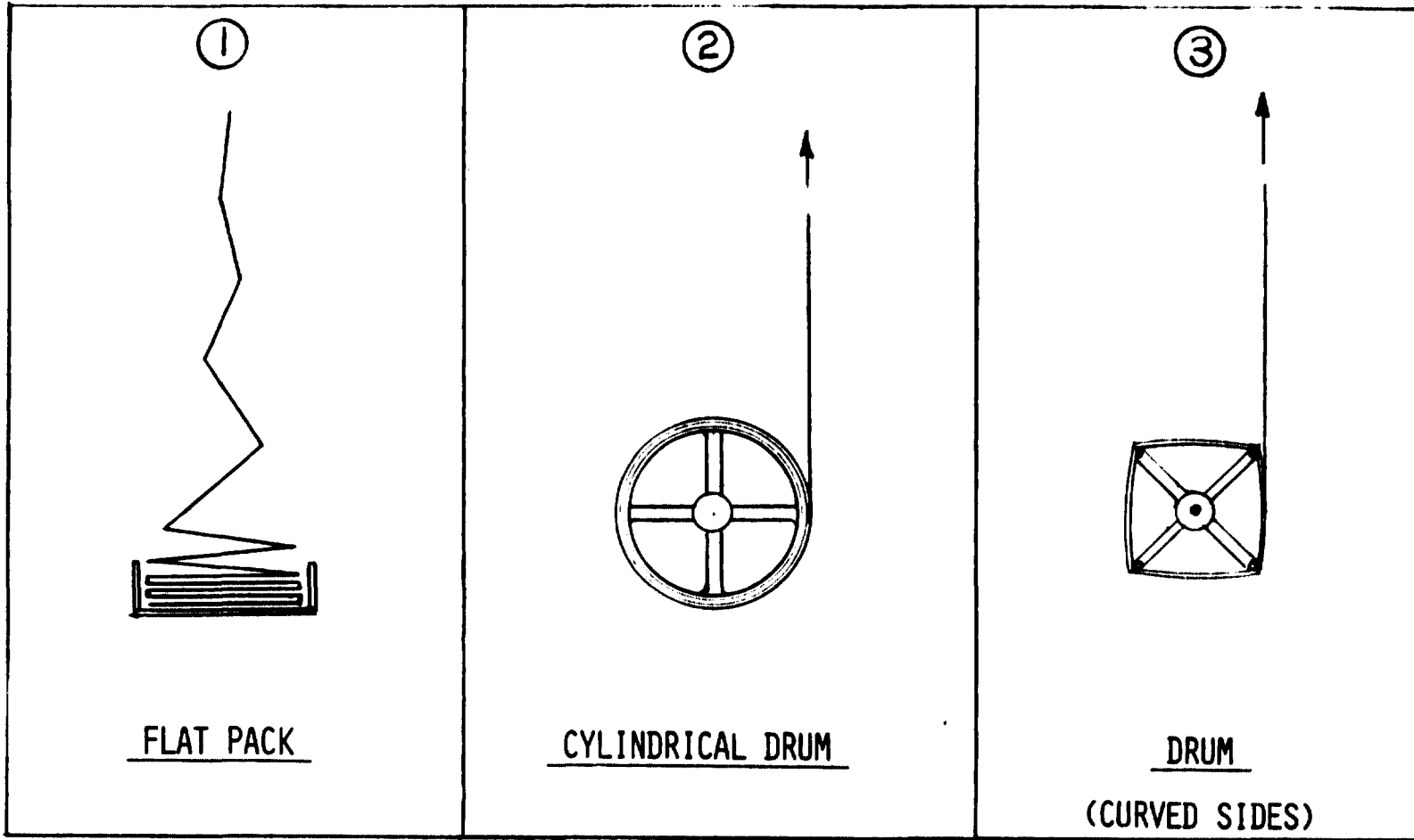
Figure 4-33. Stowage Configuration Options

4.4.5 ARRAY STOWAGE (CONTINUED)

The flat pack (foldout) approach has two distinct advantages in that the cells are packed in a basically flat condition and that the power transfer does not require a rotary device.

The rollout method offers the advantage of continuous tension on the blanket during deployment plus ease and simplicity in retraction.

The curved side concept has the obvious disadvantage of needing blank cell areas at the corners, adding length (and weight) to the system. The blanket tension will also vary with drum position unless a special spring motor is provided.

The cylindrical drum was chosen as the baseline stowage method because of its versatility and relatively low mass. Preliminary analysis shows that the blanket may be wrapped on a 10 inch drum with a reasonable margin of bending stress capability in the cells. See Table 4-16 for a comparison of the types of stowage systems.

Table 4-17. Stowage System, Key Tradeoffs

Type	Advantages	Disadvantages
1 Flat Pack	● Holds cells in flat condition for stowage and launch ● Does not require special power transfer devices	● Difficult to control foldup on retraction ● Retraction aids add weight
2 Drum (Cylindrical)	● Simplifies deploy and retract mechanisms ● Maintains tension on blanket at all times	● Blanket must be flexible ● Blanket compression forces related to blanket tension
3 Drum (Curved Sides)	In addition to 2 above ● Permits reduction of cell bending ● Adaptable to modularity	In addition to 2 above ● Requires blank substrate areas at corners in creasing blanket length

```
CYLINDRICAL DRUM CAN PROVIDE
VERSATILE LOW MASS SYSTEM
```

4.4.6 TENSIONING MECHANISMS

A flexible blanket must be maintained at a fixed level of tension throughout mission life to keep the natural frequency at the specified value. Tension is also beneficial during extension or retraction to prevent random slack in the array.

In the case of the rollout approach, a single negator spring motor inside the drum serves to maintain nearly a constant tension on the blanket. A sketch of the negator spring motor in relation to the solar array storage drum is shown in Figure 4-34. Spool A is integral with the fixed drum shaft. Spool B is free to rotate on a jack shaft that in turn is mounted on the array storage drum. When the solar array is fully stowed, the spring is fully wrapped on Spool B. As the solar array is deployed via the continuous longeron boom, the spring is unwound from Spool B and is wrapped up on Spool A. The forces stored in the spring want to wrap the spring on Spool B. As a consequence, a counterclockwise torque is applied to the storage drum. This torque results in tension T being applied to the solar array blanket. Bearing friction and friction torques are maintained at a related low level so that the tension (T) is basically proportioned to the flat characteristic of the negator spring. Extension tension will be higher than retractions tension by twice the sum of the slip ring and bearing friction equivalents.

A method of establishing tension at the end of full development of the foldout concept is illustrated in Figure 4-35. A compression spring, incorporated in the boom tip assembly, establishes the required tension range. Limit switches, which are connected electrically to the deployer control, define the limits of the tension range selected and can be used to avoid overloading of the blanket or boom structure.
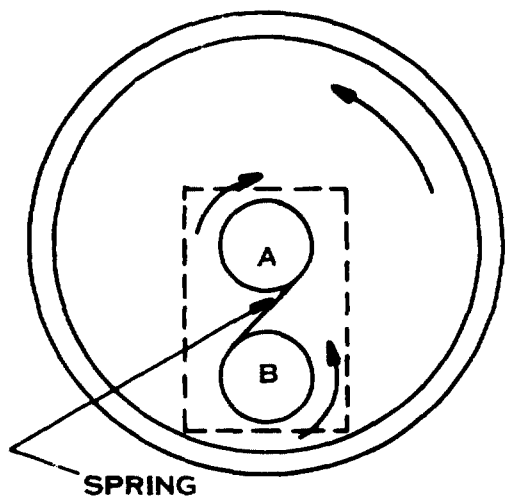
Figure 4-34. Drum Negator Spring Motor

LIMIT SWITCHES

COMPRESSED SPRING

HEADER

OPERATING RANGE
11.5 NT (2.6 LBS)
13.3 NIT (3.0 LBS)
TO 13.4 NT (3.1 LBS)
15.6 NT (3.5 LBS)

BUSHING
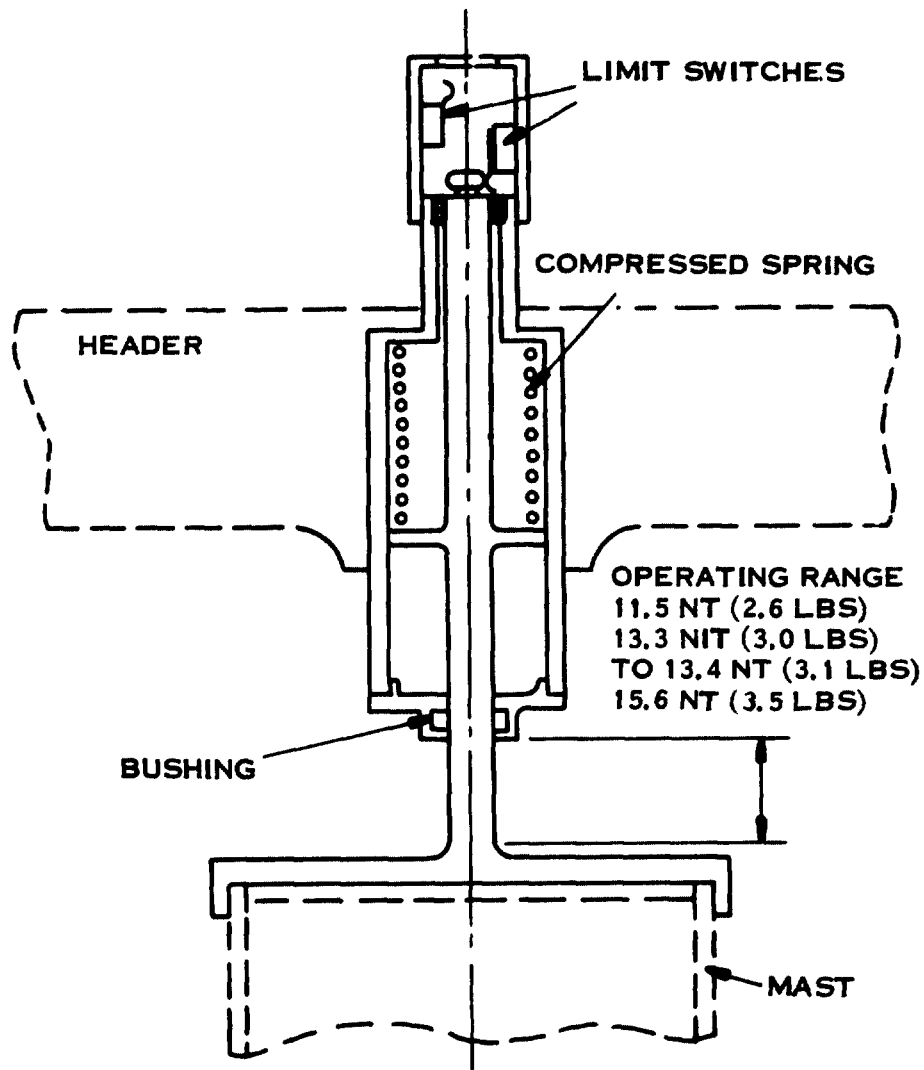
MAST

Figure 4-35. Tensioning Mechanism (Mast Tip Assembly)

4-95

4.4.7 POWER TRANSFER DEVICE CANDIDATES

Three devices, or techniques, shown in Figure 4-36, were considered for the function of power trans-
fer. The motor driven connector is a special device patterned after conventional launch disconnects.
This connector is remotely engaged as the array approaches full extension. Pilot pins engage the drum
and line up the receptacle and plug near the end of blanket travel. Intermediate array extension
positions can also be accommodated.

Both slip rings and the spiral twist cable are notable for their prior acceptance and use.

RECEPTACLE

FULL ENGAGEMENT

PRETRAVEL

LIMIT SWITCH

YOKE

CENTER SUPPORT

DRUM

KINETICS CONNECTOR
DWG. NO 1124
(MODIFIED)
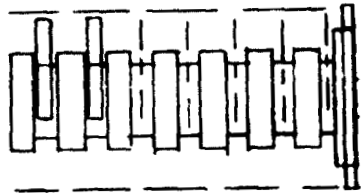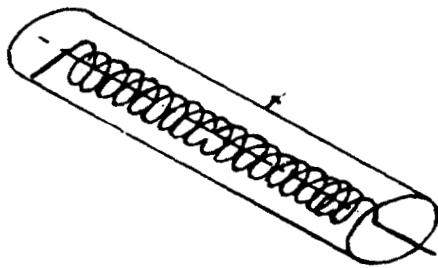
SLIP RINGS

SPIRAL TWIST CABLE
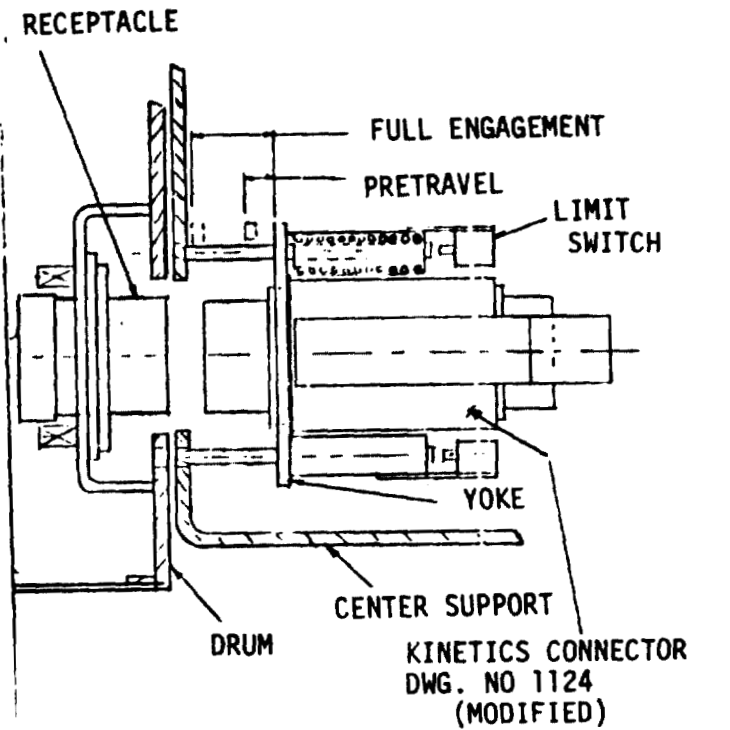
MOTOR DRIVEN CONNECTOR CONCEPT

Figure 4-36. Power Transfer Devices

4-97

4.4.7 POWER TRANSFER DEVICE CANDIDATES (CONTINUED)

Slip rings have been chosen as baseline for the power transfer mechanism. These devices are well proven in space and are passive in that they do not depend on any other related active functions. Friction torque is relatively insensitive to temperature.

The spiral twist is considered to be an approach that may exhibit an excessive torque level; which is also sensitive to low temperature conditions, especially where a large number of conductors are involved.

The motorized connector is a reasonable alternate to the slip ring. The receptacle and plug are standard hi-rel parts. Its use would become more attractive where the number of conductors and current capacity might result in an undesirable slip ring configuration.

See Table 4-18 for a summary of the power transfer trades.

Table 4-18. Power Transfer Trades

Type	Pro	Con
Slip Rings	• Space proven approach • Operable over wide temperature range with essentially *constant* torque • State of art device	• Require lubrication of brushes and bearings
Spiral Twist Cable	• Simple mechanism	• Requires long lead • Torque va: s with temperature • Requires some development
Motorized Connector	• Provides non-moving contact • Utilizes standard space proven connector elements	• Requires added mechanism and controls • Limit stowage drum to fixed positions of one revolution intervals

Selection --- Slip Rings

Alternate --- Motorized Connector

4.4.8 LAUNCH RETENTION

The cantilevered stowage drum must be supported at the outboard end during launch. A concept for implementing this function is shown in Figure 4-37.

A retention plate, located at the outboard end of the drum and hinged to a fixed support on the shuttle, is torqued toward the release position by a torsion spring. In the plate are three taper pins which engage holes. When the plate is in launch position, the end position of the leading edge member and the drum are secured both laterally and angularly. A pyro actuated bolt and nut is fired to release the retention plate.

DETAIL "A"
PIN & SOCKET

LEADING EDGE MEMBER

END SUPPORT

HEADER

SEE DETAIL "A"

RELEASED POSITION

RELOCKABLE NUT

CENTER SUPPORT

BLANKET (WRAPPED AT LAUNCH TENSION)

TORSION SPRING

SEE DETAIL "A"

DRUM ROTATION LOCK
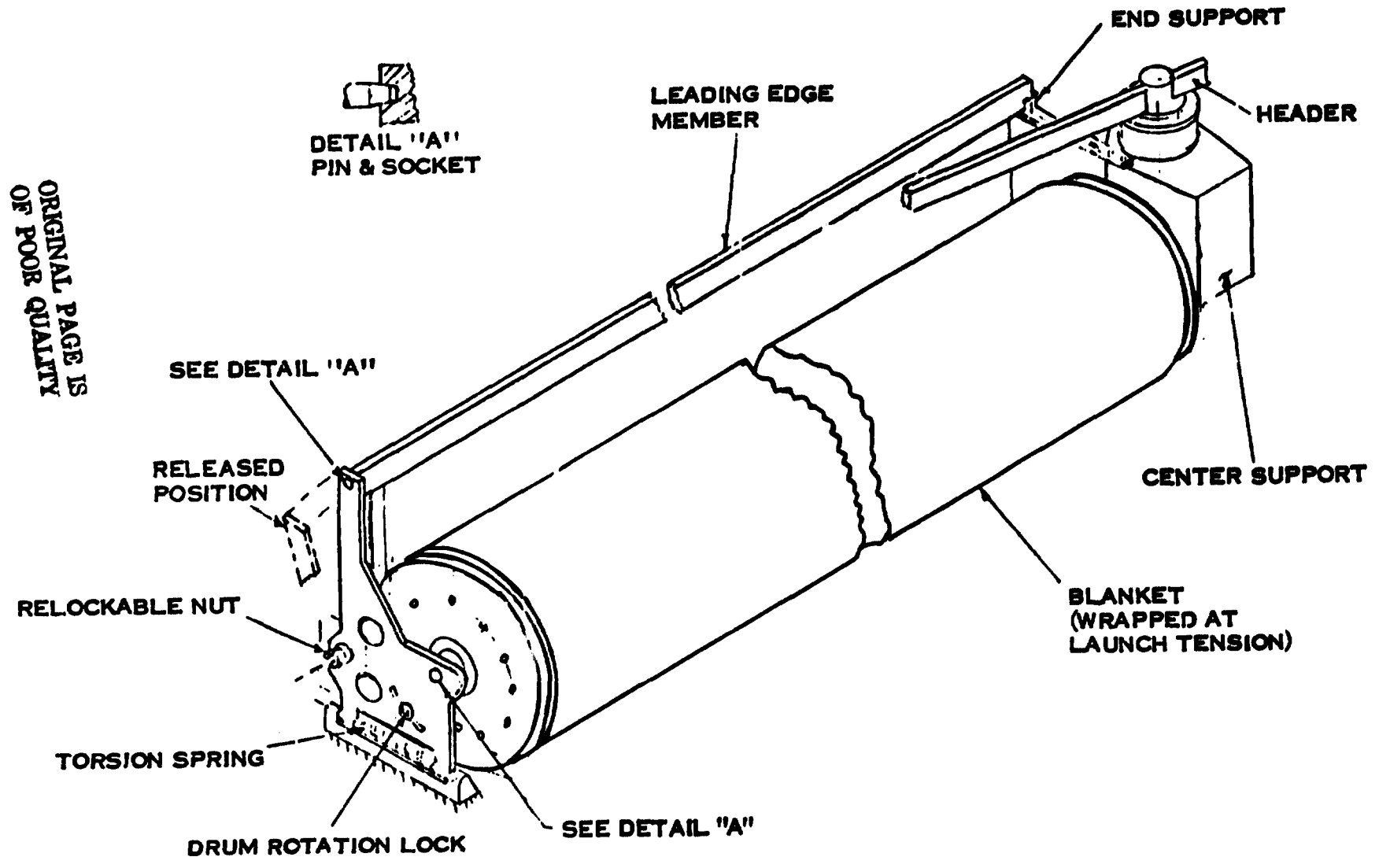
Figure 4-37. Launch Retention (Rollout)

4.4.9 SPACECRAFT INTERFACES

The center support of the array is mounted to the end of the spacecraft array shaft by means of a flange.

Electrical connections may be made with standard connectors mounted in the center support structure with power and signal functions as required.

Spacecraft interfaces is illustrated in Figure 4-38.

MECHANICAL

ELECTRICAL

DRUM INTERFACE

(CENTER SUPPORT

FLANGE INTERFACE

S/C ARRAY SHAFT

LEFT HALF

C1
POWER (40 LEADS)
POWER RETURN
TEMPERATURE SENSOR
SIGNAL GROUND

RIGHT HALF

C2
POWER (40 LEADS)
POWER RETURN
TEMPERATURE SENSOR
SIGNAL GROUND

C3
DEPLOYER MOTOR
DEPLOYER MOTOR RETURN
POSITION INDICATOR (PULSE)
SIGNAL GROUND
LIMIT SWITCH
DEPLOYER TEMPERATURE
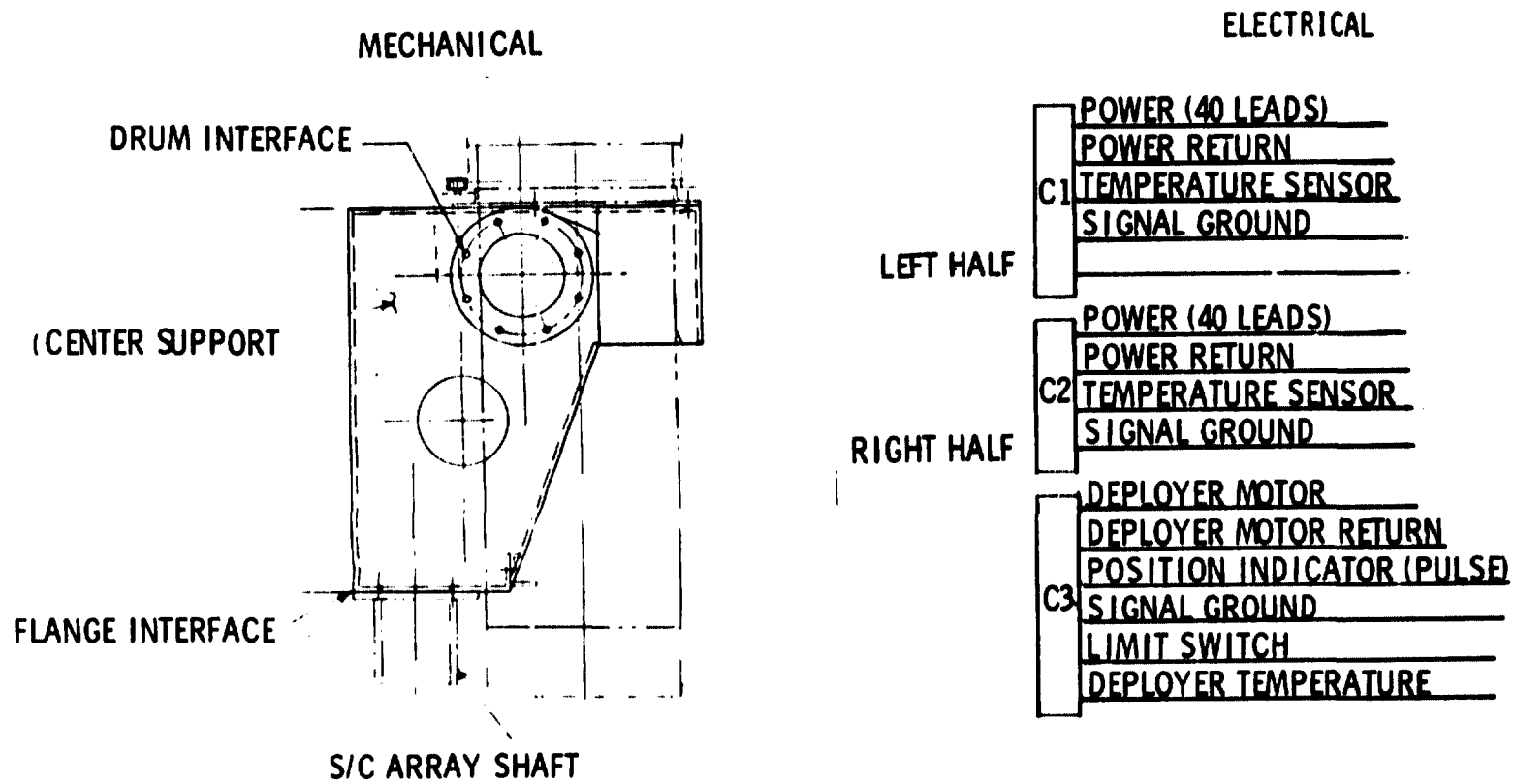
Figure 4-38. Spacecraft Interfaces

4.4.10 SHUTTLE INTERFACES

The baseline design concept for Shuttle Interface is based on the assumption that end supports for the stowage drum may be attached to the Shuttle through trunion arms and remain with the Shuttle after deployment of the spacecraft. A typical configuration is shown in the sketch of Figure 4-39.

SHUTTLE PAYLOAD BAY (15 FT. DIA. X 60 FT. LG)

LAUNCH RETENTION BRACKET

STOWED ARRAYS

TYPICAL 990 Kg SPACECRAFT

TRUNION INTERFACE WITH SHUTTLE
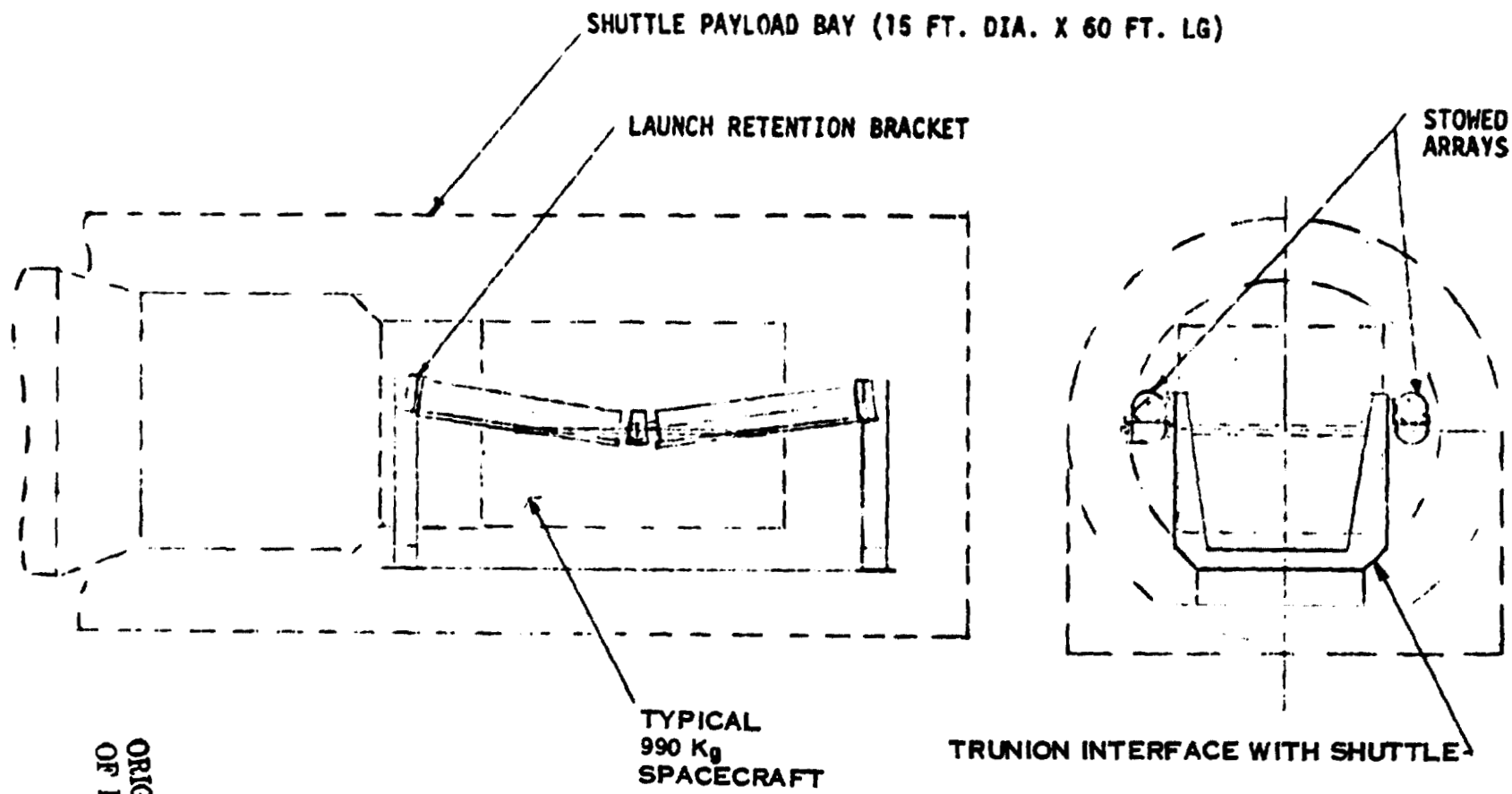
Figure 4-39. Shuttle Interface

4.5 PARAMETRIC ANALYSIS

4.5.1 VIBRO-ACOUSTIC DESIGN REQUIREMENTS

The launch and flight environments, as defined in the study Requirements Document, were analyzed for their dynamic impact on the baseline design of the 200W/kg solar array. Since a similar analysis was carried out on the 110W/kg solar array, much of the current analysis benefited from that earlier study. The principal difference was the advent of the ultra-lightweight, thin solar cells. The launch vibration, shock, static acceleration and acoustics proved to be no problem for the baseline design. The deployed array natural frequency and the quasi-static acceleration are the major constraints. See Table 4-19.

Table 4-19. Vibro-Acoustic Design Requirements

- Deployed Requirements

  - Deployed Array Dynamics: $F_n \geq 0.04$ Hertz
  - Quasi-Static Loads, Deployed Array: 1×10^{-3} G maximum

- Stowed Requirements

  - Launch Vibration, Stowed Array

    2 - 5 Hz 2.5 cm DA

    5 - 26 Hz 1.3 g (0-peak)

    26 - 50 Hz 0.09 cm

    50 - 1000 Hz 5g (0-peak)

  - Launch Acoustics, Stowed: 145 dB overall
  - Shock, Stowed Array: 20 G, 10 ms Terminal Sawtooth
  - Static Acceleration, Stowed Array: 9 G's

DEPLOYED REQUIREMENTS ARE MAJOR CONSTRAINTS

4.5 PARAMETRIC ANALYSIS (CONTINUED)

4.5.2 OPTIMIZED DEPLOYED CONFIGURATION (PLANAR)

The relationship between frequency, blanket tension and boom stiffness is shown in Figure 4-40 for a planar array of the specific mass of the baseline blanket. Aspect ratio; i.e., the ratio of array length to total array width (both halves), is the independent parameter. The final selection of an aspect ratio was made on the basis of a specific mass analysis of the selected design concepts. The principal conclusion to be drawn here is that the deployed frequency of 0.04 Hertz determines boom stiffness and tension requirements.
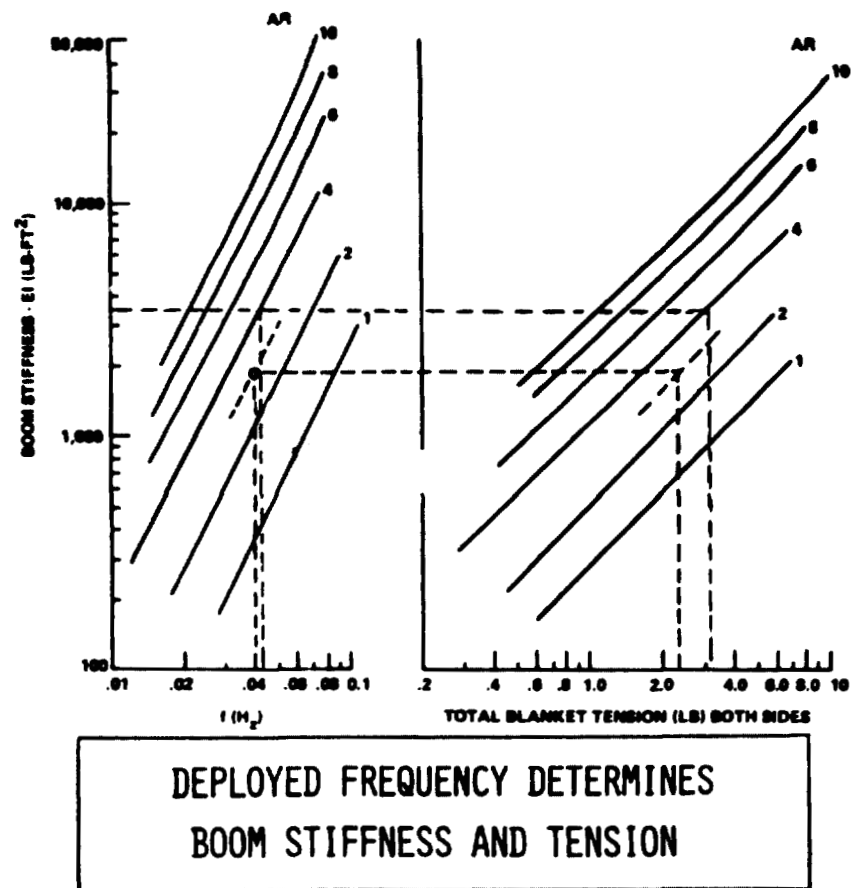
Figure 4-40. Optimized Deployed Configuration (Planar)

4.5.3 SOLAR ARRAY MASS VS ASPECT RATIO

The results of the effect of aspect ratio on mass is shown in Figure 4-41. Note that the optimum range is relatively flat in the area of aspect ratios from 3 to 5. A final calculation of the required characteristics of blanket tension for torsional stiffness and mast modulous of flexure (EI) for out of plane bending was made using the inputs shown in Table 4-20. From this analysis a blanket tension of 712 N (1.6 lbs) on each half, and a boom stiffness of 532 NM^2 (1285 $16+^{+2}$) will be sufficient to meet the design requirements. A more detailed explanation of the dynamic analysis approach is given in Appendix C.

Table 4-20. Baseline Analysis "V-Stiffened" Array

Configuration	
Aspect Ratio	4.0
Total Deployed Length	17.2 m (56.43 ft)
Total Blanket Width	4.42 m (14.5 ft)
LEM Stiffness (EI)	2060 nm^2 (5000 lb ft^2)
Blanket Mass	28 kg (61.7 lbs)
Cant Angle	8.25 degrees
Array Frequency	0.04 Hz
Results	
Required Blanket Tension	7.12 n (1.6 lbs)
Required Mast Stiffness	532 nm^2 (1285 lb ft^2)
Mast Stiffness (% of Planar)	37%
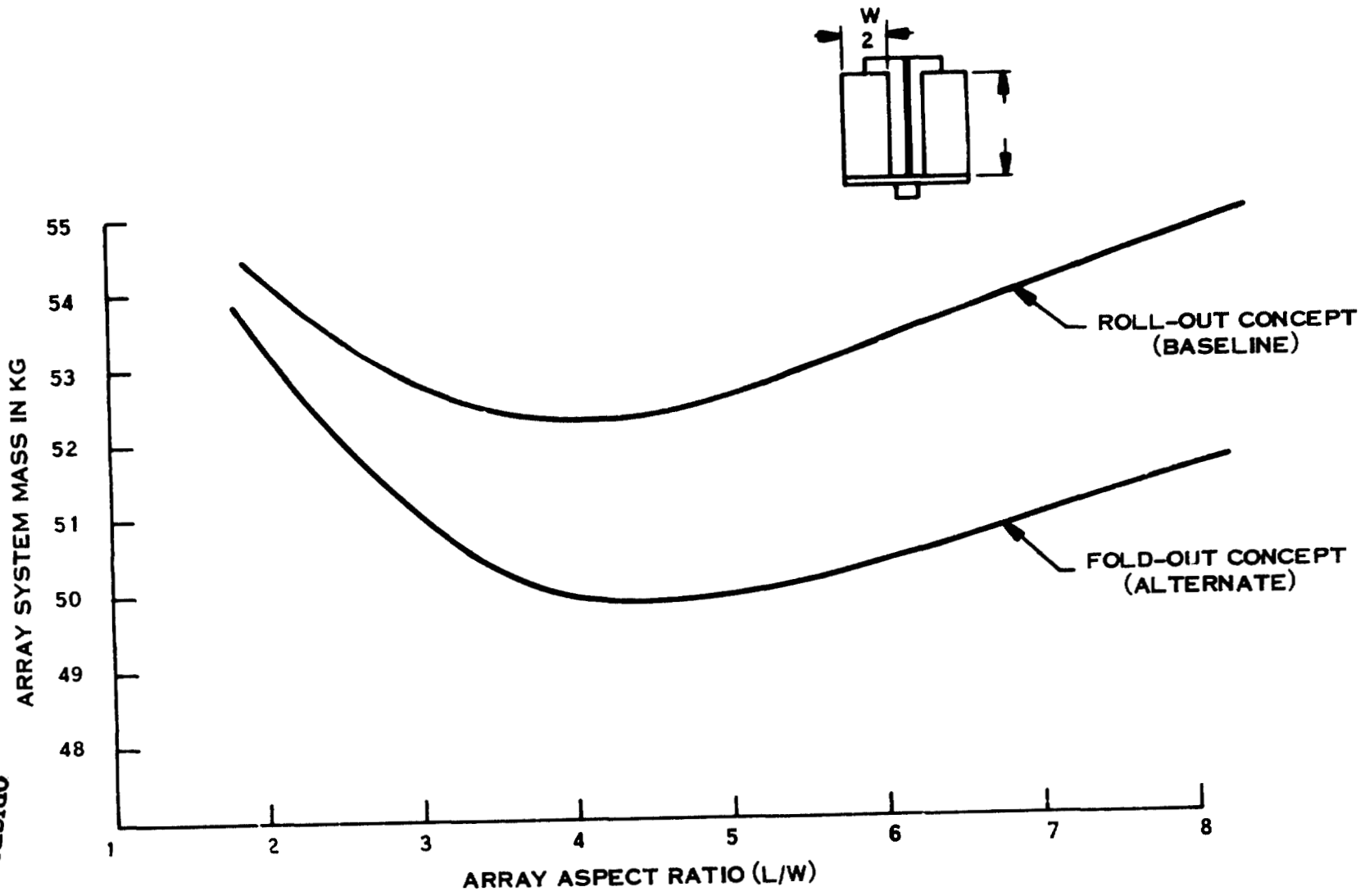
Figure 4-41. Baseline System Mass vs Aspect Ratio

4-111

4.5.4 "V-STIFFENED" ARRAY CHARACTERISTICS

Laboratory tests on a planar array show that there are three regions of different stiffness for in-plane deflections, see Figure 4-42, as follows:

Region 1: For small deflections, hysteretic behavior of the BI-STEM boom caused a relatively high stiffness. This is best predicted semi-empirically and is not predicted by simplified analytical modeling.

Region 2: For medium deflections, the tension distribution of the blankets changes such that the slope (θ) at the tip of the leading edge member is proportional to the tip deflection (δ) divided by the array length (L).

$$\theta = \delta/L$$

This results from a constraining moment at the tip of the boom due to the blanket tension and is valid until the tension shifts to the edges of the blanket.

Region 3: For large deflections, the effect of blanket tension is no longer present and the boom behaves as a cantilever. This occurs after the transitional deflection (when tension shifts to the edges of the blankets at end of Region 2).

Figure 4-42. In-Plane Force Deflection Characteristics for the RA 250 Solar Array

4.5.4 "V-STIFFENED" ARRAY CHARACTERISTICS (CONTINUED)

4.5.4.1 Out-of-Plane Tension Stiffening

In a manner similar to the in-plane stiffening of a planar array, the out-of-plane stiffening effect of a "V" configuration array may be described by an effective linear stiffness factor K_{eff} as shown in Figure 4-43. In this case the displacement of the boom tip (δ) is in the plane of the bisector of the dihedral angle formed by the two blanket halves. The resultant force shows up as a tension at the blanket edge. This tension results in a restoring moment being applied in a sense opposite to the displacement force. Thus, the "V"-configuration solar array couples in-plane tension stiffening with out-of-plane deflections.
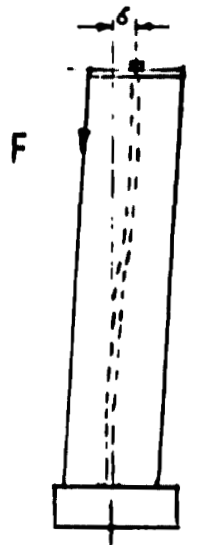
EDGE VIEW
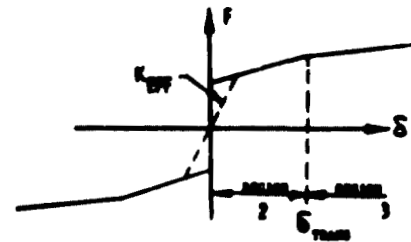
LINEARIZED MODEL

"V" CONFIGURATION COUPLES IN-PLANE
TENSION STIFFENING WITH OUT-OF-PLANE DEFLECTIONS

Figure 4-43.   Out-of-Plane Tension Stiffening

4.5.4 "V-STIFFENED" ARRAY CHARACTERISTICS (CONTINUED)

4.5.4.2 Effect of Cant Angle

Computer runs were made to determine the optimum cant angle (β), where (β) + dihedral angle = 180 degrees. The transitional force (F_t) were calculated using

$$F_t = \left[\frac{4EI}{L^3} - \frac{4T}{15L} \right] \delta + \frac{TW \sin\beta}{L}$$

where

   EI is boom stiffness

   T is for the tension in the blanket

   δ is the displacement of the boom tip

   W and L are the array width and length respectively

The transition force must be greater than 0.32 Newton to meet the quasi-static load requirement and boom stiffness must be greater than 285 N-m^2 to meet the buckling criteria. See Figure 4-44.
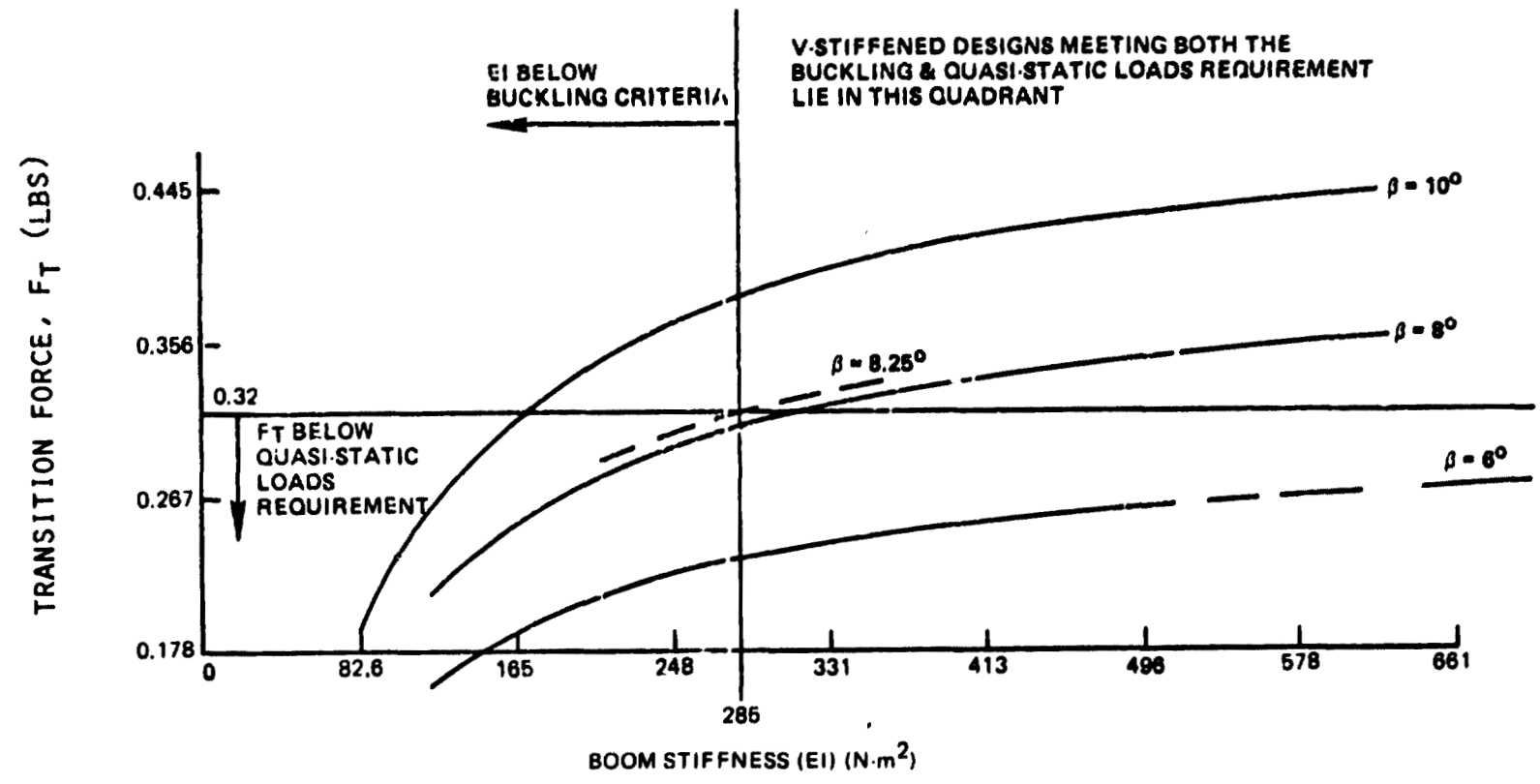
Figure 4-44. Effect of Cant Angle on Transition Force

4.5.5 BUCKLING LOAD CONSTRAINTS

The controlling factor on sizing the boom is boom buckling. See Figure 4-45. The analysis shows that lower EI values will satisfy the 0.04 Hz minimum frequency requirements.

The conservative boom stiffness required for the final design concept is plotted here against the percent of buckling load capacity. The assumed configuration is as follows:

Total deployed length	=	17.2 m (56.43 ft)
Total blanket width	=	4.42 m (14.5 ft)
LEM stiffness (EI)	=	2060 N-m^2 (5000-lb-ft^2)
Cant Angle	=	8.25°
Boom stiffness (range of values)	=	532 N-m^2 (1285 lb-ft^2)
Tension per blanket (range of values)	=	7.12 N (1.6 lbs)
Blanket mass	=	28 kg (61.60 lbs)
Boom mass	=	1.07 kg (2.36 lbs)

With a buckling safety factor of 1.25, a boom stiffness of 532 N-m^2 could be selected. This value is adequate even if the tip deflection should exceed the transitional deflection point beyond which the V-stiffening is not effective. Lower stiffness values can be applied if tip deflection can be shown to be well within the V-stiffened transition ranges.
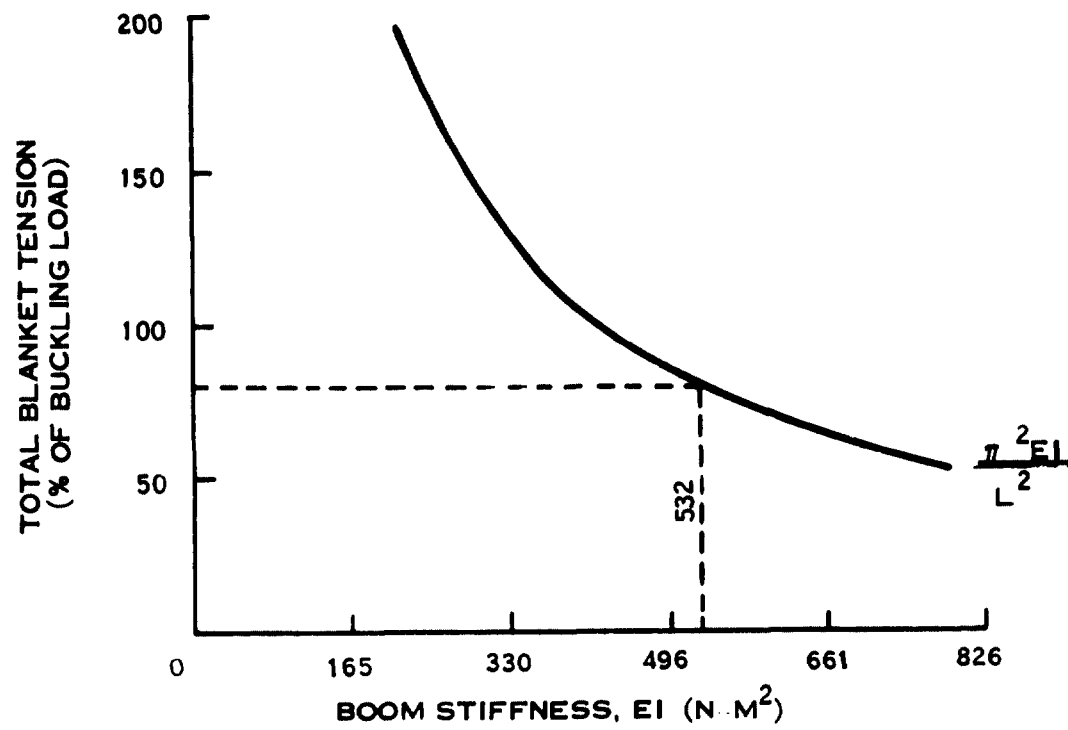
Figure 4-45. Buckling Load Constraint

APPENDIX A

BASELINE REQUIREMENTS
FOR A
200 WATT/KILOGRAM LIGHTWEIGHT
SOLAR PANEL SUBSYSTEM

General Electric Company
Space Division
P. O. Box 8555
Philadelphia, Pa. 19101

Document #200 W/Kg-2.76-004 Rev. 1
15 April 1976

Baseline Requirements

for a

200 Watt/Kilogram Lightweight

Solar Panel Subsystem

Contract No. 954393

Prepared by *Kevin M. Speight*
Kevin M. Speight, Proj. Mgr.
200 W/Kg Solar Array Study

1.0   SCOPE

1.1   This specification covers the requirements for a conceptual

         approach for a 10 kilowatt solar panel design having a

         power-to-weight ratio of 200 watts per kilogram or greater.

         This conceptual approach requires a background of information

         on the influencing parameters, their margins, the trade-offs

         considered, and the rationale developed for a light-weight

         array design as defined by the requirements in paragraph 3.0.

2.0   APPLICABLE DOCUMENT

2.1   The following document forms a part of this specification to

         the extent specified herein:

              MIL-HDBK-5   Metallic Materials and Elements for
                                         Flight Vehicle Structures

3.0   REQUIREMENTS

3.1   Conflicting requirements. In case of conflict between the

         requirements of this specification and the documents

         referenced herein, the requirements of this specification

         shall govern.

3.1.1   Deviations from standard practices. Any deviations from

         generally accepted standard practices will be approved by

         the Jet Propulsion Laboratory (JPL), after it has been

         demonstrated by analysis that the deviations will not degrade

         the overall probability of attaining the objectives of this

         effort. The burden of proof in such circumstances shall rest

         A-2

upon the contractor and not upon JPL.

3.2   Performance requirements. The solar panel shall be designed
       so that the following performance requirements can be met.

3.2.1 General. In the stowed configuration, the solar panel shall
       be supported in a manner that will prevent damage to the
       solar panel under shock and vibration loads. Upon command
       and in proper sequence, the release and deployment mechanism
       shall extend and lock the solar panel into the deployed
       position at a rate to be defined by the contractor. Upon
       command and in proper sequence, the retraction mechanism shall
       retract up to 90% of the solar panel, exposing sufficient area
       to provide up to 10% of the total power, and lock to this
       partially stowed position at a rate defined by the contractor.
       This retraction mechanism will be considered as an option.

3.2.2 Power requirement. Following launch, the deployed solar panel
       shall be capable of supplying 10 kilowatts of electrical power
       at the spacecraft interface at a solar intensity normally
       incident at 1 AU* and at the predicted solar array temperature
       at this intensity.

3.2.3 Lifetime. The solar panel shall be designed to perform over
       a period of 3 years with no greater than a 20 percent loss of
       power, disregarding solar flare proton reduction, and with no
       failures which sould prevent the panel from performing

*1 AU is defined in ASTM Spec E490-73A

successfully in both electrical and mechanical modes. Sound engineering judgement shall be exercised in regard to the depth to which the design is driven by the exclusion of single or multiple failure modes.

3.2.4   Solar panel operating temperature. The thermal characteristics of the deployed panel shall be adjusted so that the celled area maintains a maximum operating temperature of 85°C at a solar intensity normally incident at 1 AU*. The electrical character- istics of the array shall be determined over the temperature range of -100°C to +100°C.

3.2.5   Solar panel weight. The weight of the solar panel in flight configurations, including the release, deployment, and retraction mechanisms, but not including solar panel gimballing mechanisms, shall be such that the solar panel specific power equals or exceeds 200 watts per kilogram at a solar intensity normally incident at 1 AU*.

3.2.6   Packaging volume envelope. The volume and shape of the stowed solar panel, including the release, deployment, retraction and lock (an option) mechanisms, shall be determined by the contractor in order to maximize the solar panel adapta- bility to various spacecraft configurations. In these design considerations, a 2000-pound spacecraft (which includes two 10-kilowatt solar panels and a Shuttle launch vehicle) shall be assumed.

*1 AU is defined in ASTM Spec E490-73A

A-4

The following requirements shall also be included:

a) Launch vehicle shroud volume restrictions

b) Spacecraft structural interface requirements

c) Solar panel deployment complexity (reliability)

d) Solar panel gimballing (Sun tracking) requirements

e) Solar panel retraction complexity (reliability)

f) Solar panel attachment configuration requirements.

3.2.7   <u>Structural interfaces.</u> The solar panel to spacecraft attachment points shall be considered to provide the most efficient interface capable of performing the mission. Consideration shall be given to the ease with which the deployed solar panel can be gimballed (tilted or rotated) with respect to the spacecraft as required by the Sun tracking requirements. Consideration shall also be given to the requirements imposed on the spacecraft structure by the solar panel. A solar panel requiring an extremely rigid support or negligible relative motion between widely spaced support points is undesirable because meeting these requirements might result in increased spacecraft weight.

3.2.8   <u>Structural rigidity.</u> In the deployed configuration, the solar panel shall have sufficient rigidity so that its lowest cantilevered natural frequency of vibration is equal to or greater than 0.04 Hz. In the event this criteria cannot be met, i.e., the cantilevered natural frequency is less than 0.04 Hz, the

interaction of the flexibility of the solar array to the JPL
attitude control system shall be analyzed to assess the impact
of the flexibility of the solar panels on the attitude control
systems.

3.2.9   Mass center location. The solar panel shall be designed to
minimize displacement of the vehicle mass center and center of
solar pressure caused by thermal gradients and solar panel
temperatures.

3.2.10   Flatness. In the deployed configuration the solar panel blanket
celled area shall lie in a predetermined plane with a maximum
angular deviation from this plane of ten (10) degrees. This
deviation shall include deflections caused by thermal gradi
but shall not include deflections caused by dynamic mechan   al
load inputs.

3.2.11   Inspection. Release, deployment, retraction, and locking mechan-
isms, shall be designed so that, with suitable ground support
equipment, their operating functions can be inspected in a one-g
Earth field environment prior to installation on the spacecraft.

3.2.12   Reliability. The solar panel design shall incorporate design
practices that enhance the probability that the solar panel will
operate successfully in both mechanical and electrical modes.

3.3   Environmental requirements. The following environmental require-
ments shall be considered in the design of the solar panel.

A-6

3.3.1   Ground handling. The solar panel's structural, mecha-ical, a..i

electrical performance shall not be degraded because of ground

handling during manufacturing, testing, and transportation

operations.

3.3.2   Launch environment. The following environmental constraints

which represent the launch environment of the solar panel in

the stowed configuration, shall be considered in the solar

panel design.

3.3.2.1   Sinusoidal vibration. Sinusoidal vibration input levels as

shown below will be applied at spacecraft solar array interface

in three orthogonal directions, at a sweep rate of one octave

per minute.

Frequency Range (Hz)	Amplitude
2-5	1.0-inch double amplitude
5-26	1.3 g (0-pk)
26-50	0.036 inch double amplitude
5(-1000	5g (0-pk)

3.3.2.2   Acoustic. The launch acoustics environment shall be 60 seconds

of a random incidence, reverberant sound field, having the

third-octave band sound pressure levels defined in Fig. 1.
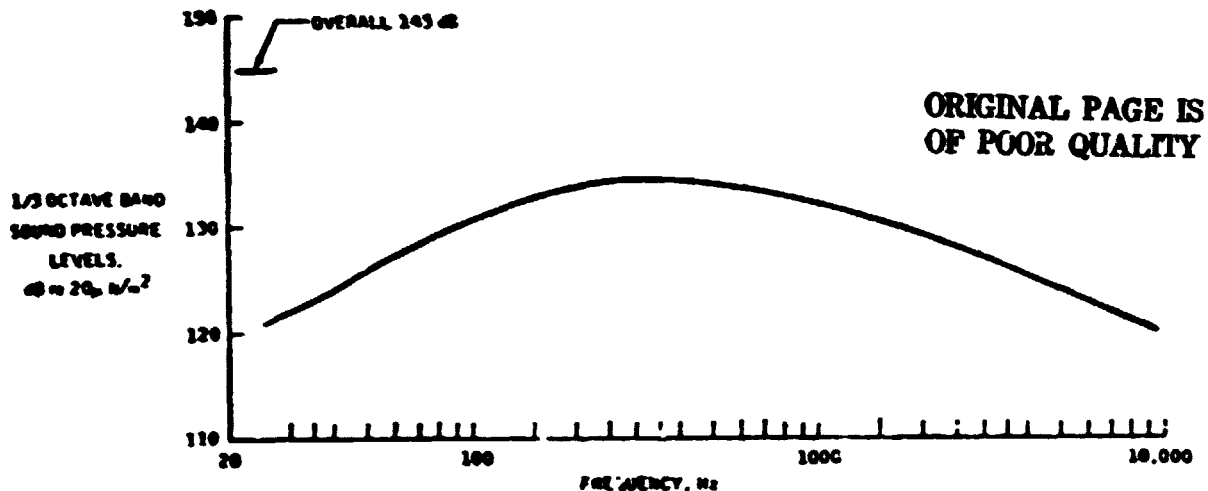
Figure 1.   Acoustic Test Levels

A-7

3.3.2.3   Shock. The worst shock environment will be a 20 g terminal

sawtooth shock pulse of 10 milliseconds duration at the spacecraft

interface in each of three orthogonal directions.

3.3.2.4   Static acceleration. The static acceleration environments shall

be 9 g's at the approximate center of mass of the solar panel

in the stowed configuration. This environment shall be considered

for the axial axes; 2 g's shall be considered for the lateral axis.

3.3.2.5   Launch pressure profile. The solar panel temperature shall be

initially at 27 $\pm6^{o}C$ and at atmospheric pressure. Figure 2

shows the pressure-time history during launch and ascent.

3.3.3   Space flight environment. The following space flight environmental

constraints shall be considered in the solar panel design.

3.3.3.1   Steady state thermal/vacuum environment. The steady state

thermal/vacuum environment shall cover the range from -130 to +140°C

and a pressure of 10^{-5} torr or less.

3.3.3.2   Thermal shock environment. The thermal shock temperature

extremes shall be -190°C and +140°C at a pressure of 10^{-5} torr

or less. The temperature time rate of change during thermal

shock shall be the natural cooling rate of the solar panel in a

simulated passage into a planetary shadow with an assumed planetary

albedo of zero, and the natural heating rate of the solar panel

in a simulated passage from a planetary shadow into a normal solar

A-5
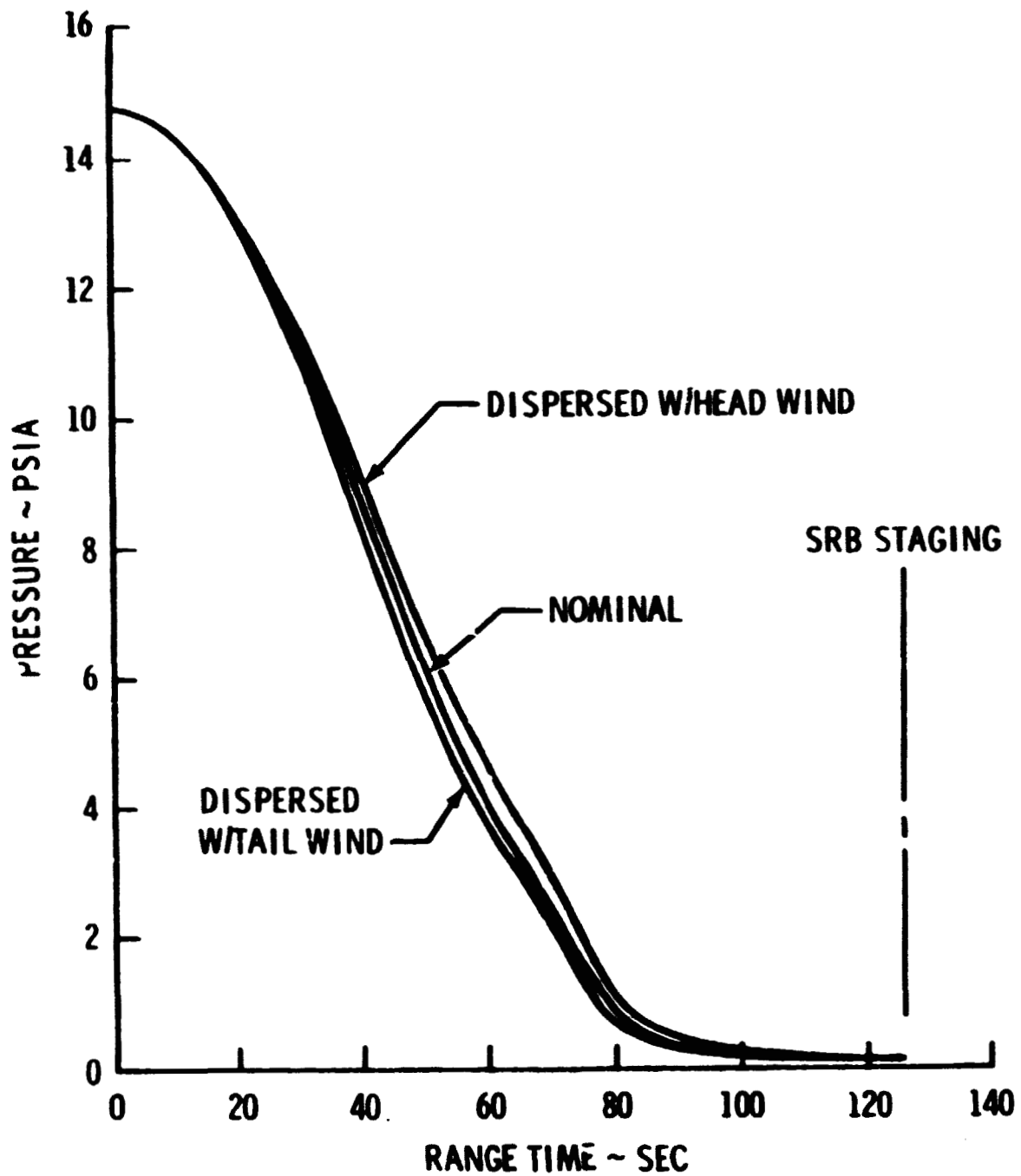
FIGURE 2. ORBITER PAYLOAD BAY INTERNAL PRESSURE
HISTORIES DURING ASCENT

flux of intensity corresponding to a steady state temperature of 140°C on the solar cells. The total thermal shock environment shall consist of 1000 complete cooling and heating cycles.

3.3.3.3   Solar flare proton radiation environment. The proton fluency for the 3-year mission shall be as defined in Table 1.

Table 1. Mission Proton Fluency

Proton Energy (Mev)	Total Fluency (Particles/cm^2)
1	2.0×10^{12}

3.3.3.4   Pyrotechnic shock environment. The solar panel assembly shall be capable of withstanding shock environments induced by the firing of any pyrotechnics that may be required for the operation of the assembly.

3.4   Materials, parts, and processes. Materials, parts, and processes used in the design of the solar panel shall conform to the requirements specified herein. Any materials, parts, and processes that are not so covered shall be subject to the approval of the JPL cognizant engineer. In every case, the contractor's selection shall assure the highest uniform quality of the solar panel.

3.4.1   Material selection criteria. The influence of the following environments and those specified in 3.3 on the design properties

A-10

of the structural, electrical, thermal control, and lubricant materials in the solar panel shall be considered:

(a) Storage at 95 percent relative humidity at $55^{\circ}C$ for 50 hours. The solar array may, however, be protected during delivery to the launch facility by use of appropriate site or ground operations facilites or equipment. If such protection is deemed appropriate, cost weight, and other impacts on the array design shall be evaluated.

(b) 10,000 thermal cycles between $-190^{\circ}C$ and $+140^{\circ}C$ at 10^{-7} torr with a 90-minute cycle, and a temperature stabilization ($< 2^{\circ}C/hr$) dwell at the extreme temperatures.

(c) 1000 thermal shocks as defined in para. 3.3.3.2 "Thermal Shock Environment".

3.4.1.1   <u>Flight environment materials.</u> The materials shall be capable of enduring the space environment without releasing any significant condensing gases which would decrease the solar cell efficiency, or could potentially lead to electrical shorts or degradation to the spacecraft system operation.

3.4.2   <u>Radiation resistance.</u> The dosage and energy levels of the particulate radiation encountered during a mission shall not produce a significant effect on the metallic structural elements. Polymeric materials shall be either shielded or selected to resist a radiation surface dosage of 10^{7} rads without decreasing the critical design properties below the design allowables.

3.4.3   **Exposed structural adhesives.** When adhesives are considered for bonding transparent or partially transparent structural components, the influence of particulate surface dosage radiation of 10^7 rads, and ultraviolet radiation equal to 1095 days of solar radiation at the rate of 2.002 calories/cm^2/minute, on the adhesive shall be considered.

3.4.4   **Diodes.** Diode isolation will be provided in the Power Conditioning circuitry. Therefore, diodes are not required on the solar array.

3.4.5   **Solar Cells.** The candidate solar cells to be used have the following characteristics:

(a) Current-voltage temperature coefficients between -100^oC and $+100^oC$ at 1 AU:

Current: 0.03 ma/^oC-Cm^2
Voltage: -2.0 mv/^oC

These values apply to all cells of any thickness between 0.003 and 0.010 inch.

(b) Physical properties:

Length: 2 to 4 Cm
Width: 2 Cm
Thickness: 0.025 Cm (.010 inch) to 0.0075 Cm (0.003 inch)

(c) Practical contact configuration. See Figure 3.

(d) Interconnecting methods:

Both weldable and solderable solar cells will be considered as available for cell thicknesses between 0.003 and 0.010 inch. The cell contacts will be silver-palladium-titanium

FIGURE 3

SOLAR CELL CONTACT CONFIGURATION

BACK SIDE CONTACTS

FULL CONTACT   PICTURE FRAME CONTACT
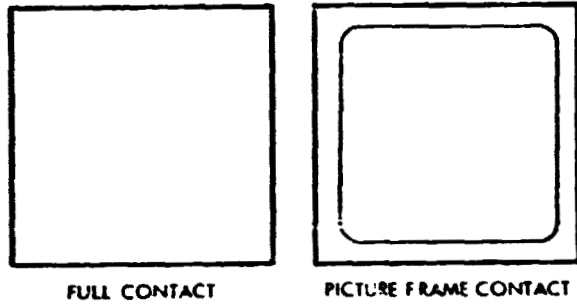
FRONT SIDE CONTACTS

BAR CONTACT   CORNER DART CONTACT   PADS
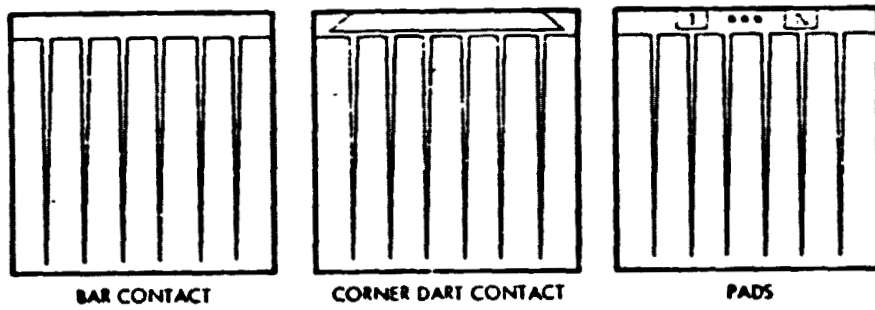
BAR CONTACT:	FULL WIDTH EITHER EDGE, 20 MILS TO ANYTHING DESIRED
WRAP AROUND CONTACT:	ANY CONFIGURATION, SPINE OR FULL WRAP
GRID LINES:	WIDTH, 2 MILS TO 8 MILS; NUMBER 3/Cm to 12/Cm

or silver-chromium. Interconnect materials will be
beryllium-copper, Kovar, molybdenum, or silver. (The
latter two in a mesh configuration have exhibited
superior overall electrical and mechanical behavior
in recent welded contact studies).

(e) Current voltage characteristics at 1 AU, 0.010 inch,
28°C. See Figure 4.

(f) Solar cell efficiency as a function of cell thickness
between 0.002 and 0.008 inch. See Figure 5.

The following assumptions may be used with regard to the
candidate solar cell data:

1. Cells as thin as 0.003-inch can be welded with little or
no degradation in performance.

2. Cells as thin as 0.003-inch can be temperature cycled
between -190°C and +140°C without incurring damage.

3. The use of alternate cells is not to be considered in the
baseline design.

4. The candidate cells described will be available in production
quantities in the timeframe necessary to fabricate actual
arrays.

5. The fill factor will not change over the temperature range
of -100°C to +100°C.

6. Cells thinner than 0.003 inch are not considered practical
and will not be used in the baseline design.
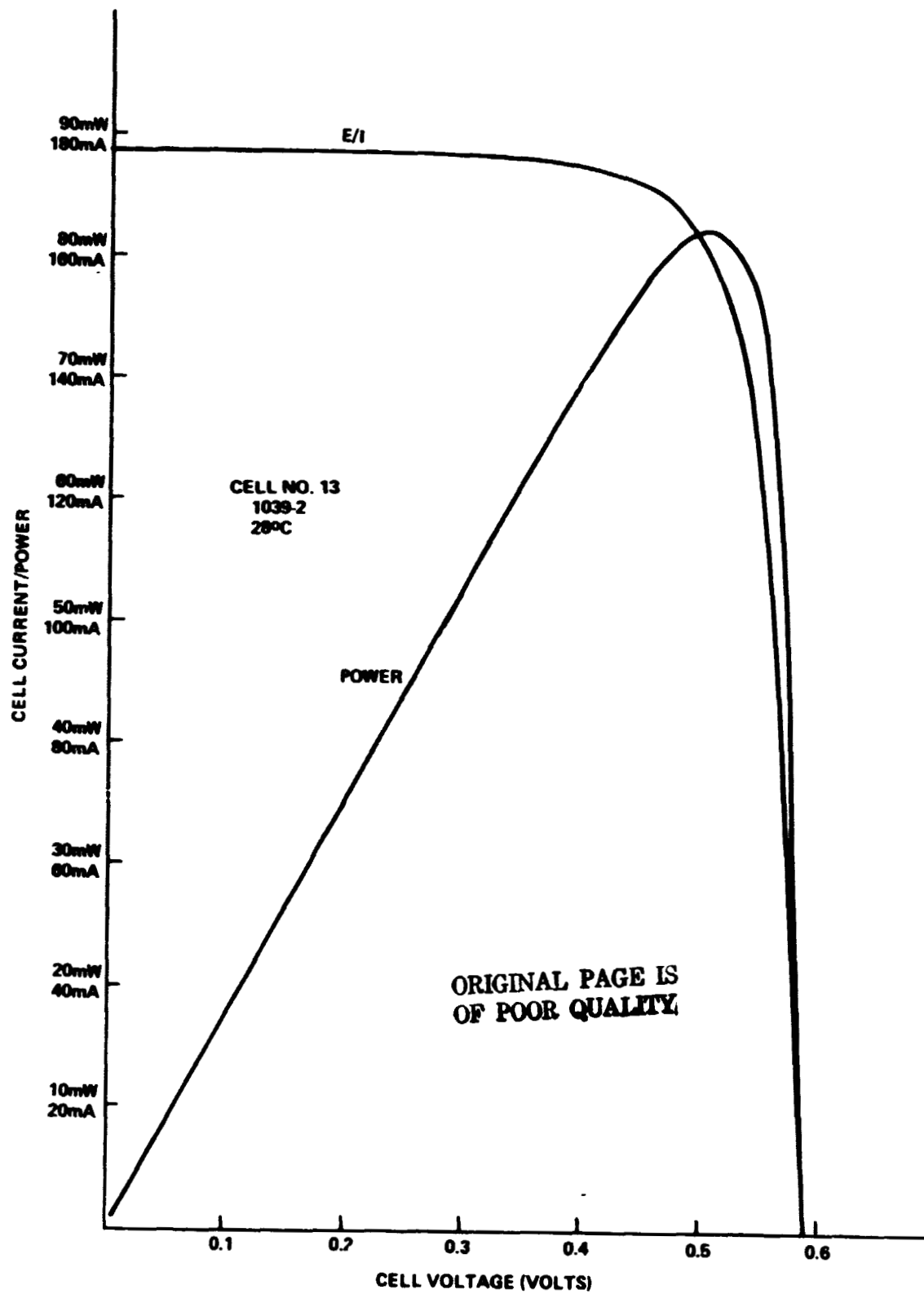
Figure 4   Typical Cell E/I and Power Curves
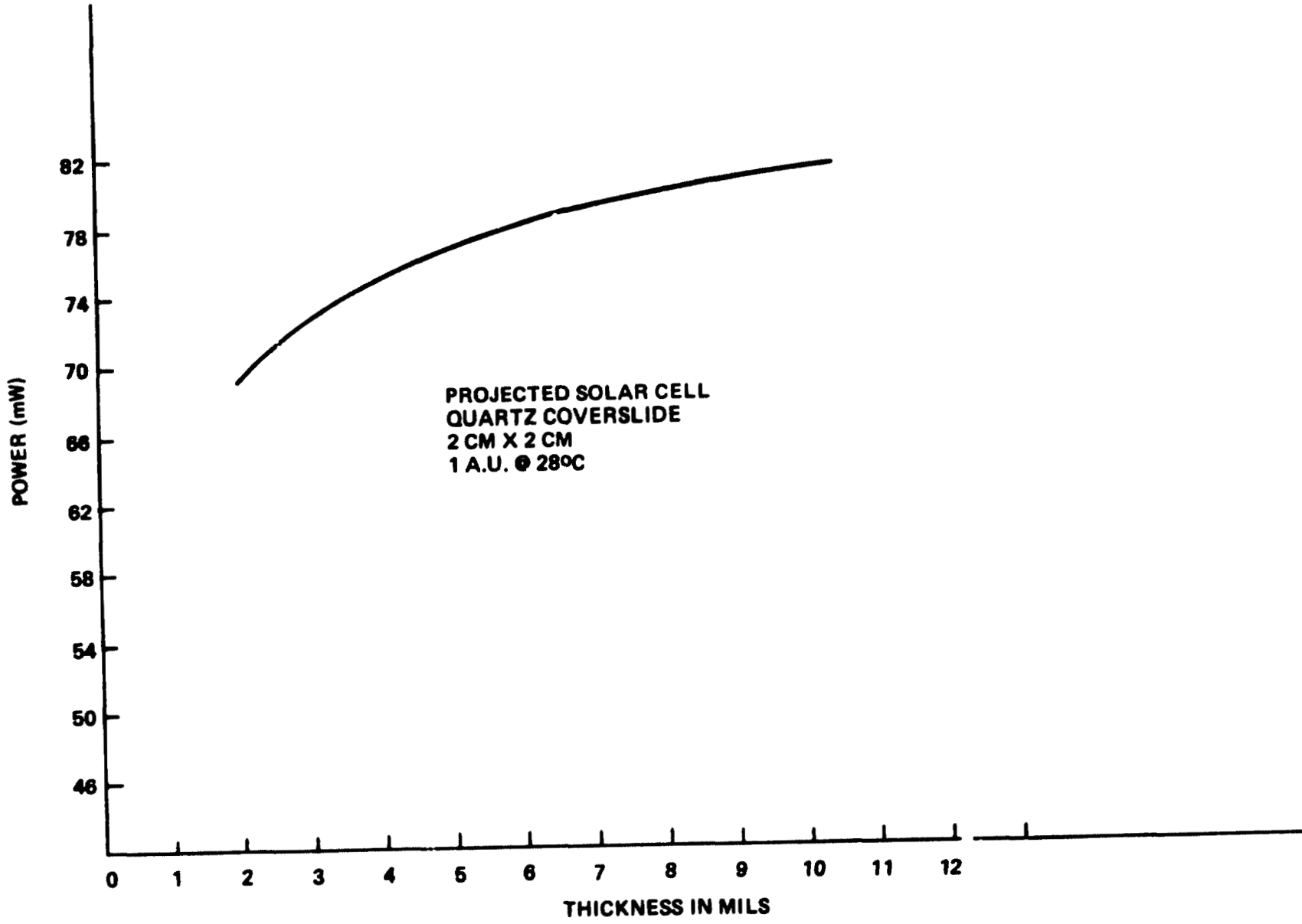
Figure 5   Cell Efficiency vs. Cell Thickness

3.4.6   Solar cell adhesives. A requirement for two separate adhesives

can exist in the solar cell area. One requirement shall be for

an adhesive used to attach the solar cells to the structures;

the second shall be to bond solar cell cover glasses to the

cells. The adhesive for bonding cover glasses to solar cells

shall be transparent to electromagnetic radiation in wavelengths

from 0.4 to 1.0 micron, and shall be resistant to ultraviolet

and particulate radiation. The adhesives shall have the

following properties:

    a) High thermal conductivity
    b) Low outgassing in the vacuum environment
    c) A modulus of elasticity compatible with the thermal
       motion of the cells and structure
    d) Repairability during the fabrication phase.

3.4.7   Solar cell adhesive thickness tolerance. Solar panel and solar

cell installation normally shall require the extensive use of

bonding materials. The thickness a.   :ea of application of

these materials, if used, shall be accurately controlled. The

designs and processes shall include control requirements and

tolerances that can be maintained in the fabrication shops.

3.4.8   Solar cell tolerances. The control of solar cell processing

through the fabrication shops shall be dependent upon the

comparison of initial testing and grading to subsequent cell

testing during the fabrication sequence. The tolerances set

by the design shall be adequate to allow a high yield of

good assemblies.

3.4.9   <u>Solar cell connections.</u> The heat required in joining solar cells can cause degradation in cell performance. The solar cell electrical connecting technique shall be compatible with solar cell interconnection methods and shall exhibit accurate temperature control for minimum power loss.

3.4.10   <u>Solar cell installation.</u> The installation of solar cell assemblies onto substrate panels and the assembly of structural component parts shall be accomplished with protective coverings on the operator's hands, or the handling shall be done with suitable mechanical devices. The configuration of these assemblies shall be designed so that the required work can be accomplished while complying with all handling restrictions.

3.4.11   <u>Thermal control coatings.</u> Degradation of thermal control coatings by the ultraviolet and particulate radiation of the flight environment shall be considered.

3.4.12   <u>Bearings and lubricants.</u> In the event bearings and lubricants are required in the solar panel design, the bearing materials shall resist the thermal excursions and particulate radiation of the flight environment. Lubricants shall not degrade; i.e., lose lubricity under flight conditions up to 1095 days, or release any condensing gases, which would case degradation to the spacecraft system. Possible occurrence of cold welding at hard vacuum shall be evaluated.

3.4.13   Part producibility. Configuration and size of parts shall be
          compatible with normal tooling practices. Very thin foil
          gage parts shall be capable of being fabricated with reasonable
          assurance that damage will not occur and that the part can be
          handled without damage when reasonable precaustions are taken.

3.4.14   Configuration of the solar panel. The configuration of the
          solar panel shall be designed so that positicning and holding
          of components and subassemblies can be accomplished to provide
          support during solar panel assembly.

3.4.15   Repair and replacement. It shall be possible for fabrication
          personnel to repair or replace any components of the solar
          panel at any time during the fabrication or ground handling
          sequence and prior to installation on the spacecraft.

3.5   Mechanical design criteria. The following criteria shall
          govern the mechanical design of the solar panel.

3.5.1   Strength and deflection requirements. All structures, with
          minimum material and geometric properties, shall have adequate
          strength and rigidity to accomplish all requirements. In the
          fulfillment of the strength and deflection requiremerts, the
          worst possible combination of simultaneously applied loads and
          environmental conditions shall be used to determine limit loads
          and design loads. Particular attention shall be given to the
          following.

3.5.1.1 <u>Dynamic loads.</u> During the loads analysis, consideration shall be given to loads induced by the solar panel's elastic and rigid-body response to dynamic excitation in the stowed and/or deployed configuration.

3.5.1.2 <u>Quasi-static loads.</u> The quasi-static loads as a result of vehicles thrust and flight maneuvers shall be 1×10^{-3}g acting upon the deployed solar array.

3.5.1.3 <u>Fatigue considerations.</u> Fatigue shall be considered in the design of structural elements by the avoidance of deleterious residual stresses and stress concentrations in conformity with good design practice. Special attention shall be given to elements subjected to repeated load cycles at high stress levels. Material selection shall include consideration of fatigue characteristics in relation to the design requirements of the structural element.

3.5.1.4 <u>Thermal considerations.</u> Consideration shall be given to deterioration of material properties and to stresses and deformation caused by temperature effects, both prolonged and transient.

3.5.2 <u>Limit load.</u> The limit load shall be the maximum load a structural element is expected to experience during its required functional lifetime, including fabrication, handling, and ground testing. no structural element with minimum material and geometric properties shall yield at limit loads or impair the required functions of the solar panel.

A-20

3.5.3   **Design load.** The design load shall be the limit load multiplied by the safety factor. No structural elemes with minimum material and geometric properties shall experience ultimate stress, failure by instability, or rupture at design load.

3.5.4   **Material properties.** Allowable material properties shall be selected to satisfy the environmental conditions that affect material properties. As a goal, metallic materials shall be in accordance with MIL-HDBK 5.

3.5.5   **Safety factors.** The safety factor is a multiplying factor applied to the limit load to allow for design uncertainties. The following safety factors shall be used as a goal:

a) Structures: 1.25
b) Structural joints, fittings, and brittle material: 1.44.

3.5.6   **Structural qualification test levels.** The environmental levels defined in 3.3 shall be considered as the qualification test levels.

3.5.7   **Structural design.** Simplicity of the analyses and tests shall be considered in the structural design. All structural components shall be amenable to either analytical or experimental demonstration of adequacy.

3.5.8   **Structural nonlinearities.** Nonlinear structural design shall be kept to minimum and used only when linear behavior is not possible.

3 5.8.1   **Energy dissipating mechanisms.** Where possible, all energy dissipating mechanisms used shall have linear force-velocity relationships over a wide range of frequencies, loads and temperatures.

3.5.8.2   **Mechanical backlash.** Particular effort shall be made to avo;d mechanical backlash in all structural connections.

3.5.9   **Separation joint preload.** Attachment of any component to another shall provide for sufficient preload so that no physical separation will occur during ultimate load conditions.

3.5.10   **Design flexibility.** Where practical, the solar panel shall be designed so that additional data and advances of technology may be incorporated at later dates.

3.5.11   **Thermal gradients.** The solar panel shall be designed to minimize thermal gradients in the plane of the solar panel.

3.5.12   **Mechanical integrity.** The solar panel shall be designed to prevent the release of loose parts or gases that could damage or impair the function of the solar panel or other spacecraft subsystems.

3.5.13   **Margins of safety.** Margins of safety are defined with respect to the limit load or the design load as:

$$MS = \frac{* \quad (\text{or} \quad ** \quad)}{\text{limit load (or design load)}} = 1$$

*Load corresponding to yield stress of a structure with minimum geometric and material properties, with consideration of environmental effects on material properties.

**Load corresponding to ultimate stress, instability, or rupture of a structure with minimum geometric and material properties, with consideration of environmental effects on material properties.

3.6   Electrical design criteria. The following criteria shall
       govern the electrical design of the solar panel.

3.6.1 Solar cell efficiency. The contractor shall establish the
       power output based on the photovoltaic characteristics of the
       JPL proposed candidate solar cells and the predicted operating
       temperature of the solar panel. This design effort shall include
       the power losses incurred during fabrication, assembly, cabling,
       and solar panel/spacecraft interfacing considerations.

3.6.2 Electrical insulation. The electrical insulation between the
       solar cells and the solar panel structure shall provide a
       maximum dielectric breakdown strength in air, at standard
       temperatures and pressure conditions, greater than three times
       the open circuit voltage of the solar panel. Leakage resistance
       under the test conditions shall be greater than 10^9 ohms per
       square centimeter of cell area.

3.6.3 Repairability. The solar cell modules shall be constructed,
       and materials shall be selected, so that any defective cell can
       be replaced in a fabrication repair area without damage to
       adjacent cells, electrical insulation, or mounting substrate.

3.6.4 Compatibility of materials. The solar cell stack shall be
       designed to use only materials that are compatible thermally,
       mechanically, and electrically with each other, with the space
       environment, and interface requirements of the solar cells
       substrate.

3.6.5   Interconnections. The solar cells shall be interconnected, both in parallel and in series by metallic conductors. These conductors shall be designed to minimize both thermal and flexural stresses on the solar cell interconnections. The electrical resistance of the interconnections (including solder, if used) shall not exceed 2 percent of the total series resistance of the solar cells. The joint shall be at least as strong as the bond between the semi-conductor meterial and the ohmic contacts. The joining materials shall exhibit stable physical and electrical characteristics in both space and terrestrial environments.

3.6.6   Magnetic field. Solar cell wiring, interconnecting and structural techniques shall be designed to minimize as far as practical the magnetic field produced by the flow of current in the solar panel.

3.6.7   Electrical conductors. The size and configuration of electrical conductors shall be determined by the following considerations:

     a)   Low weight
     b)   Low resistivity
     c)   Minimum magnetic field
     d)   Mechanical strength to endure design loads
     e)   Exterior finish to be resistant to natural and induced environments
     f)   Process adaptability
     g)   Redundancy
     h)   Thermal coefficient of expansion
     i)   Thermal shock (minimum of $30^{\circ}C$/minute) on the cells
     j)   Repairability
     k)   Conductor flexibility.

3.6.8   Conductor insulation. Conductor insulating materials shall be

selected on the basis of the following considerations:

a) Mechanical strength
b) Flexibility
c) Dielectric characteristics
d) Ease of forming or fabricating
e) Flight environment considerations
f) Weight.

3.6.9   Electrical terminals. Terminals shall be used to facilitate

maintenance, repair, and replacement of electrical components.

The following requirements for terminals shall be met:

a) Voltage drop across any terminal shall not exceed 25
    millivolts at rated load.

b) The terminals shall withstand 50 cycles of manual mating and
    unmating without replacement of parts.

c) The terminals shall be accessible for ease of wiring
    installation and for factory or field checkout.

d) The terminals shall be rigidly attached to primary or
    secondary structure.

e) The terminals shall have minimum possible weight.

f) Exterior finish of the terminals shall be resistant to both
    natural and induced environments.

3.6.10   Installation. The installation of wires, terminals, electrical

connectors, and busses shall conform to the following

requirements:

a) Busses and other wiring shall be installed in order to
    minimize as far as practical magnetic fields.

b) Installation shall withstand the rigors of normal handling
    and transportation as well as launch and operational
    maneuvers.

c) Installation shall be designed to facilitate service and
    repair activities.

3.6.11   Electrical checkout. Test terminals shall be provided on
         the solar panel to permit ground testing and checkout prior
         to launch, in a one-g Earth field, with suitable ground
         support equipment (GSE).

APPENDIX B

ATSM STANDARD SPECIFICATION E490-73a
SOLAR CONSTANT AND AIR MASS
ZERO SOLAR SPECTRAL
IRRADIANCE

ASTM Designation: E 490 – 73a

Standard Specification for
SOLAR CONSTANT AND AIR MASS ZERO SOLAR SPECTRAL IRRADIANCE[1]

This Standard is issued under the fixed designation E 490, the number immediately following the designation indicates the year of original adoption or, in the case of revision, the year of last revision. A number in parentheses indicates the year of last reapproval.

1. Scope

1.1 This specification defines the solar constant and the zero air mass solar spectral irradiance for use in thermal analysis, thermal balance testing, and other tests of spacecraft and spacecraft components and materials.

1.2 This specification is based upon data from experimental measurements made from high-altitude aircraft, balloons, spacecraft, and the earth's surface. The stated accuracies are based on the estimated accuracies of the measurements, calibrations, and radiometric scales.

2. Applicable Documents

2.1 *ASTM Standards.*
E 349 Definitions of Terms Relating to Space Simulation[2]

3. Definitions of Terms

3.1 *air mass* (optical air mass) (AM)—the ratio of the path length or radiation through the atmosphere (I_m) at any given angle, Z deg, to the sea level path length toward the zenith (I_z).

$$AM = I_m/I_z \cong \sec Z, \text{ for } Z \leq 62 \text{ deg}$$

Symbol: AM1 (air mass one), AM2 (air mass two)

3.2 *air mass zero* (AM0)—the absence of atmospheric attenuation of the solar irradiance at one astronomical unit from the sun.

3.3 *astronomical unit* (AU)—a unit of length defined as the mean distance between the earth and the sun that is, 149 597 890 ± 500 km).

3.4 *irradiance at a point on a surface* (E) —quotient of the radiant flux incident on an element of the surface containing the point, by the area of that element, measured in $W \cdot m^{-2}$

3.5 *irradiance, spectral* (E_λ)—the irradiance per unit wavelength interval at a specific wavelength, or as a function of wavelength measured in $W \cdot m^{-2} \cdot \mu m^{-1}$.

3.6 *integrated irradiance*—spectral irradiance integrated over a specific wavelength interval from λ_1 to λ_2, measured in $W \cdot m^{-2}$.

Symbol: $E_{\lambda_1-\lambda_2} = \int_{\lambda_1}^{\lambda_2} E_\lambda d\lambda$

3.7 Additional definitions will be found in Definitions E 349.

4. Solar Constant

4.1 The solar constant, based on the average of the values shown in Table 1, is 1353 $W \cdot m^{-2}$. The estimated error is ±21 $W \cdot m^{-2}$.

4.2 Table 2 summarizes the results in different units, and Table 3 presents the total solar irradiance at various planetary distances from the sun.

5. Solar Spectral Irradiance (Air Mass Zero)

5.1 The zero air mass solar spectral irradiance is based on data from the NASA 711 research aircraft experiments (1,2,3)[3] (see Table 4) with additions and revisions based on other recent measurements (16). Previously compiled solar spectral irradiances were based on ground-based measurements (17 to 25) and some measurements from rockets (26). Spectral irradiance data from the NASA Ames Research Center (27) were not included because of

---

[1] This specification is under the jurisdiction of ASTM Committee E-21 on Space Simulation.
Current edition approved Sept. 27, 1973 and Dec 27, 1973 Published January 1974
[2] 1974 Annual Book of ASTM Standards, Part 41
[3] The boldface numbers in parentheses refer to the list of references at the end of this specification.

calibration uncertainties. Further discussion on the methods of calculation and historical information can be found in Refs (3,16,28 to 31).

5.2 Table 5 presents the solar spectral irradiance in tabular form for the range from 0.115 to 1000 μm. The first column gives the wavelength (λ) in μm; the second gives the spectral irradiance (E_λ) at λ in $W \cdot m^{-2} \cdot \mu m^{-1}$; the third gives the total irradiance for the range from 0 to λ ($E_{0-\lambda}$) in $W \cdot m^{-2}$; and the fourth gives the percentage of the solar constant associated with wavelengths shorter than λ ($D_{0-\lambda}$).

5.3 Table 6 presents an abridged version of Table 5. Figure 1 plots the Standard Solar Spectral Irradiance.

5.4 The irradiance in the range from 0 to 0.115 μm (nearly 0.0025 $W \cdot m^{-2}$) is based on Hinteregger's results (32). In the 0.14 to 0.20-μm range, the values are based on Naval Research Laboratory data (17, 36), which have been adjusted downward because of data by Heath (33) and Parkinson and Reeves (34). In the range from 0.20 to 0.30 μm, the values of the Goddard Space Flight Center curve have been retained because of confirming Nimbus satellite data (33). The Epply-JPL data were used for revision in the range from 0.3 to 0.7 μm (9 to 13). The 20 to 1000-μm range (9 to 13, 16) irradiances were computed from the combined data or the brightness temperature of the sun from many different authors as quoted by Shimabukoro and Stacey (35).

REFERENCES

(1) Thekaekara, M. P., Kruger, R., and Duncan, C. H. "Solar Irradiance Measurements from a Research Aircraft," *Applied Optics*, APOPA, Vol 8, No. 8, August 1969, pp. 1713–1732.

(2) Thekaekara, M. P., et al. "The Solar Constant and the Solar Spectrum Measured from a Research Aircraft at 38,000 Feet," NASA, Goddard Space Flight Center, *Report X-322-68-304* (Greenbelt, Md.), August 1968. (Also available as *NASA TMX-63324*.)

(3) Thekaekara, M. P., "The Solar Constant and the Solar Spectrum Measured from a Research Aircraft," *NASA TR R-351*, NASNA, Nat Aeronautics and Space Administration, October 1970.

(4) Kondratyev, K. Y., and Nikolsky, G. A., "Solar Radiation and Solar Activity," *Quarterly Journal of the Royal Meteorological Society*, QJRMA, Vol 96, No. 3, July 1970, pp. 509–522.

(5) Kondratyev, K. Y., Nikolsky, G. A., Badinov, J. Y., and Andreev, S. D., "Direct Solar Radiation up to 30 km and Stratification of Attenuation Components in the Stratosphere," *Applied Optics*, APOPA, Vol 6, No. 2, February 1967, pp. 197–207.

(6) Murcray, D. G., "Balloon Borne Measurements of the Solar Constant," *Report AFCRL-69-0070*, University of Denver, January 1969

(7) Murcray, D G., Kyle T. G., Kosters, J. J., and Gast, P R "The Measurement of the Solar Constant from High Altitude Balloons," *Report AFCRL 68-0452*, University of Colorado, August 19 3.

(8) Drummond, A. J., Hickey, J. R., Scholes, W. J., nd Laue, E G., "New Value of the Solar Constant of Radiation," *Nature*, Vol 218, No. 5138, April 20, 1968, pp. 259–261

(9) Drummond A J., and Hickey, J R., "The Epplcy-JPL Solar Constant Measurement Program," *Solar Energy*, Vol 12, No 2 December 1968, pp. 217–232.

(10) Laue, E. G., and Drummond, A. J, "Solar Constant: First Direct Measurements," *Science*, Vol 161, No. 3844, August 1968, pp. 888–891.

(11) Drummond, A. J., Hickey, J. R., Scholes, W. J., and Laue, E. G., "The Eppley-JPL Solar Constant Measurement Experiment," *Proceedings of the International Astronautical Federation 17th Congress, Madrid*, Vol 2, 1966, Gordon and Breach, New York, N Y., 1967, pp. 227–235.

(12) Drummond, A. J., Hickey, J. R., Scholes, W. J., and Laue, E. G., "Multichannel Radiometer Measurement of Solar Irradiance," *Journal of Spacecraft and Rockets, Devoted to Astronautical Science and Technology*, JSCRA, Vol 4, No. 9, September 1967, pp. 1200–1206.

(13) Drummond, A. J. Hickey, J. R. Scholes, W. J. and Laue, E. G., "The Calibration of Multichannel Radiometers for Application in Spacecraft and Space Simulation Programs," *Proceedings of the International Astronautical Federation 18th Congress, Belgrade*, Vol 2, 1967, Pergamon Press, New York, N. Y., 1968, pp. 407–422.

(14) Plamondon, J. A., "The Mariner Mars 1969 Temperature Control Flux Monitor," *Jet Propulsion Laboratory Space Programs Summary 37-59*, Vol 3, October 1969, pp 162–168

(15) Willson, R. C., "New Radiometric Techniques and Solar Constant Measurements," paper presented at the 1971 International Solar Energy Society Conference, May 10-14, 1971, Goddard Space Flight Center, Greenbei., Md., "Summaries and Abstracts," p. iv-8 Willson, R C., "Active Cavity Radiometric Scale, International Pyrheliometric Scale and Solar Constant," *Journal of Geophysical Research*, JGREA, Vol 76, No. 19, 1971, pp 4325–4340

(16) Thekaekara, M P., and Drummond, A J, "Standard Values for the Solar Constant and its Spectral Components," *Nature, Physical*

Sciences, Vol 229, No. 1, Jan. 4, 1971, pp. 6 9.

(17) Johnson. F. S., "The Solar Constant," *Journal of Meteorology*, JOMYA, Vol 11, No. 6, December 1954, pp. 431 439.

(18) Moon, P., "Proposed Standard Solar Radiation Curves for Engineering Use," *Journal of the Franklin Institute*, JFINA, Vol 230, November 1940, pp. 583 617.

(19) Aldrich, L. B., and Abbot, C. G., "Smithsonian Pyrheliometry and the Standard Scale of Solar Radiation," *Smithsonian Institution Publications, Miscellaneous Collection*, SIPMA, Vol 110, No. 5, Publ. No. 3920, Washington, D.C., April 15, 1948.

(20) Aldrich, L. B., and Hoover, W. H., "The Solar Constant," *Science*, Vol 116, No. 3024, Dec. 12, 1952, p. 3.

(21) Dunkelman, L., and Scolnik, R., "Solar Spectral Irradiance and Vertical Attenuation in the Visible and Ultraviolet," *Optical Society of America, Journal*, JOSAA, Vol 49, No. 4, April 1959, pp. 356-367.

(22) Allen, C. W., "Solar Radiation," *Quarterly Journal of the Royal Meteorological Society*, QJRMA, Vol 84, No. 362, October 1958, pp. 307-318.

(23) Nicolet, M., "Sur le Problème de la Constante Solaire," *Annales d'Astrophysique*, AATRA, Vol 14, No. 3, July-September, 1951, pp. 249 265.

(24) Labs, D., and Neckel, H., "The Radiation of the Solar Photosphere from 200 Å to 100μ," *Zeitschrift für Astrophysik*, ZEASA, Vol 69, 1968, pp. 1-73.

(25) Makarova, E. A., "A Photometric Investigation of the Energy Distribution in the Continuous Solar Spectrum in Absolute Units," *Soviet Astronomy-Aj*, SAAJA, Vol 1, No. 4, April 1957, pp. 531 546.

(26) Detwiler, C. R., Garrett, D. L., Purcell, J. D., and Tousey, R., "The Intensity Distribution in the Ultraviolet Solar Spectrum," *Annales de Geophysique*, AGEPA, Vol 17, No. 3, July--September 1961, pp. 9-18.

(27) Arvesen, J. C., Griffin, R. N., and Pearson, B.

D., Jr., "Determination of Extraterrestrial Solar Spectral Irradiance from a Research Aircraft," *Applied Optics*, APOPA, Vol 8, No. 11, November 1969, pp. 2215 2232.

(28) Thekaekara, M. P., "Proposed Standard Values of the Solar Constant and the Solar Spectrum," *Journal of Environmental Sciences*, JEVSA, Vol 13, No. 4, September-October 1970, pp. 6-9.

(29) Thekaekara, M. P., "The Solar Constant and Spectral Distribution of Solar Radiant Flux," *Solar Energy*, Vol 9, No. 1, January-March 1965, pp. 7-20.

(30) Thekaekara, M. P., "Survey of the Literature on the Solar Constant and the Spectral Distribution of Solar Radiant Flux," *NASA SP-74*, NSSPA, National Aeronautics and Space Administration, Washington, D. C., 1965. (Also available as *NASA-N65-22362*).

(31) Duncan, C. H., "Radiation Scales and the Solar Constant," *Proceedings*, 4th Space Simulation Conference, American Institute of Aeronautics and Astronautics, Los Angeles, Calif., 1969. (Also available as GSFC document X-713-69-382.)

(32) Hinteregger, H. E., "The Extreme Ultraviolet Solar Spectrum and Its Variation During a Solar Cycle," *Annales de Geophysique*, AGEPA, Vol 26, No. 2, 1970, pp. 547-554.

(33) Heath, D. F., "Observations on the Intensity and variability of the Near Ultraviolet Solar Flux from the Nimbus III Satellite," *Journal of Atmospheric Sciences*, JAHSA, Vol 26, No. 5, Part 2, September 1969, pp. 1157-1160.

(34) Parkinson, W. H., and Reeves, E. M., "Measurements in the Solar Spectrum Between 1400 A and 1875 A with a Rocket Borne Spectrometer," *Solar Physics*, SLPHA, Vol 1, 1969, pp. 342 347.

(35) Shimabukoro, F. J., and Stacey, J. M., "Brightness Temperature of the Quiet Sun at Centimeter and Millimeter Wavelengths," *Astrophysical Journal*, ASJOA, Vol 152, No. 6, June 1968, pp. 777-782.

TABLE 1 Solar Constant

Platform	Detector	Year	Solar Constant, W m²	Ref
NASA 71 aircraft	Hy-Cal pyrheliometer	1967	1358	1,2,3
NASA 711 aircraft	Angström 7635	1967	1349	1,2,3
NASA 711 aircraft	Angström 6618	1967	1343	1,2,3
NASA 711 aircraft	cone radiometer	1967	1358	1,2,3
Soviet balloon	U of Leningrad actinometer	1961 1968	1353	4,5
U of Denver balloon	Eppley pyrheliometer	1969	1338	6,7
Eppley-JPL high-altitude aircraft	Eppley pyrheliometer	1966 1968	1360	8 to 13
Mariner VI and VIII spacecraft	cavity radiometer	1969	1353	14
JPL balloon	cavity radiometer	1968 1969	1368	15
Average estimated error			1353 ± 21	

611

TABLE 2 Solar Constant Conversion Factors

Solar constant = 1353 W·m⁻² (±21 W·m⁻²) [preferred unit]

= 0.1353 W·cm⁻²
= 135.3 mW·cm⁻²
= 1.353 × 10⁶ erg·cm⁻²·s⁻¹
= 125.7 W·ft⁻²
= 1.940 cal·cm⁻²·min⁻¹ (±0.03 cal·cm⁻²·min⁻¹)
= 0.0323 cal·cm⁻²·s⁻¹
= 429.2 Btu·ft⁻²·h⁻¹
= 0.119 Btu·ft⁻²·s⁻¹
= 1.937 Langleys·min⁻¹

The calorie is the thermochemical calorie-gram and is defined as 4.1840 absolute joules. The Btu is the thermochemical British thermal unit and is defined by the relationship: 1 Btu (thermochemical)/(°F × lb) = 1 cal·g (thermochemical)/(°C × g).

The Langley, however, is defined in terms of the older thermal unit the calorie·g (mean), that is, 1 Langley = 1 cal·g (mean)·cm⁻²; 1 cal·g (mean) = 4.19002 J

TABLE 3 Solar Irradiance at the Planets

Planet	Solar Irradiance, W·m⁻²		
	Mean	Perihelion	Aphelion
Mercury	9029.0	14309.0	6211.0
Venus	2586.0	2621.0	2551.0
Earth	1353.0	1399.0	1309.0
Mars	583.0	709.0	487.0
Jupiter	50.0	55.2	45.5
Saturn	14.9	16.6	13.4
Uranus	3.68	4.07	3.34
Neptune	1.496	1.50u	1.493
Pluto	0.870	1.556	0.555

TABLE 4 Spectral Irradiance Instruments On Board the NASA 711 Galileo Research Aircraft, Used for Obtaining the GSFC Curve of Solar Spectral Irradiance (Refs 1, 2, 3)

Instrument	Energy Detector	Type of Instrument	Aircraft Window Material	Wavelength Range, μm
Perkin-Elmer monochromator	1P28 tube, thermocouple	LiF prism	sapphire	0.3 0.7 0.7 4
Leiss monochromator	EMI 9558QA, PbS cell	quartz double prism	Dynasil quartz	0.3 0.7 0.7 1.6
Filter radiometer	phototube	dielectric thin films	Dynasil quartz	0.3 1.2
P-4 interferometer	1P28 or R136 PbS cell	Soleil prism	Infrasil quartz	0.3 0.7 0.7 2.5
I-4 interferometer	thermistor bolometer	Michelson mirror	Irtran 4	2.6 15

612

TABLE 5 Solar Spectral Irradiance—Standard Curve

λ = wavelength, μm.
E_λ = solar spectral irradiance averaged over small bandwidth centered at λ, W·m⁻²·μm⁻¹
$E_{0-\lambda}$ = integrated solar irradiance in the wavelength range 0 to λ, in W·m⁻².
$D_{0-\lambda}$ = percentage of solar constant associated with wavelengths shorter than λ, and solar constant = 1353 W·m⁻²

NOTE—Lines indicate change in wavelength interval of integration.

λ	E_λ	$E_{0-\lambda}$	$D_{0-\lambda}$
.115	.007	.0025	.0001
.120	.008	.0048	.0002
.125	.007	.0070	.0005
.130	.007	.0071	.0005
.140	.030	.0073	.0005
.150	.070	.0078	.0005
.160	.230	.0093	.0006
.170	.630	.0136	.0010
.180	1.250	.0230	.0016
.190	2.710	.0428	.0031
.200	10.7	.1090	.0081
.210	22.9	.2778	.0205
.220	57.5	.6794	.0502
.225	66.5	.9850	.0728
.230	66.7	1.3140	.0971
.235	59.3	1.6290	.1204
.240	63.0	1.9356	.1430
.245	72.3	2.2730	.1680
.250	70.6	2.6306	.1944
.255	104.0	3.0666	.2266
.260	130	3.6516	.269
.265	185	4.4391	.328
.270	232	5.4016	.405
.275	204	6.5716	.485
.280	222	7.6366	.564
.285	315	8.9791	.663
.290	482	10.9716	.810
.295	584	13.6366	1.007
.300	514	16.3016	1.210
.305	603	19.1741	1.417
.310	689	22.6041	1.655
.315	764	26.0366	1.924
.320	830	30.0216	2.218
.325	975	34.5341	2.552
.330	1059	39.6191	2.920
.335	1081	44.9691	3.323
.340	1074	50.3566	3.721
.345	1069	55.7141	4.117
.350	1093	61.1191	4.517
.355	1083	66.5591	4.919
.360	1068	71.9366	5.316
.365	1132	77.4366	5.723
.370	1181	83.2191	6.150
.375	1157	89.0641	6.502
.380	1120	94.7566	7.003
.385	1098	100.3016	7.413
.390	1098	105.7916	7.819
.395	1189	111.5091	8.241
.400	1429	118.0541	8.725
.405	1644	125.7366	9.293
.410	1751	134.224	9.920
.415	1774	143.036	10.572
.420	1747	151.039	11.222
.425	1693	160.439	11.858
.430	1639	168.769	12.473
.435	1663	177.024	13.083
.440	1810	185.706	13.725
.445	1922	195.036	14.415
.450	2006	204.056	15.140
.455	2057	215.014	15.891
.460	2066	225.321	16.653
.465	2048	235.606	17.413
.470	2033	245.809	18.167
.475	2044	256.001	18.921
.480	2074	266.296	19.681
.485	1976	276.421	20.430
.490	1950	286.236	21.155
.495	1960	296.011	21.878
.500	1942	305.766	22.599
.505	1920	315.421	23.312
.510	1882	324.926	24.015
.515	1833	334.214	24.701
.520	1833	343.379	25.370
.525	1852	352.591	26.059
.530	1842	361.826	26.742
.535	1818	370.976	27.418
.540	1783	379.979	28.084
.545	1754	388.021	28.737
.550	1725	397.519	29.340
.555	1720	406.131	30.017
.560	1695	414.669	30.646
.565	1705	423.169	31.276
.570	1712	431.711	31.907
.575	1719	440.269	32.541
.580	1715	448.074	33.176
.585	1712	457.441	33.889
.590	1700	465.971	34.439
.595	1682	474.576	35.066
.600	1666	482.796	35.603
.605	1647	491.079	36.295
.61	1635	499.204	36.902
.62	1602	515.469	38.098
.63	1570	531.329	39.270
.64	1544	546.899	40.421
.65	1511	562.174	41.550
.66	1486	577.159	42.657
.67	1456	591.069	43.744
.68	1427	606.284	44.418
.69	1402	620.429	45.855
.70	1369	634.284	46.879
.71	1344	647.849	47.882
.72	1314	661.139	48.946
.73	1290	674.159	49.826
.74	1260	686.909	50.761
.75	1235	699.304	51.691
.76	1211	711.614	52.595
.77	1185	723.594	53.600
.78	1159	735.314	54.348
.79	1134	746.779	55.194
.80	1109	757.994	56.023
.81	1085	760.944	56.834
.82	1060	779.694	57.627
.83	1036	790.176	58.601
.84	1013	800.619	59.158
.85	990	810.434	59.899
.86	968	828.224	60.622
.87	947	829.794	61.330
.88	926	839.164	62.022
.89	908	848.334	62.770
.90	891	857.329	63.365
.91	880	866.184	64.019
.92	869	874.929	64.665
.93	858	883.564	65.304
.94	847	892.009	65.934
.95	837	900.569	66.556
.96	820	908.794	67.168
.97	803	916.909	67.768
.98	785	924.849	68.355
.99	767	932.609	68.928
1.00	748	940.184	69.484
1.05	688	975.504	72.105
1.10	653	1007.109	74.435
1.15	535	1035.309	76.519
1.20	465	1060.009	78.404
1.25	436	1083.884	80.189
1.30	397	1104.759	81.652
1.35	358	1123.634	83.067
1.40	337	1141.009	84.331
1.45	312	1157.234	85.530
1.50	288	1172.234	86.639
1.55	267	1186.109	87.605
1.60	245	1198.909	88.611
1.65	223	1210.609	89.475
1.70	202	1221.234	90.261
1.75	188	1230.784	90.967
1.80	159	1239.259	91.593
1.85	142	1246.784	92.199
1.90	126	1253.484	92.644
1.95	114	1259.484	93.000
2.00	103	1264.909	93.409
2.1	90	1274.559	94.2024
2.2	79	1283.009	94.8269
2.3	69	1290.609	95.3734
2.4	62	1296.959	95.4500
2.5	55	1302.009	96.2903
2.6	40	1307.959	96.6710
2.7	43	1312.509	97.0073
2.8	39	1316.609	97.3103
2.9	35	1320.309	97.5038
3.0	31	1323.509	97.8277
3.1	26.0	1326.459	98.0303
3.2	22.6	1328.809	98.2179
3.3	19.2	1330.979	98.3724
3.4	16.6	1332.769	98.5047
3.5	14.6	1334.329	98.6208
3.6	13.5	1335.734	98.7238
3.7	12.3	1337.024	98.8192
3.8	11.1	1338.194	98.9056
3.9	10.3	1339.244	8.9847
4.0	9.5	1340.254	99.0579
4.1	8.70	1341.1641	99.12571
4.2	7.80	1363.9891	99.19618
4.3	7.10	1342.7341	99.24124
4.4	6.50	1343.4141	99.29150
4.5	5.92	1344.0351	99.33740
4.6	5.35	1344.5906	99.37905
4.7	4.86	1345.1091	99.41670
4.8	4.47	1345.5757	99.45127
4.9	4.11	1346.0041	99.48290
5.0	3.79	1346.3499	99.51219
6	1.8200	1349.2049	99.71950
7	.9960	1350.6099	99.82335
8	.5850	1351.3974	99.88155
9	.3670	1351.8734	99.91673
10	.2410	1352.1774	99.93920
11	.1650	1352.3804	99.95420
12	.1170	1352.5216	99.96462
13	.0851	1352.6224	99.97209
14	.0634	1352.6907	99.97750
15	.0481	1352.7524	99.98170
16	.037100	1352.7950	99.98465
17	.029100	1352.8291	99.98730
18	.02310	1352.8542	99.98923
19	.0186	1352.8751	99.99077
20	.015200	1352.8920	99.99202
25	.006170	1352.9454	99.99596
30	.002970	1352.9603	99.99765
35	.001600	1352.9707	99.99850
40	.000942	1352.9800	99.99897
50	.000391	1352.9927	99.99944
60	.00019700	1352.9996	99.99967
80	.00006160	1352.9981	99.99986
100	.00002570	1352.9994	99.99991
120	.00001260	1352.9994	99.99995
150	.00000523	1352.9997	99.99997
200	.00000216	1352.9998	99.99999
250	.00000070	1352.9999	99.99999
300	.00000034	1352.9999	99.99999
600	.00000011	1352.9999	99.99999
1000	.00000000	1353.0000	100.00000

613

TABLE 6 Solar Spectral Irradiance—Standard Curve, Abridged Version

λ = wavelength, μm.
E_λ = solar spectral irradiance averaged over small bandwidth centered at λ, W m^{-2} μm^{-1}.
$D_{o,\lambda}$ = percentage of the solar constant associated with wavelengths shorter than λ, and solar constant = 1353 W m^{-2}

λ	E_λ	$D_{o,\lambda}$	λ	E_λ	$D_{o,\lambda}$	λ	E_λ	$D_{o,\lambda}$
0.115	.007	1×10^{-4}	0.43	1639	12.47	0.90	891	63.37
0.14	.03	5×10^{-4}	0.44	1810	13.73	1.00	748	69.49
0.16	.23	6×10^{-4}	0.45	2006	15.14	1.2	485	78.40
0.18	1.25	1.6×10^{-3}	0.46	2066	16.65	1.4	337	84.33
0.20	10.7	8.1×10^{-3}	0.47	2033	18.17	1.6	245	88.61
0.22	57.5	0.05	0.48	2074	19.68	1.8	159	91.59
0.23	66.7	0.10	0.49	1950	21.15	2.0	103	93.49
0.24	63.0	0.14	0.50	1942	22.60	2.2	79	94.83
0.25	70.9	0.19	0.51	1882	24.01	2.4	62	95.86
0.26	130	0.27	0.52	1833	25.38	2.6	48	96.67
0.27	232	0.41	0.53	1842	26.74	2.8	39	97.31
0.28	222	0.56	0.54	1783	28.08	3.0	31	97.83
0.29	482	0.81	0.55	1725	29.38	3.2	22.6	98.22
0.30	514	1.21	0.56	1695	30.65	3.4	16.6	98.50
0.31	689	1.66	0.57	1712	31.91	3.6	13.5	98.72
0.32	830	2.22	0.58	1715	33.18	3.8	11.1	98.91
0.33	1059	2.93	0.59	1700	34.44	4.0	9.5	99.06
0.34	1074	3.72	0.60	1666	35.68	4.5	5.9	99.34
0.35	1093	4.52	0.62	1602	38.10	5.0	3.8	99.51
0.36	1068	5.32	0.64	1544	40.42	6.0	1.8	99.72
0.37	1101	6.15	0.66	1486	42.66	7.0	1.0	99.82
0.38	1120	7.00	0.68	1427	44.81	8.0	.59	99.88
0.39	1098	7.82	0.70	1369	46.88	10.0	.24	99.94
0.40	1429	8.73	0.72	1314	48.86	15.0	4.8×10^{-2}	99.98
0.41	1751	9.92	0.75	1235	51.69	20.0	1.5×10^{-2}	99.99
0.42	1747	11.22	0.80	1109	56.02	50.0	3.9×10^{-4}	100.00
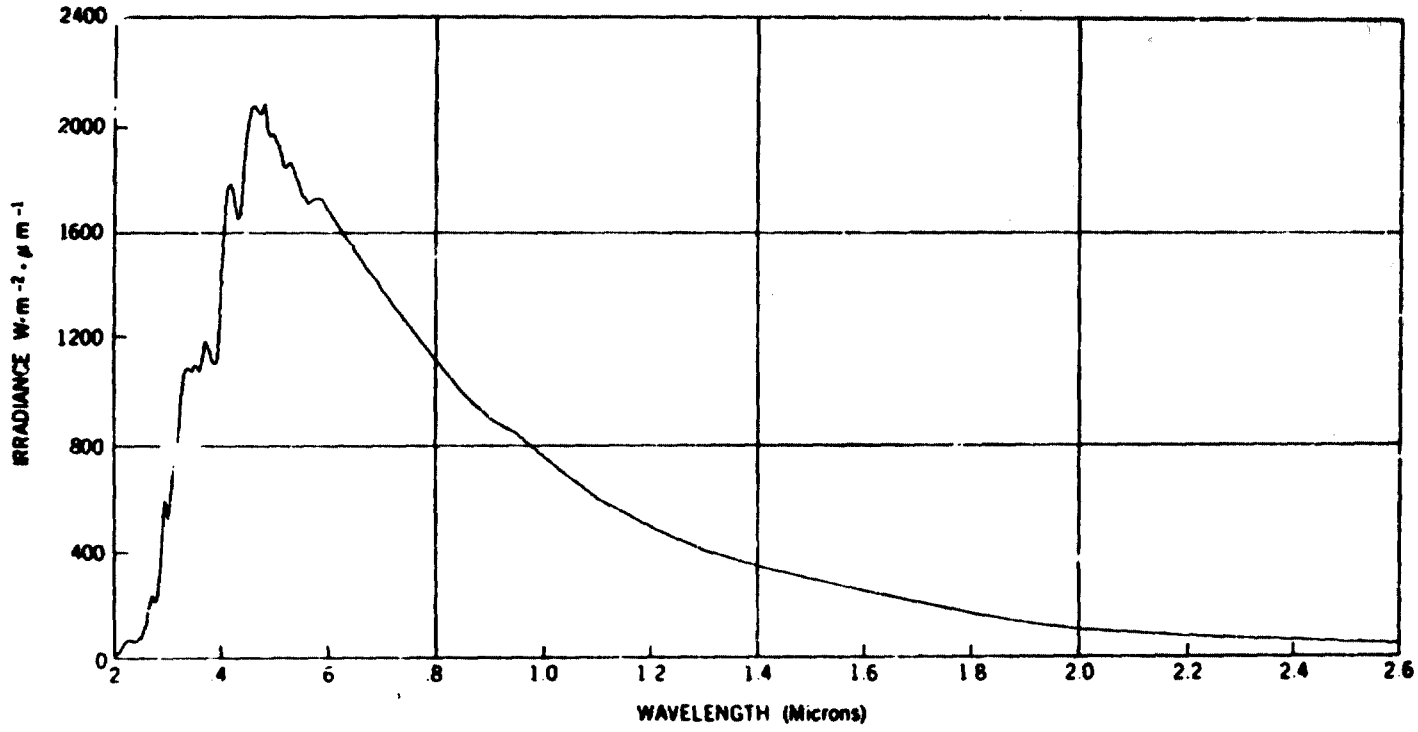
FIG. 1 Solar Spectral Irradiance.

APPENDIX C
PARAMETRIC ANALYSES

2.5 PARAMETRIC ANALYSES

2.5.1 GENERAL

This section describes the dynamic parametric analysis performed on both a planar and V-stiffened array configurations. The results of the analyses and their impact on the design of a 200 watt per kilogram solar array are discussed.

2.5.2 PLANAR ARRAY - VIBRATION STUDIES

2.5.2.1 Introduction

Parametric studies performed during the 110 W/kg solar array study formed the basis for establishing the optimum structural configuration characteristics of the 200 W/kg array. The design requirements for an interplanetary mission were essentially the same with a minimum deployed array natural frequency of .04 Hertz and a deployed array quasi-static load capability of 1×10^{-3} g's. The launch environment is that of the Space Shuttle instead of the Titan-Centaur, but this change only affects the stowed configuration and is not extensively different. In this report, only the deployed array vibration studies are being considered.

The following discussion reviews much of the investigations, techniques, and optimization studies which were conducted on the 110 W/kg array. A preliminary configuration was selected based on the findings of the earlier study and the new guidelines for lighter weight, more efficient solar cells.

Computer codes for determining minimum boom bending stiffness and blanket tension to meet the .04 Hertz frequency were updated and results are presented for the new baseline configuration.

2.5.2.2 Background Data

The configuration selected for the 110 W/kg interplanetary mission is shown in Figure 2-1. It consists of two Kapton solar cell blankets supported by a tubular Beryllium leading edge member, and a single deployable articulated steel longeron ASTROMAST. A flat pack design was used for the stowed solar array. Table 2-12 presents a total system mass summary for the system. The total weight of 87.5 kilograms was split almost equally between the mass of the solar cell blankets and the supporting and packaging structure. The goal of 200 W/kg necessitates the 87.5 kilograms be reduced to about 50 kilograms and indicates the need to reduce weight in all areas.

Figures 2-20 and 2-21 present the first anti-symmetric (torsion) and symmetric (bending) frequency versus blanket tension characteristics for a planar array. As indicated by the curves, their crossover point gives the maximum natural frequency for a minimum blanket tension. Figures 2-22, 2-23, and 2-24 graphically present the results of optimized boom stiffness and tension versus natural frequency and minimum system weight. The overall conclusion derived from these parametric variation studies was that a three to one aspect ratio was the minimum weight design for baseline configuration shown in Figure 2-1.

In view of the extensive optimization analyses performed during the 110 W/kg study, a planar baseline configuration was selected which closely matched the findings from the earlier investigation. However, it is shown in subsequent discussions that the optimized planar array with just the lighter and more efficient solar cells does not meet the desired weight goal of 50 kilograms. Further weight reductions and/or configuration changes are indicated.

Table 2-12   Total System Mass Summary - 110 W/kg Array
(Baseline Configuration for Interplanetary Mission)

Item		Mass (kg)
Solar Cell Blankets (see Table 2-6 for detail breakdown)		48.5
Stowage and Support Structure		30.6
Frame	11.0	
Container Bottom	3.6	
Container Cover	4.0	
Container Mechanisms	0.1	
Center Fitting	0.8	
Leading Edge Member	3.1	
End Retention Fittings	1.0	
End Retention Cable Cutters	0.9	
End Retention Mechanisms	0.4	
Blanket Tension Mechanisms	1.2	
Interlayer Cushioning	2.5	
Container Foam	1.8	
Coatings	0.1	
Fasteners	0.1	
Deployment Mechanism		8.4
Mast	3.1	
Canister	5.3	

Total   87.5

Figure 2-20   Symmetric and Antisymmetric
Frequency Vs. Tension (ASTROMAST)
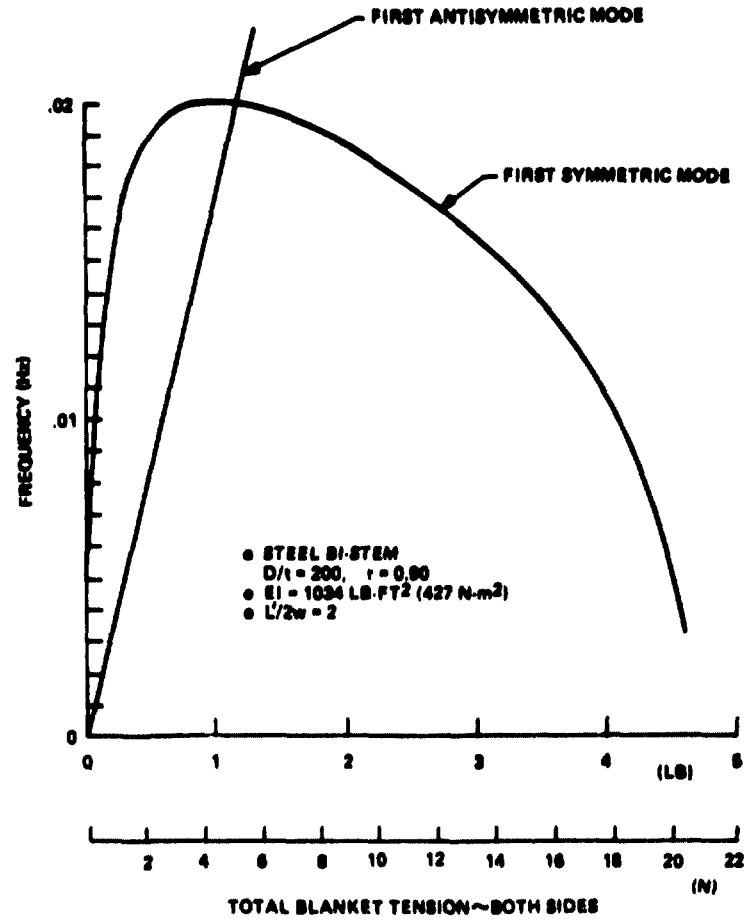
Figure 2-21   Symmetric and Antisymmetric
Frequency Vs. Tension (BI-STEM)
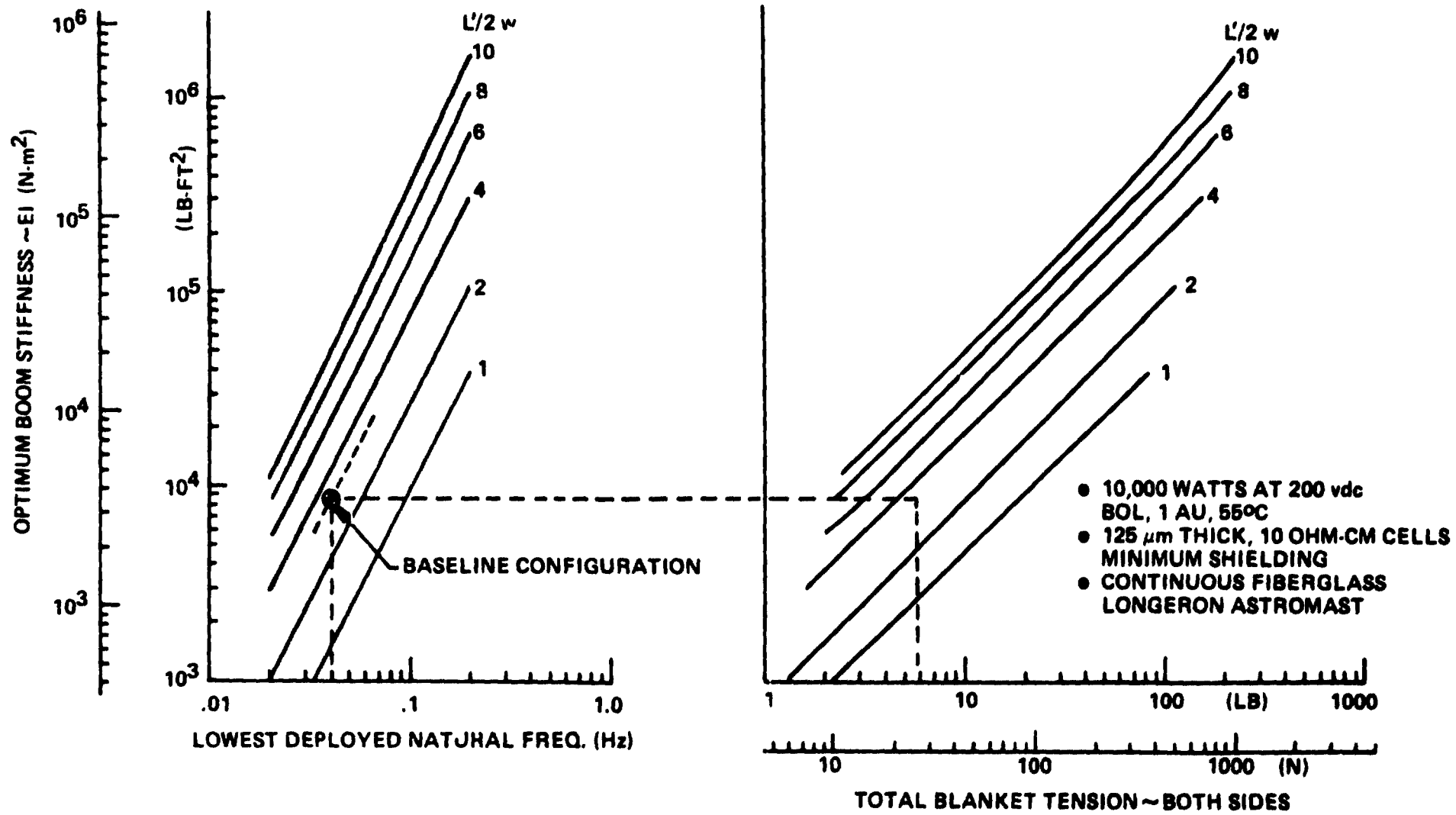
Figure 2-22 Optimum Boom Stiffness and Tension Vs. Frequency
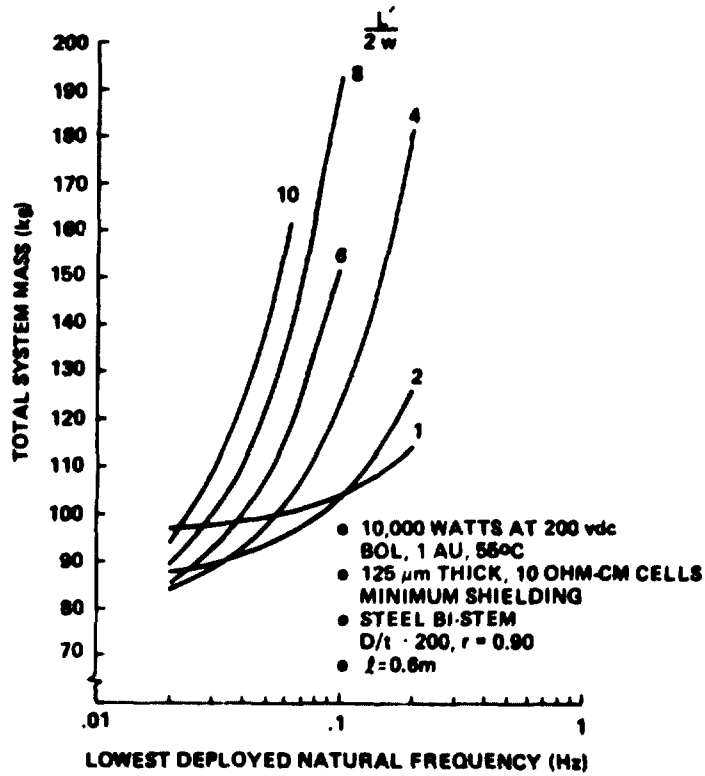
Figure 2-23 Total System Mass Vs.
Deployed Natural Frequency ASTROMAST
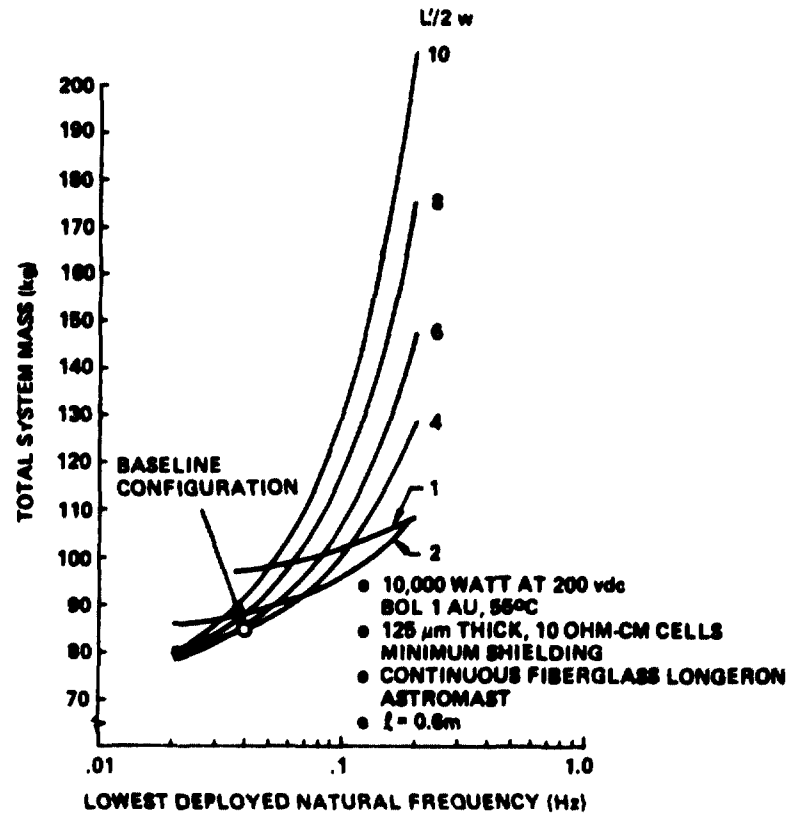
Figure 2-24 Total System Mass Vs.
Deployed Natural Frequency BI-STEM

2.5.2.3 Planar Array Computer Codes

The dynamics analysis required to determine the optimum boom stiffness and tension of the planar array was performed using a discrete parameter model used for previous analyses on the 30 W/lb. and 110 W/kg studies, and verified by test. The model used a five by two discretization as shown in Figure 2-25. Because of the symmetry of the solar array configuration, only half the array was analyzed with appropriate boundary conditions to determine either the symmetric or antisymmetric array modes. Each blanket was represented by 10 rectangular elements that describe the out-of-plane stiffness caused by the blanket tension. The leading edge member (LEM) and boom were modeled using beam elements and included the effect of axial preload on the boom stiffness. The leading edge member was free to rotate relative to the boom about the longitudinal axis of the array. A consistent mass representation was used. The boom density was varied in accordance with the boom stiffness as shown in Figure 2-20 for the continuous longeron ASTROMAST and articulated steel ASTROMAST booms. The analyses were performed using the appropriate subroutines in a DYNAMO II program that enabled the parameters to be varied over the range of interest. (See Table 2-13)

2.5.2.4 Deployed Analysis

2.5.2.4.1 Optimum Blanket Tension

The initial analysis performed was to determine the optimum blanket tension necessary to meet the .04 Hz frequency requirements for both symmetric and torsional vibration. Since the LEM rotates freely on the end of the boom, boom stiffness does not affect the torsional frequency calculations of the array, and the tension required to meet the torsional frequency criteria can,
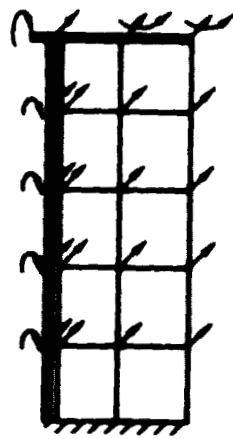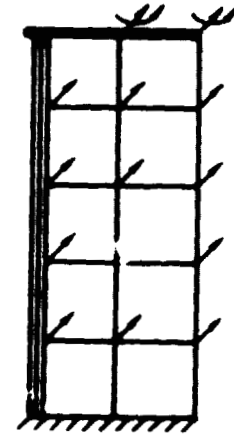
(a) SYMMETRIC　　　　　　　　　**(b) ANTI-SYMMETRIC**

Figure 2-25　Finite-Element Model of Two-Blanket,
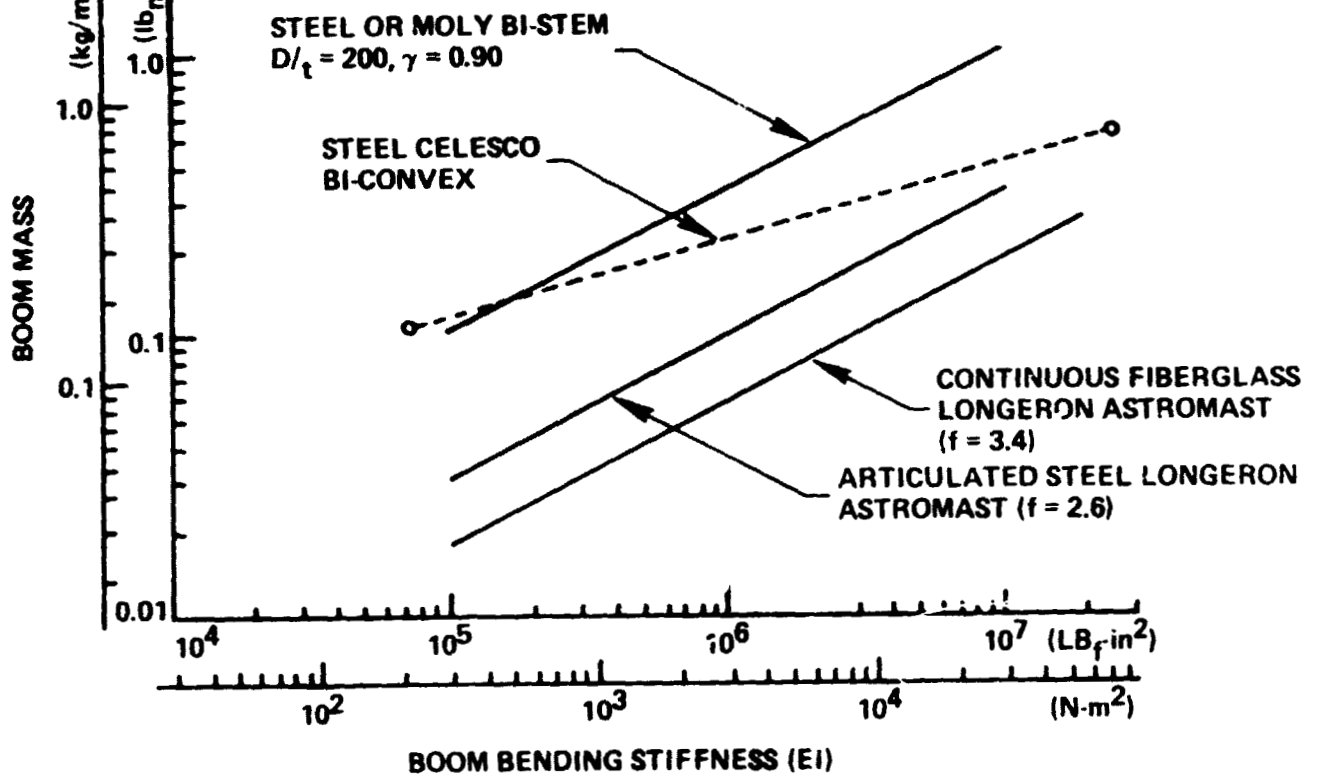Single-Boom Solar Array

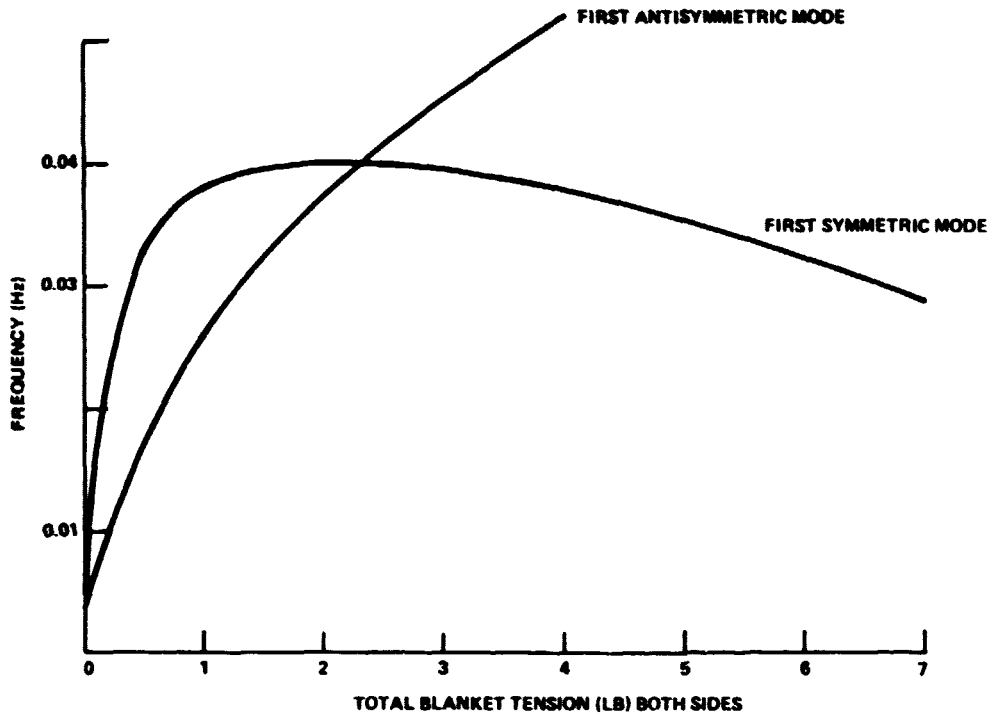Figure 2-26　Deployable Boom Mass Vs. Bending Stiffness

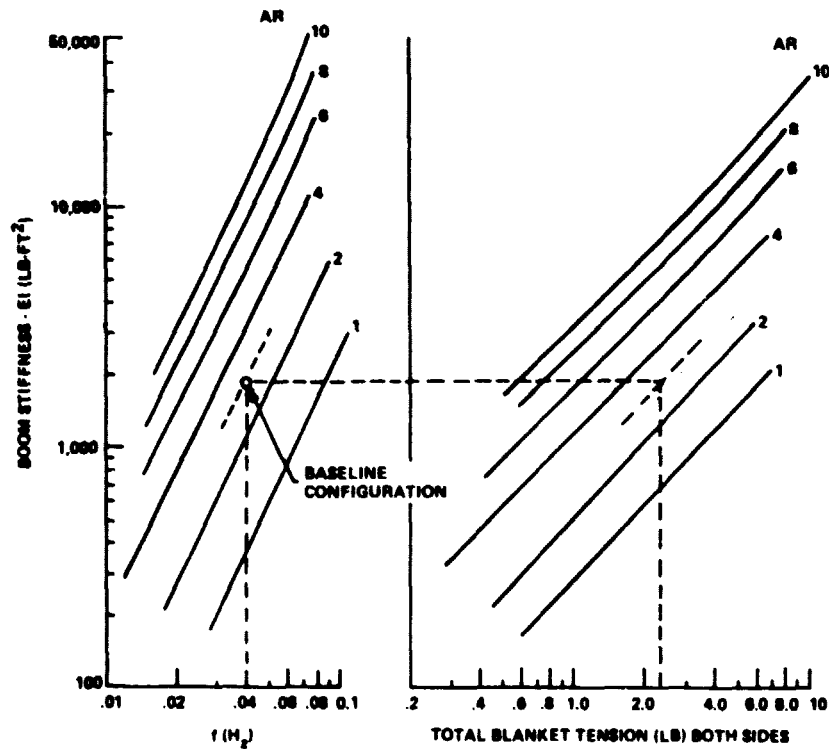Figure 2-27   Effect of Blanket Tension
On Lowest Natural Frequency

Figure 2-28   Boom Stiffness As A Function of
Frequency and Tension

therefore be determined solely from the information given above. This was done utilizing the rectangular membrane finite element program developed for determining the anti-symmetric frequencies of the 110 W/kg array. Once this value of tension was determined it was input, along with the data in Table 2-14, into the symmetric analysis program, to determine the boom stiffness necessary to meet the .04 Hz criteria for out-of-plane bending.

The results have been plotted in Figure 2-27 from which it can be seen that the optimum tension for the baseline system is approximately 2.4 lbs. (both sides).

Table 2-13 contains a summary of information acquired from the computer codes for use in the present 200 W/kg study.

Table 2-13   200 W/kg Baseline Planar Array Computer Runs

Run No.

SAS002	Effect of tension on torsional frequencies.
SAS003	Effect of EI variation on symmetric frequenceis assuming: - Fiberglass ASTROMAST - Tension equal to that required for a torsional frequency of .04 Hz.
SAS004	Effect of EI variation on symmetric frequencies assuming: - Articulated steel ASTROMAST - Tension equal to that required for a torsional frequency of .04 Hz.
SAS005	Effect of tension variation on symmetric frequency.

Table 2-14   Baseline Configuration - Planar Array

Aspect Radio	(AR)	3	
Length	(L)	14m	46 ft.
Width (total)	(W)	4.68m	15.3 ft.
Blanket Mass	(M)	24.97 kg	$55.06/g_c$ slugs
Blanket Density	(ρ)	$.381 \text{ kg/m}^2$	$.078/g_c$ slugs
Required Frequency	(f)	.04 Hz	

2.5.2.4.2 Effect of Aspect Ratio

In this analysis, data calculated for the 110 W/kg study was modified to represent the 200 W/kg array. Figure 3-100 of the 110 W/kg final report[1] presents a plot of optimum boom stiffness (EI) vs. fundamental frequency (f) and optimum blanket tension for various aspect ratios. Since the primary equation in the determination of the tension required for .04 Hz in torsion is that for tension in a stretched string,

$$TS = \frac{4 \text{ W}^2}{\pi^2} \text{ X } \rho L^2$$

the tension scale on this plot was shifted by ratioing the tension values by ρL^2 of the baseline 200 W/kg blanket to the ρL^2 of the 110 W/kg blanket. The boom stiffness scale of the plot was then similarly shifted by ratioing the values on this scale by TL^2. The results are shown in Figure 2-28 of this report.

---

[1] Reference 1

Computer runs were made for the 200 W/kg baseline that verified that the results are sufficiently accurate for evaluation of the 200 watt/kg configurations.

2.5.3 V-STIFFENED ARRAY-VIBRATION STUDIES

2.5.3.1 Introduction

Parametric studies performed for the 110 W/kg solar array as well as the current 200 W/kg study indicated that further reductions in required boom stiffness and overall system weight can be obtained from a minor variation of the planar design to a canted or V-stiffened one. The 110 W/kg study was able to meet its system weight goal with a planar array. However, as shown in the previous section, the planar configuration cannot meet the system weight requirement unless a significant mass reduction is made in the stowage and support structure. The following discussion presents a review of the earlier investigations into V-stiffening effects and a 200 W/kg baseline configuration is established which nearly meets the system weight goal.

2.5.3.2 Background Data

A "V"-stiffened solar array configuration was conceived as a means of obtaining significant increases in the minimum array resonant frequency without added complexity. Thus, it is possible to meet a specified deployed natural frequency requirement with reduced boom stiffness (and reduced total system weight) when compared with a planar array geometry. This concept, shown in Figure 2-11, uses the slight angle of the array blankets to enable observed in-plane stiffening resulting from the redistribution of blanket tension to provide out-of-plane stiffness. Static tests and analysis of the in-plane behavior showed that the array blanket tension was redistributed such that the
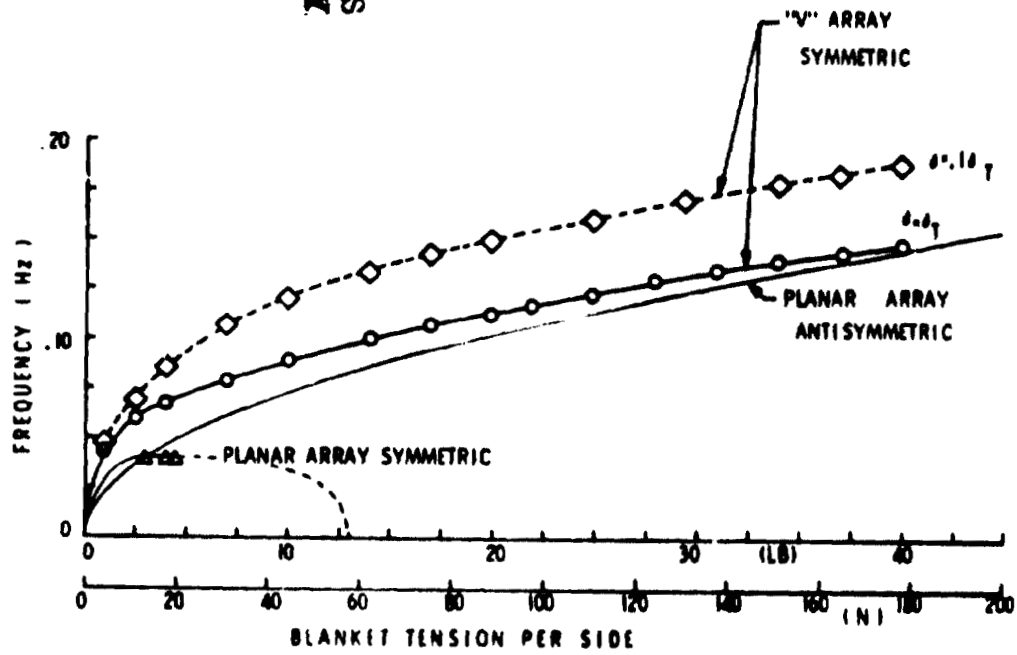
Figure 2-29   Effect of Blanket
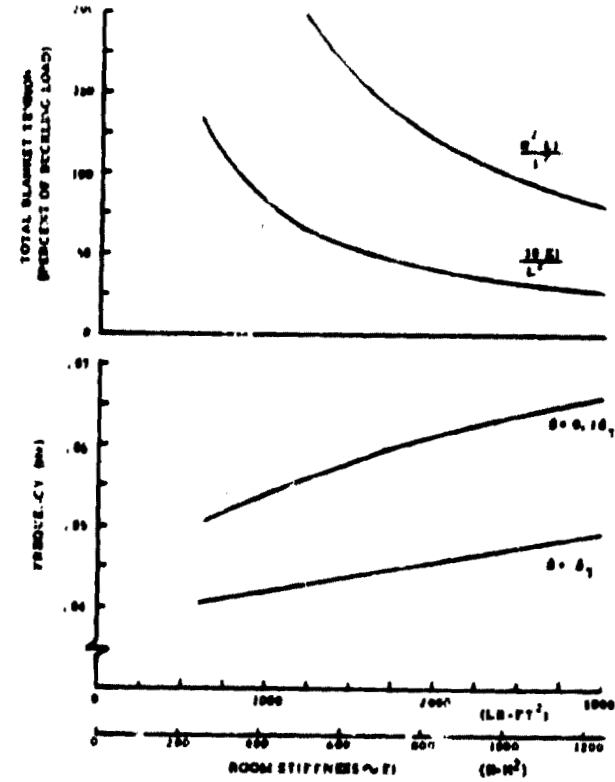Tension on Solar Array Frequency

Figure 2-30   Effect of Boom Stiffness On
"V" Configuration Solar Array Characteristics

array rotated about one edge. In effect, the blanket provided a moment con-
straint to the tip of the deployable boom until an edge tension condition
was achieved after which the boom behaved as a cantilever. By canting the
blankets and centering the boom within the blankets, this boom tip constraint
can be used to stiffen the array for symmetric out-of-plane motion.

The effect of the canted blankets will also provide stiffening for torsional
motion of the array. For a given boom, the tip constraint will enable greater
tension to be applied without buckling the boom; hence, an increase in the tor-
sional frequency. In addition, the boom will be required to bend during tor-
sional vibration with some increase in the frequency. (Because of the high in-
plane stiffness, the array will tend to twist about the center of the "V" caus-
ing bending of the boom.)

Figure 2-29 graphically illustrates the effect of blanket tension on natural
frequency for a "V"-stiffened array. There is no crossover or hump maximum
frequency for the symmetric mode as exists for the planar array. Conversely,
for a given frequency, "V"-stiffening permits the use of lower blanket tensions
and subsequently lighter weight support structure. Figure 2-30 presents the
results of an investigation into minimum allowable boom stiffnesses and boom
buckling limits. It is apparent that the "V"-stiffened array does not have
an optimum boom stiffness and blanket tension for a given frequency similar to
the planar array. The following discussion further investigates these trends
and has resulted in the selection of a minimum weight configuration.

2.5.3.3 V-Stiffened Array Computer Code

Tests on a planar array indicated that there were three regions of different
stiffnesses for in-plane deflections as shown in Figure 2-31a and described
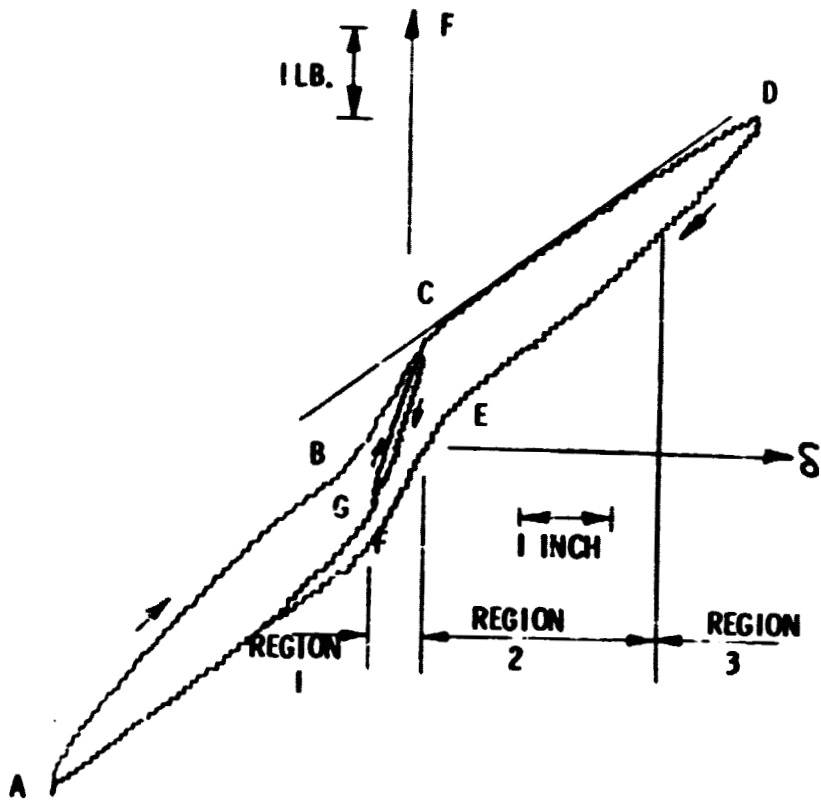
(a) Measured on RA250
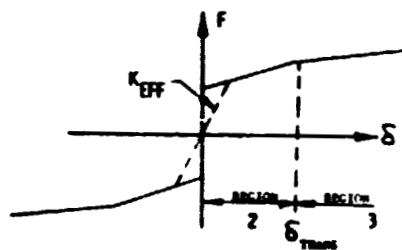
ORIGINAL PAGE IS
OF POOR QUALITY

(b) Linearized

Figure 2-31   In-Plane Force-Deflection Characteristic

below:

Region 1: For small deflections, hysteretic behavior of the BI-STEM boom
caused a relatively high stiffness. This is best predicted semi-empirically
and is not predicted by simplified analytical modeling.

Region 2: For medium deflections, the tension distribution of the blankets
changes such that the slope (Θ) at the tip of the leading edge member is pro-
portional to the tip deflection (δ) divided by the array length (L).

$$\Theta = \delta/L$$

This results from a constraining moment at the tip of the boom due to the
blanket tension and is valid until the tension shifts to the edges of the
blanket.

Region 3: For large deflections, the effect of blanket tension is no longer
present and the boom behaves as a cantilever. This occurs after the transi-
tional deflection (when tension shifts to the edges of the blankets at end of
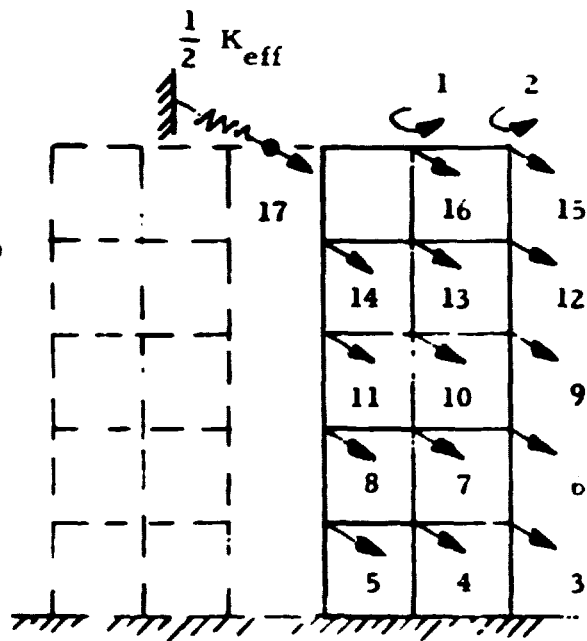Region 2).

Using the idealized representation shown in Figure 2-31b, an effective linear
stiffness (K_{eff}) can be defined for a selected amplitude of motion. Although
other methods could be used to arrive at a linearized stiffness, this appears
to be a reasonable estimate. It is conservative for large amplitudes in that
the stiffness is higher than predicted, but may be unconservative for small
amplitudes because the Region 1 stiffness is not included in the stiffness
representation.

C-16
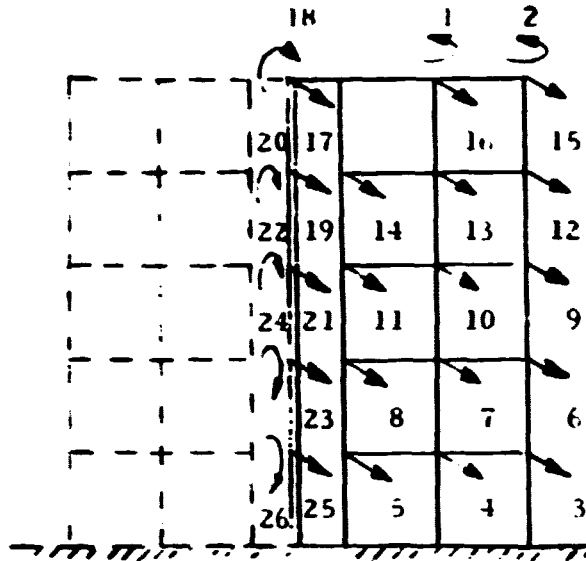
NOTE: SYMMETRY BOUNDRY CONDITIONS
IMPOSED ALONG BOOM $\mathrel{C_L}$

(a) Planar Solar Array

$\frac{1}{2} K_{eff}$

NOTE: K_{eff} USED TO
REPRESENT BOOM
STIFFNESS WITH IN-
PLANE BLANKET
TENSION EFFECT.

(b) "V"-Configuration Solar Array

Figure 2-32   Symmetric Models

2.5.3.3.1 Symmetric Vibration Analysis

The approach used in performing this symmetric vibration analysis of the "V" stiffened array was to use the existing planar model of the blankets and revise the boom stiffness representation to reflect the effect of the blanket tension redistribution. The original analytical model of the array is shown in Figure 2-32a. The revised model of the array is shown in Figure 2-32b, where the major modification is to replace the boom finite element model by an effective linear spring (K_{eff}). This appears reasonable in that the cant angle of the array being considered is small (on the order 10^0) so that significant area is not added to the array due to the change in the projected area. The resulting change in the membrane stiffness due to the small angular rotation should not be significant, but should actually increase the blanket stiffness. Therefore, the main effect seems to be the revised boom stiffness.

Consider the out-of-plane deflections of the "V" stiffened array shown in Figure 2-33a and the free body diagram of the Leading Edge Member (LEM) shown in Figure 2-33b. These diagrams are identical to those of Reference 2 except for the modified width which now becomes the projected width; i.e., w is replaced by $w \sin\beta$. The force deflection relation (ref. 1) neglecting root flexibility (α) becomes:
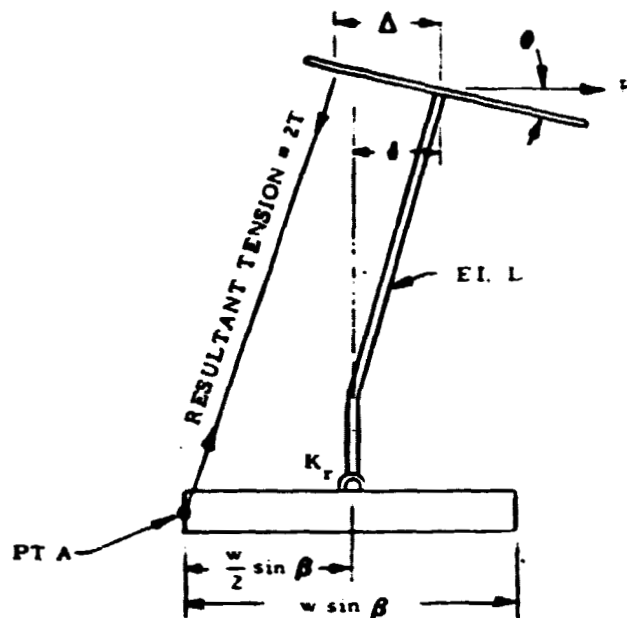
$$F = \left[\frac{4 \, EI}{L^3} - \frac{4T}{15L} \right] \delta + \frac{Tw \sin\beta}{L} \qquad (1)$$

where:
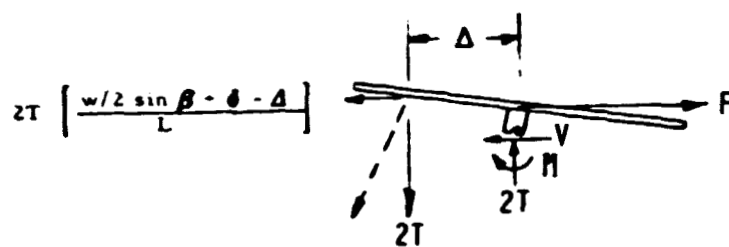
T = tension per blanket

EI = Boom Stiffness

w = Half width of array

C-18

(a)

Edge View of Deflected Array

$$2T \left[\frac{w/2 \sin \beta + \phi - \Delta}{L} \right]$$

$$V = \frac{6 E I \phi}{L^3 (1 + 4\alpha)} - \left[\frac{11 + 76\alpha + 160\alpha^2}{5 (1 + 4\alpha)^2} \right] \frac{T\phi}{L}$$

$$M = \frac{2 E I \phi}{L^2 (1 + 4\alpha)} + \frac{T\phi (1 + 12\alpha)}{15 (1 + 4\alpha)^2}$$

(b)

Figure 2-33   Force Diagram at Outer End of Array

and the limiting deflection at which the transition from Region 2 to Region 3 occurs (Ref. 1 and 2) neglecting root flexibility, becomes:

$$\delta_{TRANS} = Tv \sin\beta \left[\frac{2\ EI}{L^2} + \frac{T}{15} \right]^{-1} \qquad (2)$$

Using K_{eff} to linearize the boom stiffness over the range of applicable deflections and neglecting root flexibility:

$$K_{eff} = \frac{F}{\delta} = \left[\frac{4\ EI}{L^3} - \frac{4T}{15L} + \frac{Tv\ \sin\beta}{L} \right] \frac{1}{\delta} \qquad (3)$$

where $1/2\ K_{eff}$ is added to the stiffness matrix of the analytical model at coordinate 17.

It will be noted that the tension effect on the boom stiffness is included in the linearized stiffness. As the tension is increased, the boom stiffness decreases as indicated by the first two terms of Equation 3. When $2T = \dfrac{30\ EI}{L^2}$, the boom stiffness becomes zero and the K_{eff} is due only to the initial offset value. From the buckling standpoint, the buckling load in Region 2 is increased from $\dfrac{\pi^2\ EI}{L^2}$ to $\dfrac{30\ EI}{L^2}$, an increase of approximately 3 to 1.

The mass of the boom is included in the boom tip coordinate using one-fourth of the boom mass.

2.5.3.4 Deployed Analysis

2.5.3.4.1 Assessment of Stiffening Effects

An evaluation of the effectiveness of the V-stiffened configuration was performed using the baseline configuration (Ref. 12) as a point of reference. The following values were assumed for the parameters specified:

Total Deployed Length   =   14 m (46 ft.)

Total Blanket Width   =   4.68 m (15.34 ft.)

Boom Stiffness (EI)   =   625 nt-m^2 (2000 lb.-ft.^{2})

LEM Stiffness (EI)   =   2060 nt-m^2 (5000 lb.-ft.^{2})

Blanket Mass   =   24.97 Kg (55.06/g_c slugs)

Tension per Blanket   =   5.78 nt (1.3 lbs.)

The effect of the cant angle on the array characteristics can be seen from the previous analytical expressions. The deflection at which transition occurs is directly proportional to the sine of the angle (Equation 2) so that the transitional deflection can be increased, if necessary, by increasing the angle (e.g., a 15 degree angle would result in approximately 50 percent increase in the transition deflection over that provided by a 10 degree angle). For a given deflection, the effective boom stiffness is increased significantly due to the increase in the offset force (3). On the other hand, the effective boom stiffness at the transitional deflection can be shown to be

$$K_{eff} = \frac{6\ EI}{L^3} - \frac{3T}{15L} \qquad (4)$$

which is not affected by the cant angle.

The fundamental symmetric resonant frequency determined from the analytical model is shown in Figure 2-34 for the range of tension values investigated. For comparison, the symmetric and antisymmetric frequencies of the baseline planar array are also shown. The "V" array frequency is shown for oscillation amplitudes equal to the transitional deflection and one-tenth the transitional deflection. It should be noted that the small amplitude curve is questionable due to neglecting the Region 1 stiffness.
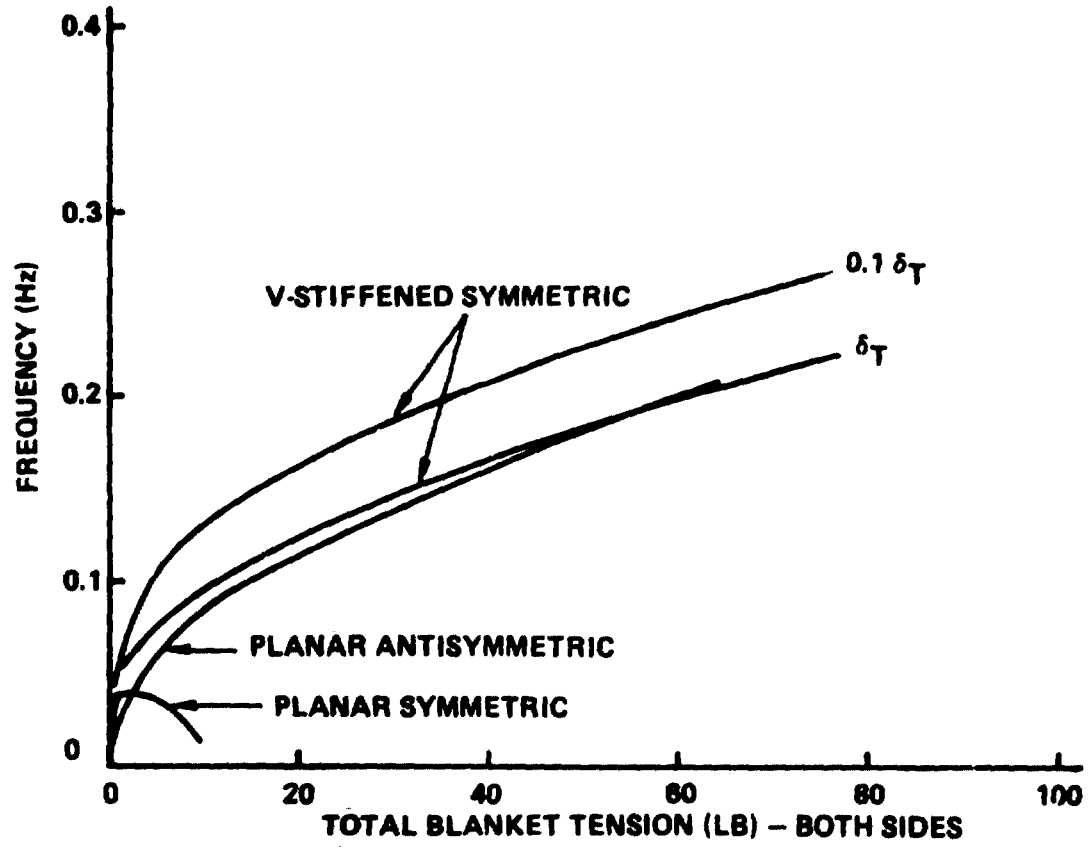
Figure 2-34   Effect of Blanket Tension on Solar Array Frequency

From Figure 2-34 it is apparent that the tension required to meet the .04 Hz torsional frequency and the boom stiffness required to meet the .04 Hz symmetric frequency criteria for the planar array, results in a greatly increased symmetric frequency for a small (10°) amount of V-stiffening. Therefore, using this tension value (needed for .04 Hz torsion) allows the boom stiffness to be significantly decreased while still obtaining .04 Hz in out-of-plane bending.

For baseline design, the required blanket tension (per side) of a planar configuration was determined to be approximately 5.8 nt (1.2 lb). The tension was set at this value and the boom stiffness varied through the range of practical interest.

The range of boom stiffness that was considered practical was based on the buckling load of the array for the required tension value. If a conservative design approach is used, a criteria that the buckling load of the cantilever boom is not exceeded could be selected. Alternately, a less conservative criteria is that the buckling load of the boom with the blanket restoring moment acting would not be exceeded. Using the first criteria, the boom could not buckle for any range of deflections whereas the second criteria would result in boom buckling if the tip deflection was greater than the transitional deflection. From Figure 2-35 applying a safety factor of 1.25 to the buckling load an EI of 285 nt-m^2 (690 lb-ft^2) satisfies the first criteria and an EI of 91 nt-m^2 (220 lb-ft^2) satisfies the second criteria.

The calculated symmetric frequencies for this boom stiffness range satisfies the 0.04 Hz requirement for oscillations at the transitional deflection and a large margin is indicated for smaller oscillation amplitudes. Consequently, the controlling factor is boom buckling.
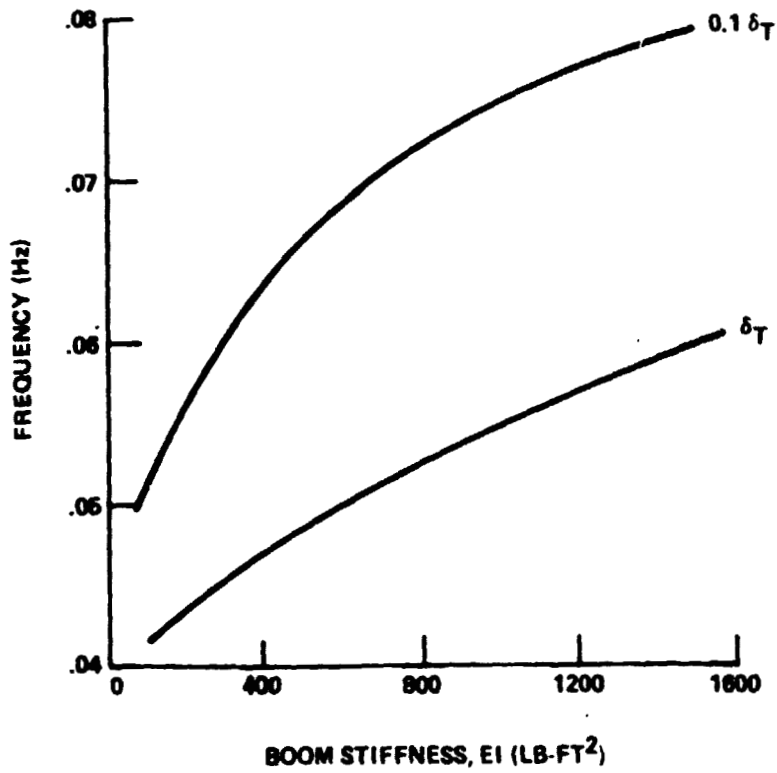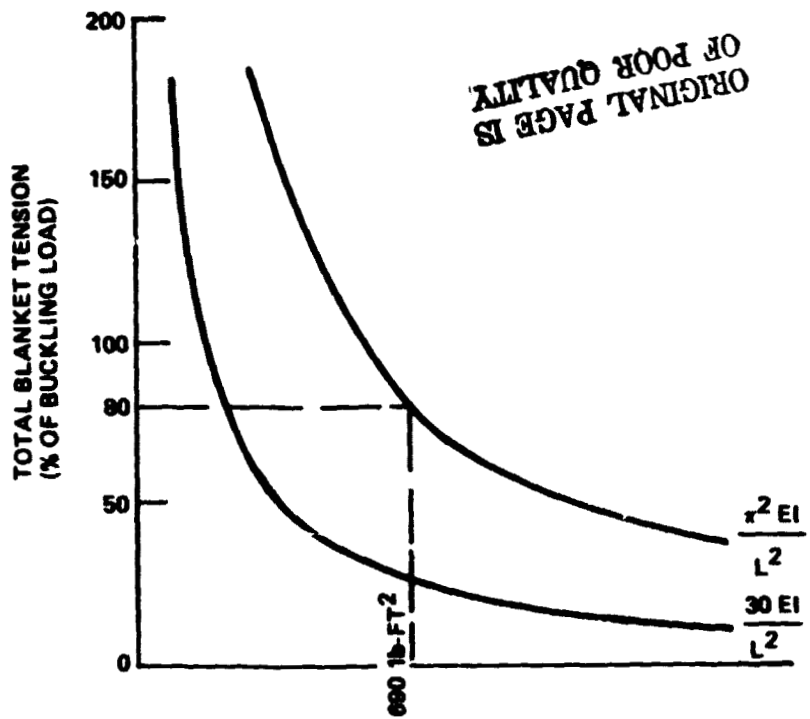
Figure 2-35   Effect of Boom Stiffness on "V" Configuration
Solar Array Characteristics

2.5.3.4.2 Force Deflection Characteristics

To determine the optimum cant angle (β) of the blankets, computer runs were made to calculate the frequency in out-of-plane bending over a range of boom stiffnesses for cant angles of 6°, 8°, and 10°. The transition forces (F_t) were calculated from equation (1) for each boom stiffness (EI) at each cant angle and are plotted vs. EI in Figure 2-36.

The loads produced by the quasi-static acceleration requirement $(10^{-3}$ g's) set by JPL must not exceed the transition force or the effects of V-stiffening will be lost. A 1.25 safety factor applied to an approximate blanket plus boom weight of 57 lbs. multiplied by 10^{-3} results in a minimum transition force requirement of .071 lb.

The intersection of the horizontal line drawing at $F_t=.07$ on Figure 2-36 gives the minimum boom stiffness needed to meet this criteria for each of the cant angles. A blanket cant angle of approximately 6.25° is seen to result in a design which meets exactly, both the transition force and boom buckling criteria. The use of any other cant angle would require a design which exceeds one or both of these requirements.
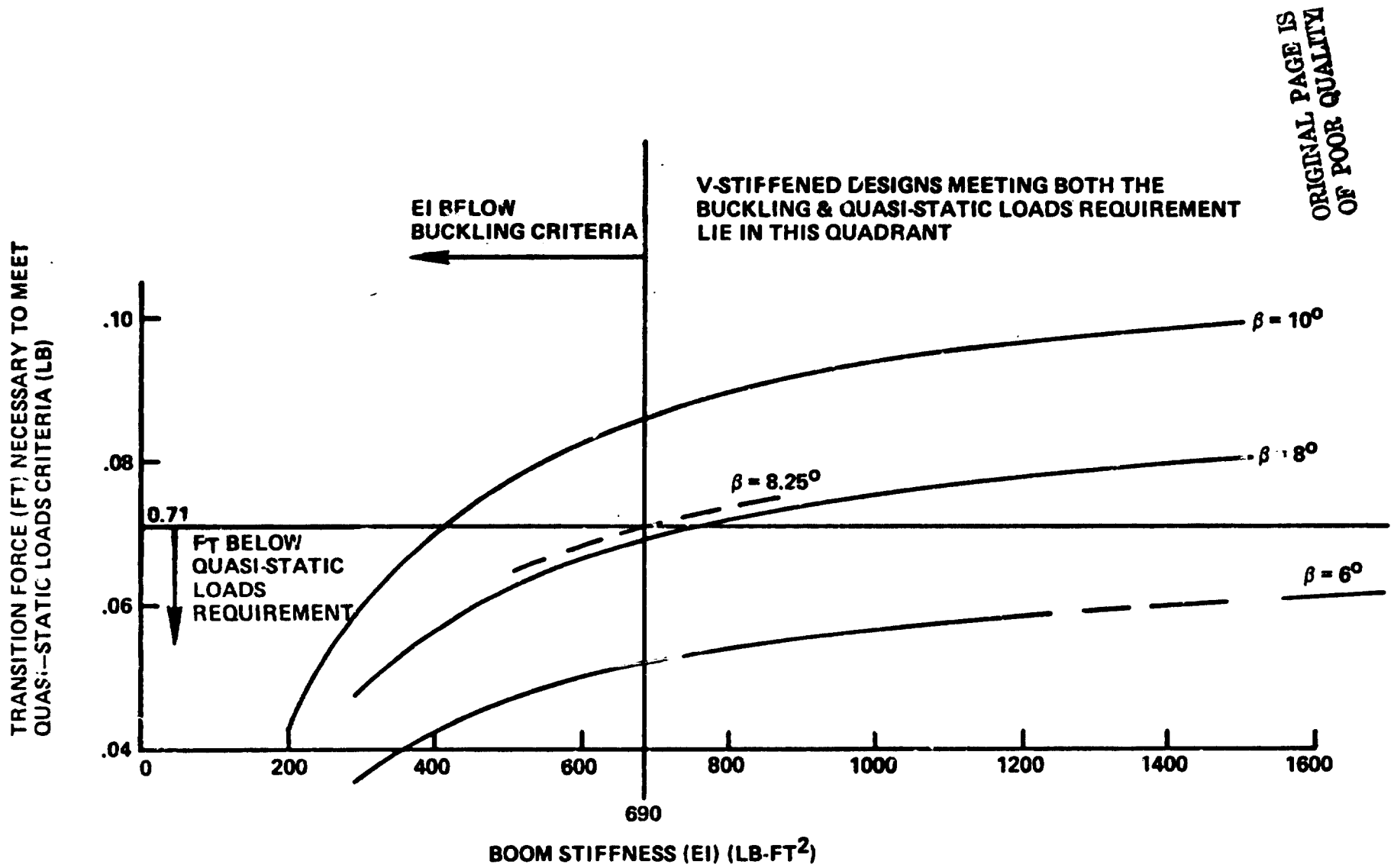
Figure 2-36   Effect of Blanket Cant Angle on Boom Stiffness